AD NUMBER

AD484265

NEW LIMITATION CHANGE

TO

Approved for public release, distribution unlimited

FROM

Distribution authorized to U.S. Gov't. agencies and their contractors; Critical Technology; JUN 1966. Other requests shall be referred to Air Force Aero Propulsion Laboratory, Attn: APIP, Wright-Patterson AFB, OH 45433.

AUTHORITY

AFAPL ltr, 4 May 1973

484265

HIGH RATE (5-MIN) MISSILE

BATTERY PROGRAM

M. A. VERTES
J. E. OXLEY
S. COHEN

TECHNICAL REPORT AFAPL-TR-66-50

JUNE 1936

484265

NOTICES

When Government drawings. specifications. or other data are used for any purpose other than in connection with a definitely related Government procurement operation, the United States Government thereby incurs no responsibility nor any obligation whatsoever, and the fact that the Government may have formulated, furnished, or in any way supplied the said drawings, specifications, or other data, is not to be regarded by implication or otherwise as in any manner licensing the holder or any other person or corporation, or conveying any rights or permission to manufacture, use, or sell any patented invention that may in any way be related thereto.

This document is subject to special export controls and each transmittal to foreign governments or foreign nationals may be made only with prior approval of the Air Force Aero Propulsion Laboratory.

Copies of this report should not be returned to the Research and Technology Division unless return is required by security considerations, contractual obligations, or notice on a specific document.

HIGH RATE (5-MIN) MISSILE
BATTERY PROGRAM

M. A. VERTES
I. E. OXLEY
S. COHEN

FOREWORD

This is the final report prepared by Leesona Moos Laboratories, Great Neck, New York on Air Force Contract AF 33(615)2680 under Task No. 817304, High Rate (5-Min) Missile Battery Program, of Project No. 8173, Static Energy Conversion. Principal contractor personnel consisted of Dr. H. G. Oswin, Principal Investigator; Mr. M. A. Vertes, Project Engineer; Dr. J. E. Oxley, Electrochemist and S. Cohen, Chemical Engineer. The work was conducted during the period of June 15, 1965 through March 18, 1966. This work was administered under the direction of the Static Energy Conversion Branch, Aerospace Power Division, Air Force Aero Propulsion Laboratory, Research and Technology Division and the Air Force Systems Command, USAF, Wright-Patterson Air Force Base, Ohio. Mr. G. H. Miller, APIP-2, is the Project Officer for the Laboratory.

This report was submitted by the authors on April 11, 1966 and approved by Dr. H. G. Oswin of Leesona Moos Laboratories.

All, or many, of the items compared in this report were commercial items that were not developed or manufactured to meet government specifications, to withstand the tests to which they were subjected, or to operate as applied during this study Any failure to meet the objectives of this study is no reflection on any of the commercial items discussed or on any manufacturer.

Publication of this report does not constitute Air Force approval of the reports findings or conclusions. It is published only for the exchange and stimulation of ideas.

ABSTRACT

Thi: report describes the work carried out at Leesona Moos Laboratories under Contract No. AF 33(615)2680 toward development of two operating batteries, a 28 volt nominal and a 1000 volt nominal battery. The three main phases of the program were:

- Literature search and experimental investigation of electrode couples.

- Cell development.

- Design analysis.

The aluminum/oxygen and zinc/oxygen battery systems were studied in the 15 second to 5 minute discharge time range. The results of the parametric studies, conceptual design studies, and thermal analysis to date have shown that the weights of the aluminum/oxygen and zinc/oxygen batteries a re penalized to a major extent by the need for eat sinks at rates longer than 15 seconds. This is the result of irreversible thermodynamic losses which appear as waste heat during discharge of the cell.

In all cases, the most reversible aluminum anodes found have been the materials supplied by Olin. These alloys have demonstrated consistent superiority over and above high purity and commercial purity aluminum. These alloys provide superior cell voltages to zinc in potassium hydroxide but this advantage is lost because of the greater percent of irreversibility and hydrogen evolution.

TABLE OF CONTENTS

LIST OF ILLUSTRATIONS

SECTION I

INTRODUCTION

This report details the work carried out at Leesona Moos Laboratories (LML) under Contract No. AF33(615)2680. The main p   .ion of the work was the experimental and analytical investigation of the aluminum/oxygen system. The objective was to develop this system into two operating batteries: a 28 V nominal and a 1000V nominal battery. Detailed studies showed that the aluminum anodes require considerably greater research effort than allowed within the scope of the program before development of the battery could start, and the Contracting Agency, Air Force Aero Propulsion Laboratory, then decided that the remaining effort should be redirected to characterizing the limitations of the aluminum/oxygen system, determining the applicability of zinc/oxygen for very high rates and to provide a zinc/air, zinc/oxygen battery laboratory evaluation unit for AFPL.

Most of the work reported here in olving experimentation and the majority of the analytical work was directed towards the development of the two working batteries and, namely, the characterization of the aluminum/oxygen system, its expected operational limitations and identification of its weight-controlling factors. The results of the study are presented in Sections II through V. Section VI contains conclusions and recommendations with respect to high energy density batteries and with special attention to the aluminum/oxygen couple.

SECTION II

TECHNICAL APPROACH

To meet the original objectives of the program, namely development of two batteries within a given period of time, a three-pronged technical approach was taken at LML consisting of (a) literature search and experimental investigations of electrode couples, (b) cell development and (c) design analysis.

In order to give a better understanding to the reader on the thinking behind the selection of aluminum/oxygen as a system for high-rate/high-energy density battery, some of the requirements and goals of the original program are listed below:

1. The conventional battery shall have a nominal 28V rating. The voltage shall not vary more than 20% from open circuit to full load.

2. The pile construction battery shall have a nominal output voltage of 1000 volts. The voltage shall not vary more than 10% from open circuit to full load.

3. The cells of the pile-type construction shall be capable of delivering 3.5 amperes for 1.5 minutes.

4. The cells for the conventional type battery shall be capable of delivering 43 amperes for 5 minutes and 855 amperes for 15 seconds.

5. The cell shall be capable of being started up and operated at any temperature in the range -35°F to +150°F without the addition of any external energy.

6. The battery shall be capable of starting up and operating in any position.

7. The battery shall be capable of starting up and operating in a zero gravity environment.

8. The external battery case temperature shall not rise above 250°F due to internal heating when the battery is placed in ambient air.

9. As a goal, the conventional battery weight shall be .85 lbs.

10. As a goal, the pile construction battery weight shall be .875 lbs.

11. As a goal, both battery designs shall have an energy density of 4 watt-hours/cu. in.

In order to illustrate the difficulty of the task, consider a battery having 100 watt-hours capacity and weighing .85 lbs. and also having an energy density of 4 watt-hours/cu. in. This battery would have a specific gravity of .94 or less than that of water.

At the start of the program the basic choice had been made between the three major types of cell: (1) molten salt, (2) aqueous, (3) non-aqueous.

One of the system requirements is that the cells be capable of start-up and operation in temperature range of -35°F to $+150^\circ$F without the addition of any external energy. Another requirement was that the temperature of the external battery case must not rise above 250°F. These requirements preclude the use of molten salt electrolytes.

Non-aqueous electrolytes have at least an order of magnitude lower conductivity than aqueous electrolytes. At the required high current drain this would have resulted in excessive resistance losses. In addition, very little is known of the electrode kinetics of such electrolytes and considerable research effort would have been required before any development could start.

These considerations limited the selection of the couples to those that are operable in aqueous media. Couple combinations were then selected on the basis of available data such as AH/#, theoretical OCV, stability, reversibility. For many couples of interest, information was lacking. On the basis of data from all available sources, aluminum/oxygen and zinc/oxygen were the prime and second choices. After the couples were selected, data from the literature and from Leesona projects was assembled. Experimental investigations commenced to gather the information needed to permit a detailed characterization of the couples. Parallel studies of the complete battery system were also initiated at this time to enable the determination of the relative weights and volumes of the various components of the battery.

In order to meet the goal of 100 WH/#, a minimum theoretical (based on equivalent weight of couples and OCV) value of 400 WH/# was used as a criterion: the factor of four being considered minimal for the particular low-energy, high-rate requirement. Table I lists some of the combinations reviewed: only five of these are less than 400 WH/#.

The stability of the couples with respect to the solvent - water - is of course a very important criterion which eliminates many of the more electroposition couples in Table I, in particular the alkali and alkaline-earth metals.

4

Table 1.   Electrochemical Couples Possessing High Theoretical Power Density

Couples		Watt Hours/Pound	E^o
$2Al + 3CuF_2$	$2AlF_3 + 3Cu$	353	1.735
$2Al + 3CuO$	$Al_2O_3 + 3Cu$	515	2.06
$2Al + 3/2O_2$	Al_2O_3	1874	2.71
$2Al + 3Cl_2$	$AlCl_3$	860	3.14
$2B + 3/2O_2$	B_2O_3	2130	2.04
$Be + CoF_2$	$BeF_2 + Co$	351	1.53
$Be + 1/2O_2$	BeO	2950	3.02
$Be + CuO$	$BeO + Cu$	648	2.36
$2Li + CuF_2$	$2LiF + Cu$	749	3.55
$2Li + 1/2O_2$	Li_2O	2365	2.91
$2Li + CuO$	$Li_2O + Cu$	587	2.25
$2Li + 2CuO$	$Li_2O + Cu_2O$	329	2.34
$3Li + CoF_3$	$3LiF + Co$	965	3.64
$Mg + CuCl_2$	$MgCl_2 + Cu$	332	2.16
$Mg + CuF_2$	$MgF_2 + Cu$	566	2.92
$3Mg + 2CoF_3$	$3MgF_2 + 2Co$	550	2.29
$4Mg + Co_3O_4$	$4MgO + 3Co$	572	1.98
$2Mg + NiO_2$	$2MgO + Ni$	850	2.44
$2Mg + O_2$	$2MgO$	1860	3.09
$Mg + AgO$	$MgO + Ag$	491	2.98
$Mg + 2AgF$	$MgF_2 + 2Ag$	310	3.53
$Mg + Cl_2$	$MgCl_2$	796	3.12
$2Na + CuCl_2$	$2NaCl + Cu$	414	3.07
$2Na + CuF_2$	$2NaF + Cu$	510	3.09
$Ca + CuF_2$	$CaF_2 + Cu$	604	3.51
$Ca + 1/2O_2$	CaO	1360	3.14
$2Zn + O_2$	$2ZnO$	485	1.62
$Zn + Cl_2$	$ZnCl_2$	345	1.93
$Ti + O_2$	TiO_2	1030	1.69

5

Equally important criteria for a high-rate, high energy-density cell are Faradaic efficiency of the couples and rates of the electrochemical processes - the current density. Both of these must be maximized to achieve good energy density in high-rate cells.

After evaluating possible combinations by these criteria, the following systems were considered most suitable:

1. aluminum/oxygen

2. magnesium/oxygen

3. zinc/oxygen

4. aluminum/chlorine

Work was primarily restricted to Al/O_2. However, because of the effects encountered with aluminum anodes especially in KOH, a brief investigation of (1) Cl_2/Cl^- couple (to permit use of aluminum anodes in chloride electrolyte) and (2) Mg/Mg^{++} (to determine whether it exhibited greater reversibility than Al/Al^{+++}) was carried out.

SECTION III

PARAMETRIC STUDIES OF ELECTRODE COUPLE

3.1 ALUMINUM ANODES

The electropositive nature of aluminum is usually modified by its tendency to passivate in the presence of oxidizing anions. This is not the case in strong alkaline solutions when the passive oxide dissolves rapidly continually leaving a fresh metal surface exposed. To use aluminum successfully as a battery anode, a protecting but not passivating oxide layer is required in the presence of a concentrated electrolyte.

Most attempts to improve the anodic discharge of aluminum have involved either the modification of electrolytes or the use of alloys. For a primary battery the aim should be to promote a high dissolution rate while retaining high hydrogen over-voltage characteristics on the surface. Thus, it is desirable to modify the metallurgical properties of aluminum in such a way that aluminum can be rapidly ionized while preserving the integrity of the "protecting" oxide layer. The role of alloy additives is, of course, specific to any given metal/electrolyte system and requires a sound understanding of the metallurgical properties, and the defect nature of the surface oxide. It has been shown, for example, that the addition of mercury to aluminum although it possesses very high hydrogen over-voltage causes aluminum to become very reactive probably because the aluminum oxide cannot adhere to the highly amalgamated metal surface. "Combustion" of amalgamated aluminum has been observed in the presence of air, resulting in a very finely dispersed oxide phase. The Metals Division of Olin Mathieson supplied LML with aluminum-tin alloys which met some of these requirements. The alloys were developed by Olin for use as sacrificial anodes. The alloys offer a significant advantage over ordinary commercial or high-purity aluminum.

The Olin alloys are a series of tin-containing systems which are treated specifically to produce oxide coatings with improved cation conductivity. It is claimed (R) that the presence of stannic ions in the oxide lattice increases the concentration of positive carriers significantly resulting in an increased ratio of ionic conductivity to electronic conductivity.

Thus, the transfer of aluminum ions through the oxide layer is enhanced without increasing electronic conductivity. This is an important consideration since electronic conductivity is one of the parameters which help control hydrogen evolution on the surface. This is shown in the sketch on the following page.

7

metal/oxide interface

oxide/electrolyte interface

Al oxide

Al^{+++} - - - - $\begin{cases} OH^- \\ H_2O \end{cases}$

Al

H$_2$ + OH$^-$

H$_2$O

ϵ
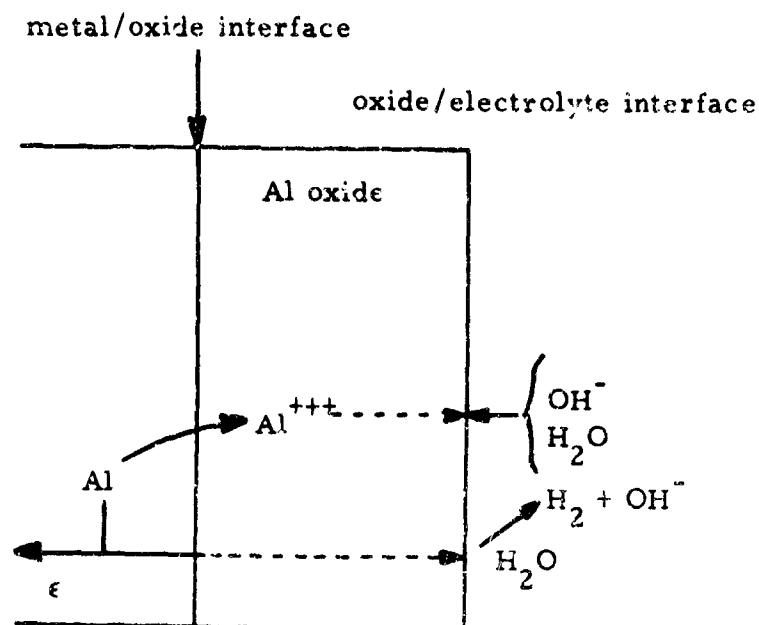
Schematic of Transfer of Aluminum Ion Through Oxide Layer

The processes are shown schematically - the aluminum ionizing at the metal/oxide interface, forming aluminum ions and releasing electrons into the metal. The aluminum ions travel across the adherent oxide layer because of the potential gradient which exists across this dielectric phase to the oxide/electrolyte interface where they form an adherent or non-adherent oxide layer in the presence of H_2O and OH$^-$ ions. The electrons released by the oxidation step can be removed through the metal phase to provide useable electrical energy or they can "leak" through electron-conducting paths in the adherent oxide layer to the oxide/electrolyte interface where they can discharge H_2O molecules forming H_2 gas and OH$^-$ ions as shown. Thus, a low electron-conductivity is very important in the oxide layer since it controls this "leakage" current and, therefore, H_2 evolution. The Clin alloys containing a homo-geneous dispersion of Sn^{++++} in the adherent oxide layer though increasing cation (Al^{+++}) transport, apparently do not increase the electron-transport, thus providing a "semi-passive" state - an oxide which permits the anodic process to occur while limiting the undesirable cathodic process (H_2 evolution).

In spite of this progress, however, the alloys do not provide a complete answer to H_2 evolution and irreversibility which will be shown in the following sections to be limiting factors.

8

a. Selection of Electrolytes

One of the goals of the program was to provide a battery capable of retaining >90% of its ampere-hour capacity after six months storage at 120°F. For high energy density batteries, this can only be achieved by using the reserve concept. A further requirement is start-up at temperatures as low as -35°F; this requires an electrolyte which is liquid at this temperature.

For batteries using oxygen-depolarized cathodes, the optimum electrolyte is potassium hydroxide. The electrochemical reduction of oxygen in potassium hydroxide proceeds more efficiently in potassium hydroxide than in any other electrolyte studied. All concentrations of potassium hydroxide between 25.5 and 39.7% are liquid at -35°F; the specific conductivity is high; there are several lightweight plastics that can be used as materials of construction in potassium hydroxide and can be considered as battery construction materials.

If the anodes oxidize to the hydroxide form, water must be supplied from the electrolyte. However, because of the high solubility of KOH, which is increased as the battery temperature increases during discharge, the electrolyte can become more concentrated and still remain liquid.

In chloride electrolytes, more water is needed for form soluble sales, e.g., $AlCl_3$ and $6H_2O$, $MgCl_2 \cdot 6H_2O$ than in the KOH solutions. Further, the conductivity of chloride electrolytes is much lower than KOH. These two factors make chloride electrolytes less favored than KOH for high rate, high energy cells.

Properties of these electrolytes are compared in Table II.

b. Aluminum Anodes in Chloride Electrolytes

Figure 1 summarizes the data obtained with pure aluminum and the Olin aluminum alloys in KCl and $AlCl_3$ electrolytes. The behavior of the alloys was considerably superior to that of pure aluminum. The improvement of approximately 700 millivolts in the open circuit voltage, indicates considerably greater reversibility of the alloys compared with pure aluminum. The improvement in reversibility is a direct result of the addition of tin to the oxide layer.

While hydrogen evolution was improved over that observed with pure Al (it was estimated to be equivalent to passing a current of 5 ma/cm^2), it was still estimated to be too high because it would reduce Faradaic efficiency, but more importantly the formation of gas bubbles in the electrolyte at zero-G conditions would result in high impedance. It also generates waste heat and would introduce hydrogen into an oxygen atmosphere.

Table II.   Properties of Selected Electrolytes

Solution	EUTECTIC					SAT. SOL'N @ -35°F		
	Wt. %	Freezing Pt. °F	Sp. Cond. ohm⁻¹ cm⁻¹ @65°F	Boiling Pt. °F	Sp. Gravity @68°F	Wt. %	Sp. Cond. ohm⁻¹ cm⁻¹ @65°F	Sp. Gravity @68°F
$AlCl_3$	25.3	-67	0.115	222	1.21	27.4	0.11	1.23
$ZnCl_2$	51	-79.6	0.09	248	1.57	40	0.09	1.5
$MgCl_2$	21.6	-28.4	0.135	227.8	1.18	-	-	-
$CaCl_2$	22.8	-67	0.162	231.1	1.28	31.6	0.162	1.29
NH_4Cl	18.6	+3.6	0.30	219.7	1.05	-	-	-
NaCl	23.3	-5.95	0.17	224.4	1.17	-	-	-
KCl	19.75	+12.1	0.26	218.3	1.13	-	-	-
KOH	31	-86	0.54	237.2	1.25	25.5 / 39.7	0.54 / 0.44	1.21 / 1.40

10

Anode	Manufacturer	Electrolytes
✗ A159	Dow	2.5MKCl
⊙ MRLA6	Olin Mathieson	2.5 MKCl
▢ MRL12226	Olin Mathieson	25%/AlCl$_3$
△ MRLA6	Olin Mathieson	25%/AlCl$_3$

Ambient Temperature
Galvanostatic Test
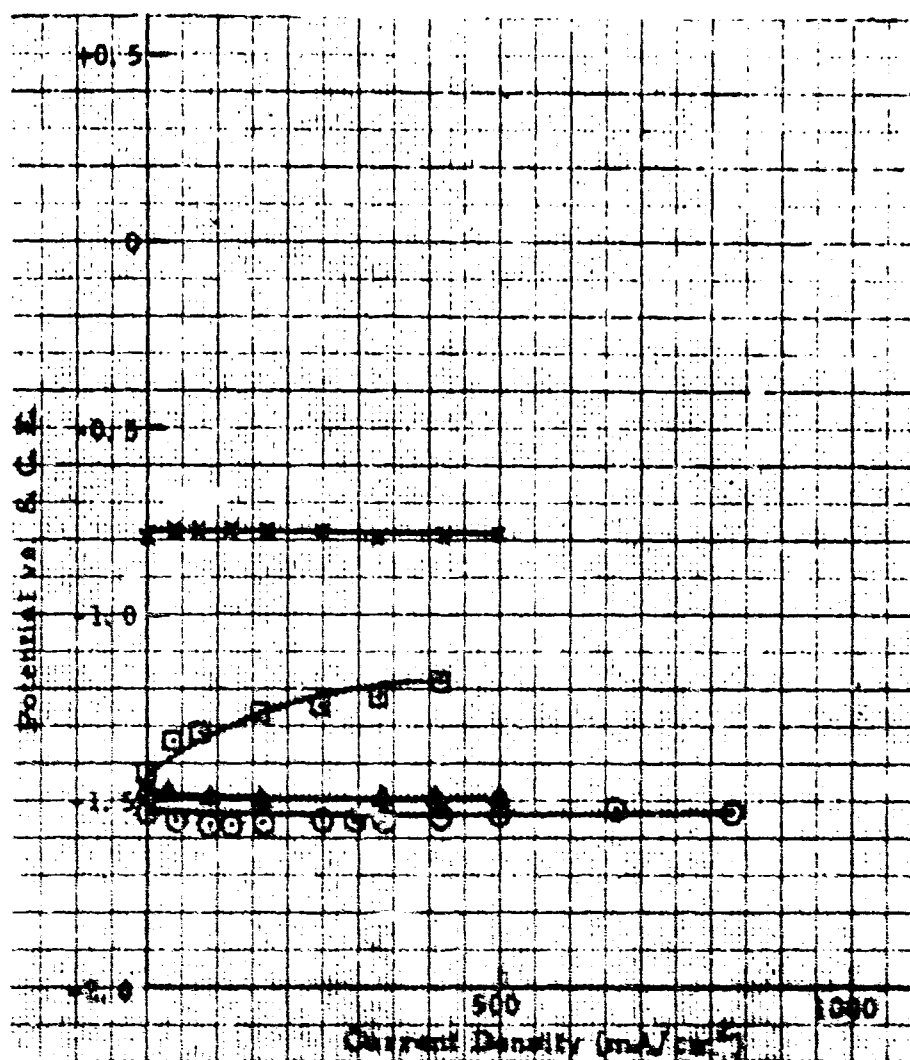
Figure 1.   Performance Data for Aluminum Anode in Chloride Electrolytes

11

In addition to Olin, other aluminum suppliers were asked to provide suitable anode materials for this program. Aluminum Company of America, (New Kensington, Pa. Research Laboratories) has developed an aluminum alloy for use in flashlight-type dry cells with a manganese dioxide depolarizer, which is described in patent numbers 2,796,456 and 2,838,591. These anodes are used in chloride electrolyte with a chromate inhibitor to provide a good wet shelf life. Samples of this electrode material, although developed by Alcoa for chloride electrolytes, were tested in 30(w)% KOH electrolyte. Considerable gassing was observed which was not reduced by the addition of a chromate inhibitor. On the other hand, there was no gassing observed when the aluminum chloride - ammonium chromate electrolyte was used. However, no current was obtained from such an aluminum/oxygen cell because of the low limiting current on oxygen electrode in this electrolyte. Previous experience with oxygen electrodes in aluminum chloride electrolyte had demonstrated limiting current densities up to $0 \, mA/cm^2$ could be obtained with an oxygen depolarized cathode. It is assumed that the addition of chromate to the electrolyte inhibited the reduction of oxygen. From these limited experiments it was concluded that Alcoa alloys M-372 and M-373 could not be used for this application.

c.   Studies of Aluminum Oxidation in KOH

A detailed investigation of the electrochemical behavior of aluminum in KOH was undertaken. It was hoped that this study would reveal the causes for the three main shortcomings of the presently available aluminum alloys, viz: gassing during discharge, high polarization from thermodynamically calculated reversible potential, and poor low temperature start-up. Three types of measurement have been employed to date; potentiostatic current/ voltage curve, galvanostatic charging curves and metallographic examination of the alloys and pure aluminum after polarization at different potentials. An important objective was to determine the relative contribution to overall inefficiency and heat generation of IR losses in the oxide film and activation polarization.

(1)   Experimental Methods

All electrochemical measurements were performed in the cell shown in Figure 2. This is a three-electrode system comprising a working electrode, counter electrode and reference electrode. A special holder was constructed for the working electrode which permits the use of small (0.5 cm^2) aluminum foil samples. The electrodes could be replaced rapidly and the area exposed to the electrolyte was clearly defined by the use of a close-fitting rubber gasket. Platinum gauze was used for the counter electrode. The reference electrode was mercury/mercury oxide. A Luggin capillary from the reference compartment was positioned close to the working electrode. Such arrangement allows the current/voltage characteristics of any test electrode to be determined free of interference from electrolyte resistance and the

12
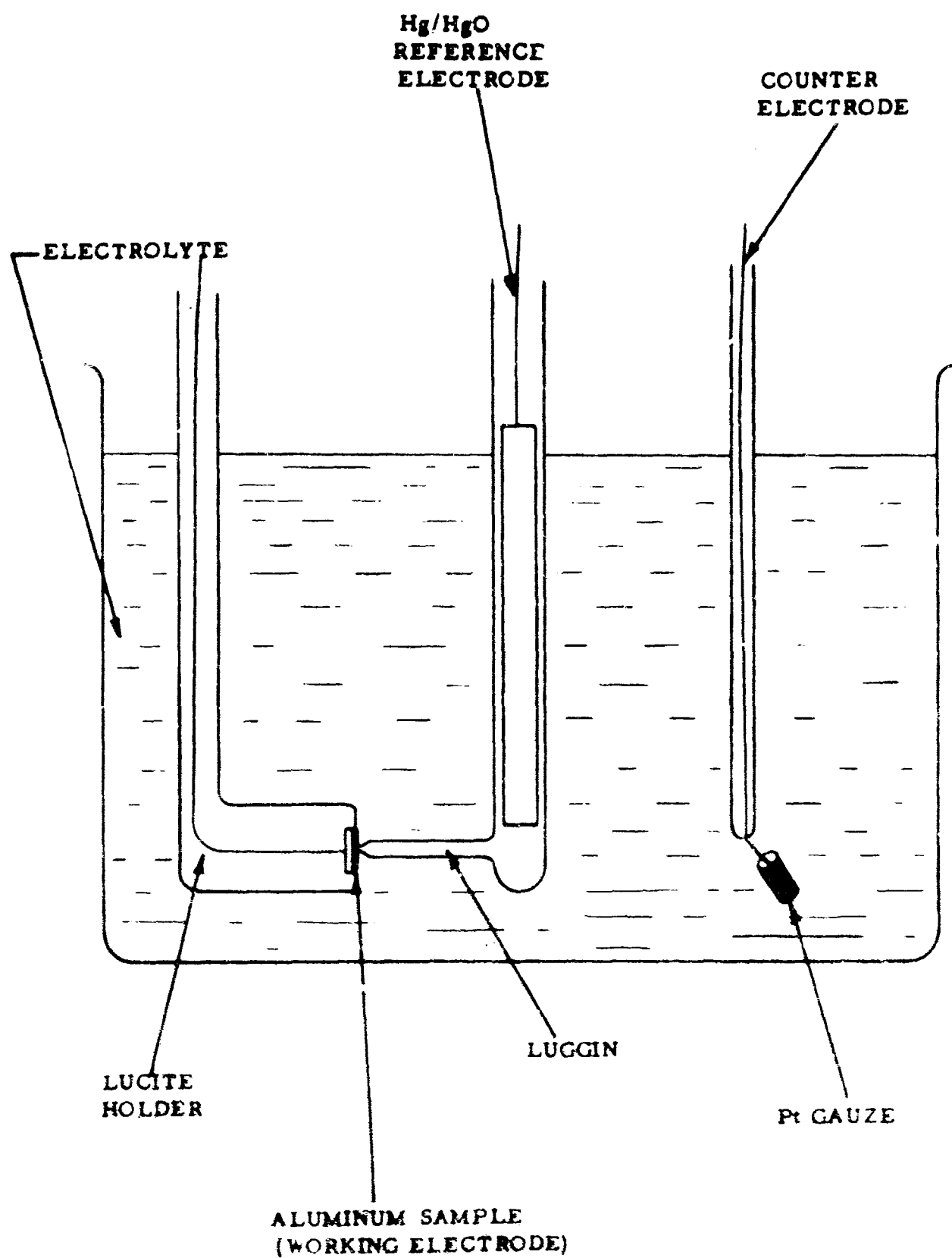
Figure 2.   Experimental Test Cell

13

polarization behavior of a counter electrode. A Wenking potentiostat was used for the controlled potential studies. Potentials were measured using a high impedance differential voltmeter (John Fluke Manufacturing Company), and a Tektronix oscilloscope was employed for the recording of charging curves and transient current/time characteristics.

All measurements were made in 30(w)% KOH. The following electrode materials were tested:

(a)	pure aluminum	99.9%
(b)	pure aluminum	99.999%
(c)	Olin alloy	A6
(d)	Olin alloy	12226
(e)	Olin alloy	12228
(f)	Olin alloy	44835
(g)	Olin alloy	44836
(h)	Olin alloy	13166
(i)	Alcoa alloy	M-372
(j)	Alcoa alloy	M-373
(k)	Alcoa alloy	CB-75-T4
(l)	Clevite alloy (14% porous)	102965

(2) Current Voltage Curves

Potentiostatic current/voltage curves for the above materials are shown in Figures 3 through 7. Olin alloy 44836 gave the best performance in terms of both high anodic currents and most negative OCV. This finding represents a marked improvement over the performance of pure aluminum. However, the Olin alloy 12226 gave the lowest gassing rate during discharge. The overvoltage of 44836 exceeded that of high purity (99.999%) aluminum which is indicative of the role of the oxide layer in governing the hydrogen evolution process at aluminum since in the absence of an oxide layer the addition of heavy metal "impurities" would normally be expected to lower the hydrogen overvoltage. A notable feature in both the Olin alloys and the pure aluminum was the occurrence of current oscillations. The nature (amplitude and frequency) and potential region in which oscillations were found varied for the different materials. Thus, in the case of the 12226 alloys, oscillations occurred between -1.0V and -1.2V vs. Hg/HgO. Whereas, for pure aluminum (99.9%) they were found between +1.6V and +1.8V vs. Hg/HgO. No oscillations were found for 99.999% Al. Oscillations were very regular for the 12226 alloy as shown in Figure 4, but for the 44835 and 44836 they were irregular and no definite structure was apparent. The occurrence of

Figure 5. Potentiostatic Current-Voltage Curve

Current Density (mA/cm²)

Volts vs. Hg/HgO

+600
+400
+200
0
-200
-400
-600

-2.0
-1.6
-1.2
-0.8
-0.4
+0.4
+0.8
+1.2
+1.6
+2.0

99.999% Pure Al
Olin Alloy A6
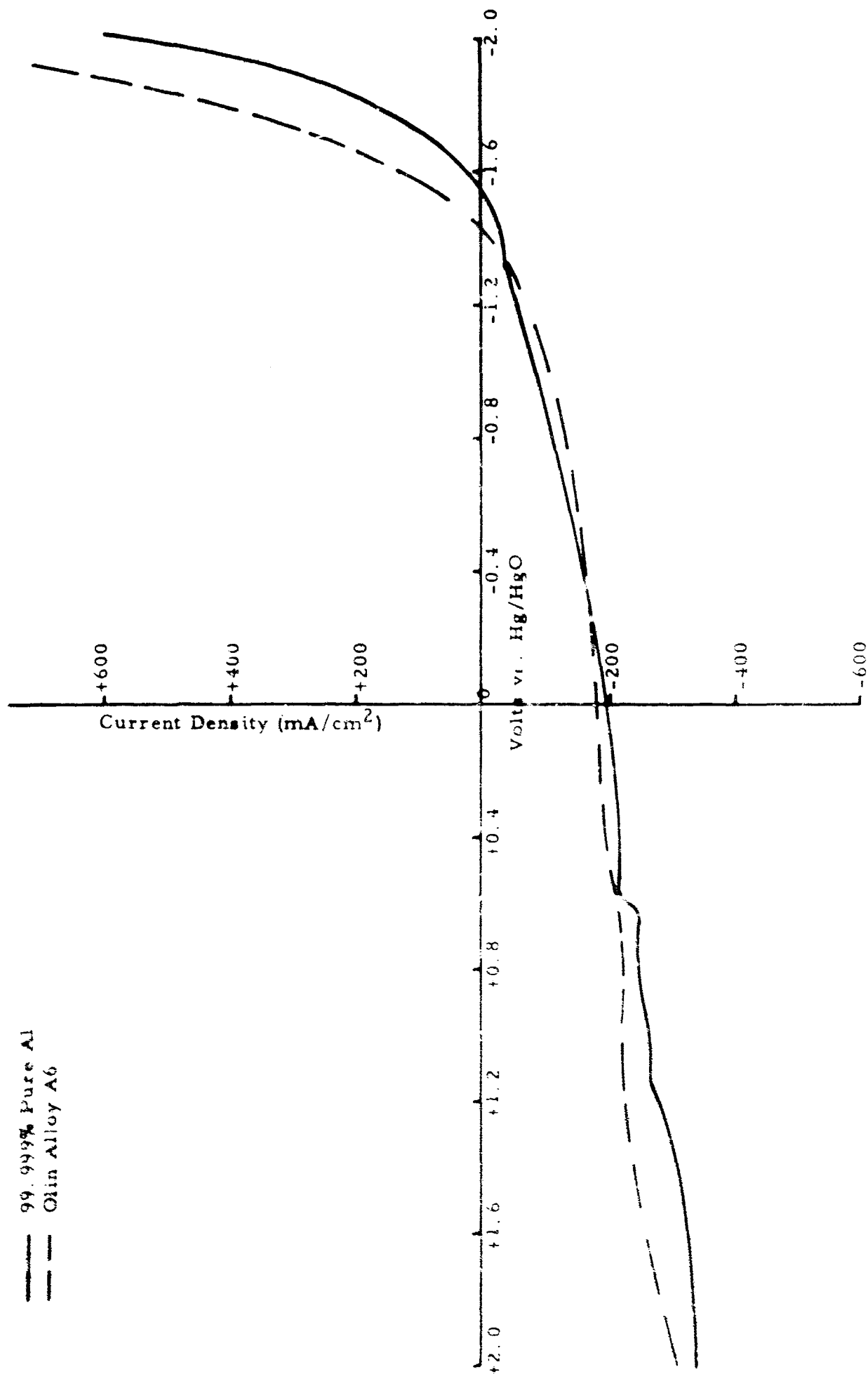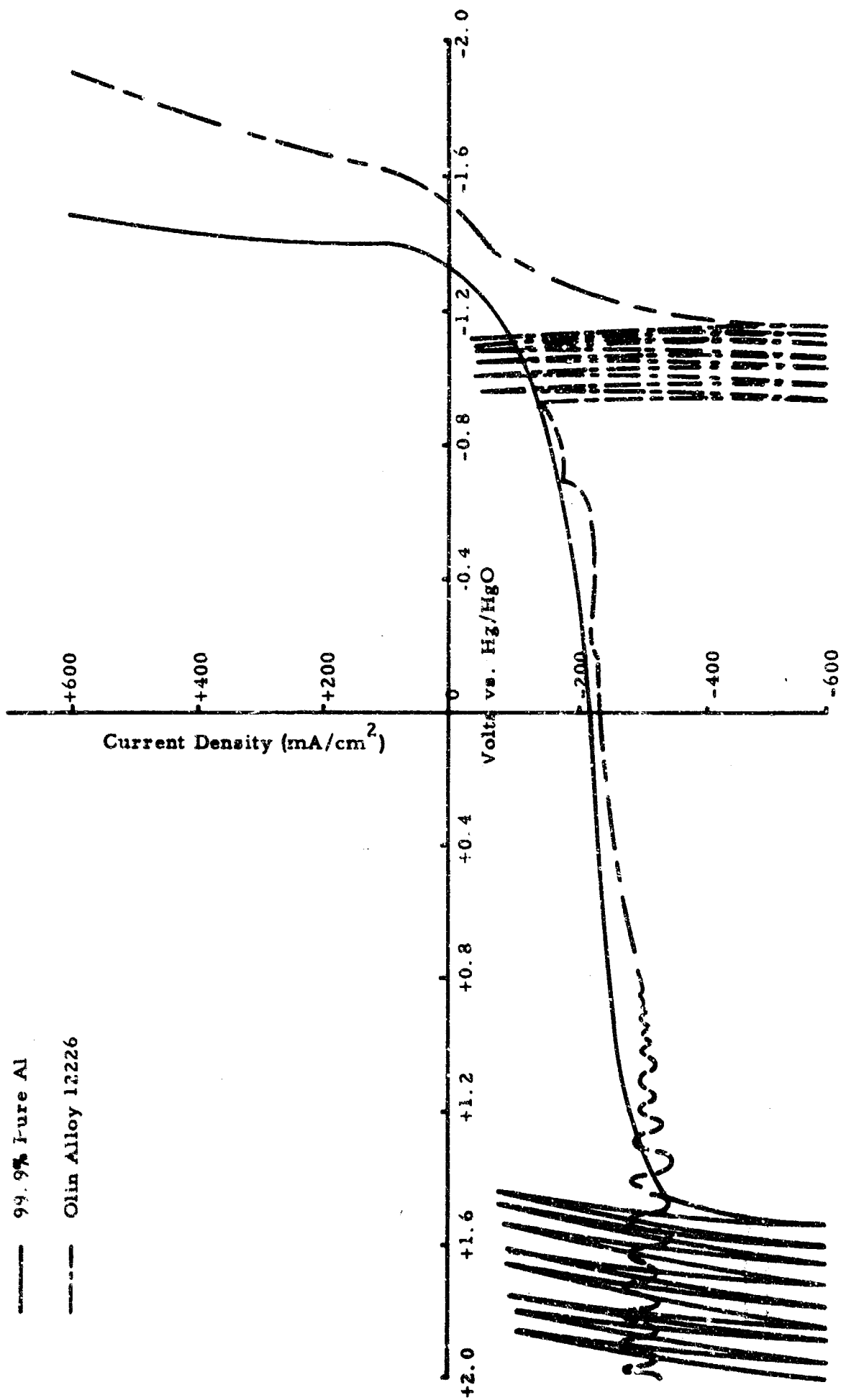
Figure 4. Potentiostatic Current-Voltage Curves

99.9% Pure Al

Olin Alloy 12226

Figure 5.   Potentiostatic Current-Voltage Curves

Current Density (mA/cm²)

Volts vs. Hg/HgO

——— Olin Alloy 44836

— — — Olin Alloy 44835

17
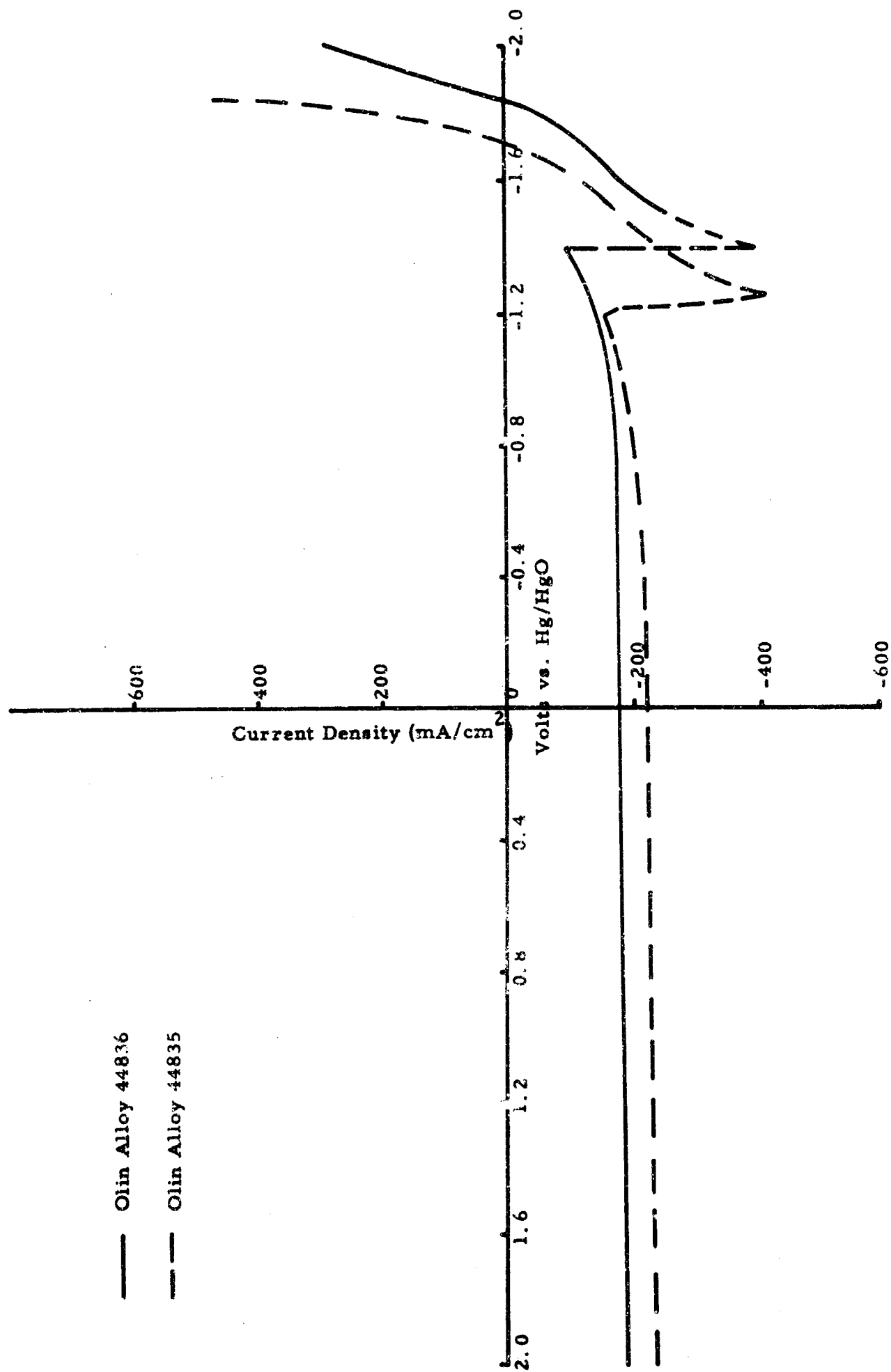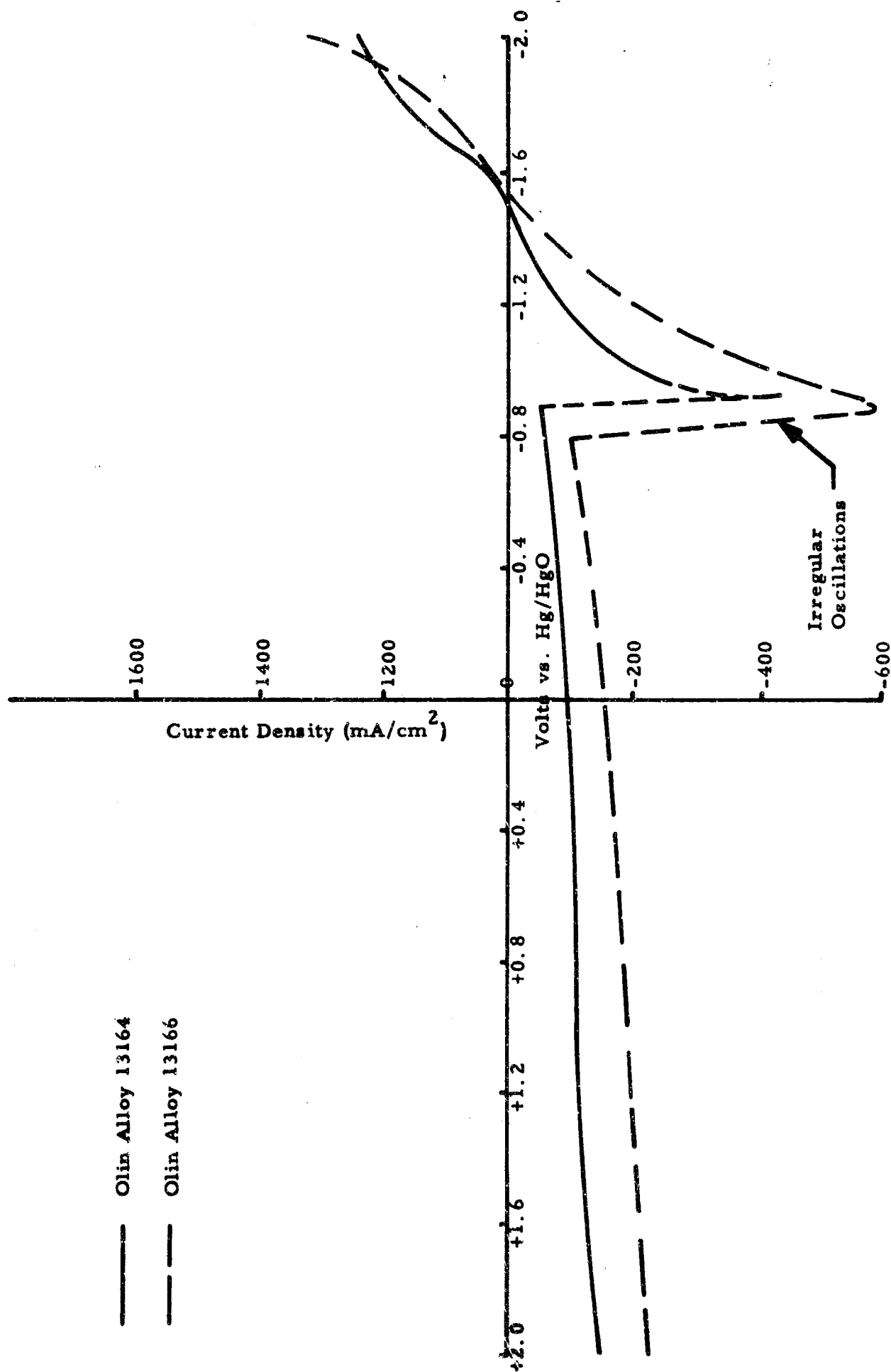
Figure 6.   Potentiostatic Current-Voltage Curve

Olin Alloy 13164
Olin Alloy 13166

Irregular
Oscillations

Current Density (mA/cm^2)

Volts vs. Hg/HgO

18
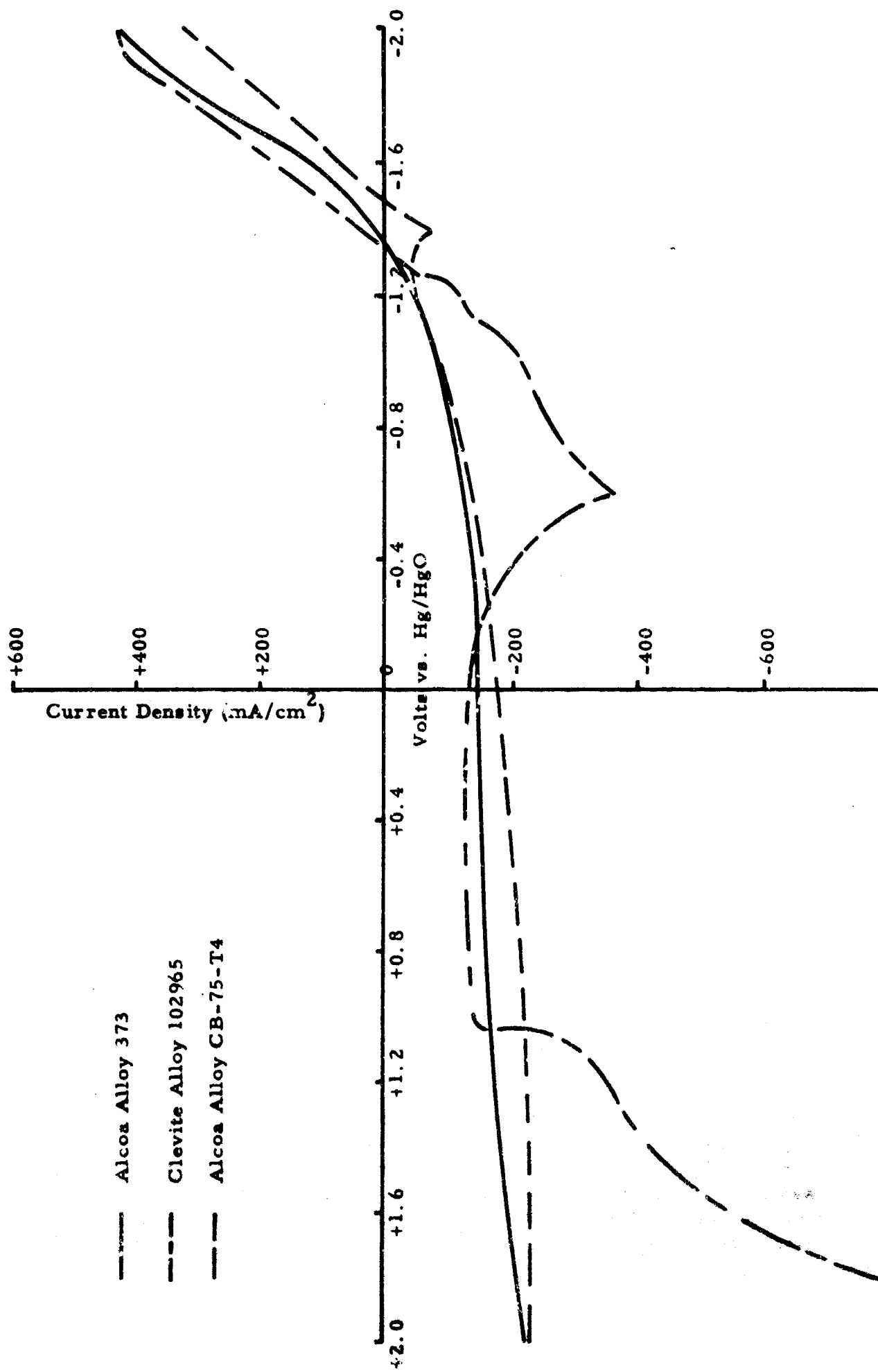
Figure 7.   Potentiostatic Current-Voltage Curves

Current Density (mA/cm^2)

Volts vs. Hg/HgO

+600 +400 +200 0 -200 -400 -600

+2.0 +1.6 +1.2 +0.8 +0.4 0 -0.4 -0.8 -1.2 -1.6 -2.0

——— Alcoa Alloy 373

– – – Clevite Alloy 102965

— — Alcoa Alloy CB-75-T4

19

such oscillations is characteristic of the formation and dissolution of passive films and has been reported in other systems. The dissolution process apparently occurs via a different mechanism on whether the potential is anodic or cathodic to the oscillation region. This was clearly revealed by metallographic examination of the samples. At anodic potentials, dissolution takes place preferentially along grain boundaries and results in the formation of deep troughs. This is described in further detail below.

The effect of adding chloride ion to the KOH electrolyte was briefly investigated since it had been found earlier certain Olin alloys performed better in chloride electrolyte. The current/voltage behavior was only slightly changed by additions up to $10^{-2}M$ of KCl.

The effect of stirring the electrolyte was also investigated in order to determine whether the rate limiting step in any way was associated with mass transport of reaction products away from the electrode/electrolyte interface. The only effect was to lower the current slightly in the hydrogen evolution region and to increase the current at very anodic potentials.

(3) Metallographic Studies

Three samples were subjected to a careful metallographic analysis; (1) 99.999% Al, (2) Olin alloy 12226, and (3) Olin alloy 44836. The electrodes were held potentiostatically at different potentials in the range -2 volts to +2 volts vs. Hg/HgO for 25 minutes. They were then removed from solution and photographed at a magnification of 30 times. Figures 8, 9, and 10 show photographs for the three materials respectively after polarization at three potentials; (a) in the hydrogen evolution region where the net current is cathodic (c. -1800 mV), (b) in the region of the initial rise in anodic current (c. -1400 mV) (prior to the oscillation region in case of the alloys), and (c) at an anodic potential (c. -1000 mV).

Noticeable differences and trends can be seen from these photographs. Grain boundaries were very distinct in the case of the alloys, whereas none at all were visible for pure aluminum. In the case of alloy number 44836, dissolution occurs at potentials cathodic to the open circuit value where the net current is cathodic. This was found at potentials down to -2 volts and indicates that this particular alloy is intrinsically more active than apparent from the current/voltage curve. This finding would clearly take on more significance if it were found possible to inhibit hydrogen evolution at such cathodic potentials since it clearly indicates that oxidation is occurring at potentials closer to the reversible potential. At potentials cathodic to the oscillation region, dissolution occurred preferentially along grain boundaries. This was particularly true for alloy 44836 at -1.8 volt where scarcely any dissolution was apparent on the surface of the grains. In particular, the potentiostatic studies indicate that aluminum oxidation can occur in KOH at potentials nearer to the reversible Al/Al^{+++} couple. This occurs specifically in the

20
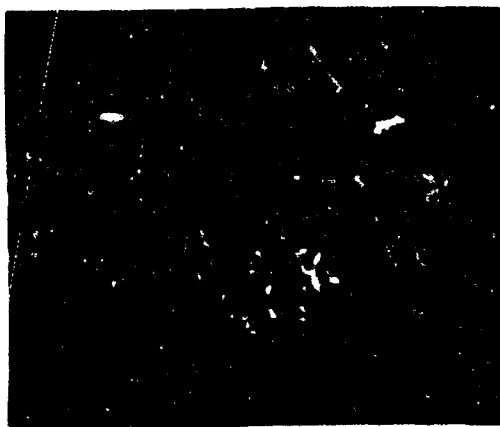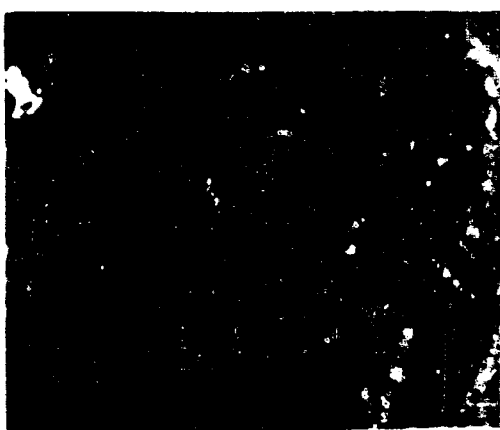
— 2.0 VOLTS

— 1.5 VOLTS
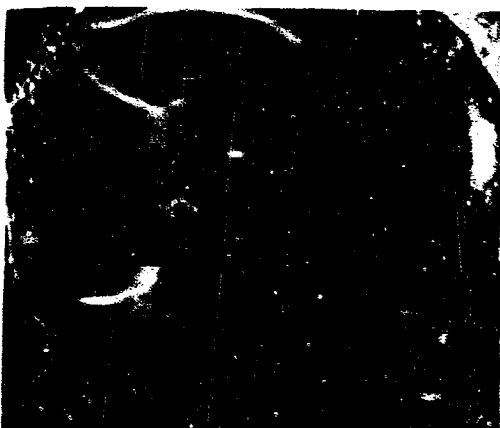
— 0.0 VOLT

FIGURE 8. PHOTOMICROGRAPHS OF 99.999 % PURE ALUMINUM AFTER POLARIZATION AT DIFFERENT POTENTIALS FOR 25 MINUTES. (MAG 8X).

21
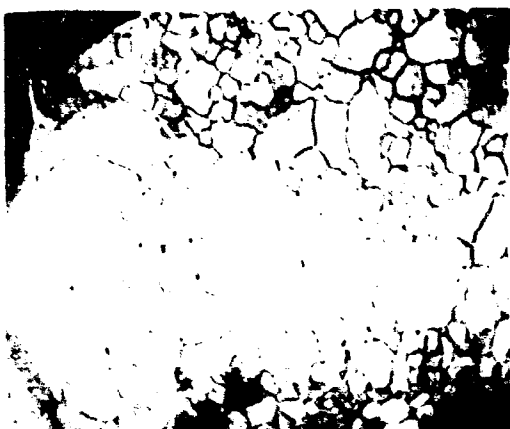
— 1.8 VOLTS

— 1.6 VOLTS
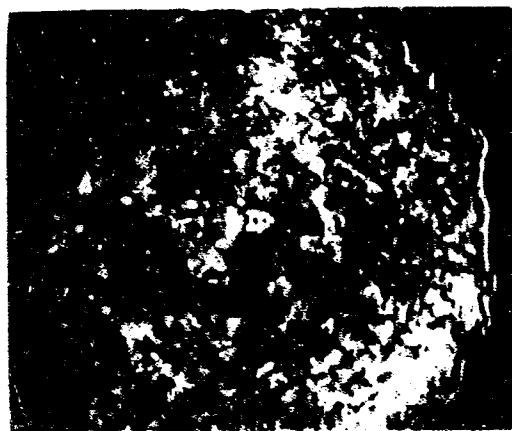
— 1.0 VOLT

FIGURE 9. PHOTOMICROGRAPHS OF OLIN MATHIESON ALLOY #12226 AFTER
POLARIZATION AT DIFFERENT POTENTIALS FOR 25 MINUTES. (MAG 8X)

— 1.8 VOLTS
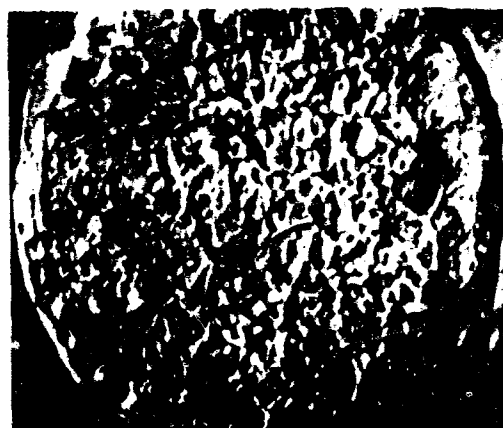
— 1.25 VOLTS
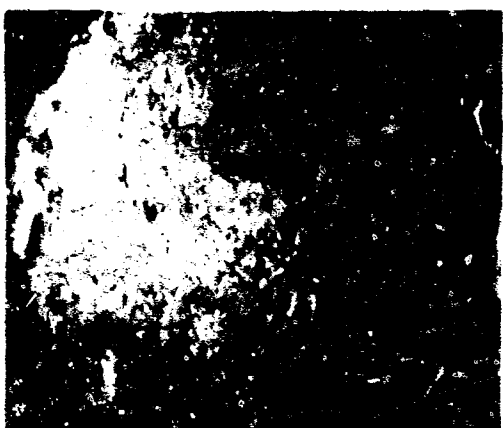
— 1.0 VOLT

FIGURE 10. PHOTOMICROGRAPHS OF OLIN MATHIESON ALLOY #44036 AFTER
POLARIZATION AT DIFFERENT POTENTIALS FOR 25 MINUTES. (MAG 8X).

23

grain boundary regions of Olin alloy 44836 where presumably the oxide layer is less passive and permits the anodic process to occur at these more negative potentials. Operation of an aluminum anode at these potentials with the elimination of gassing would provide significantly improved cell performance. At potentials anodic to the oscillation region, dissolution was even over the entire surface. For pure aluminum, of course, dissolution was fairly even over the entire potential range. Figure 11 shows a photograph of a 44836 sample which was polarized in the oscillation region. The two different types of attack were seen to take place simultaneously. The occurrence of preferential etching along grain boundaries is probably related to two factors; firstly, the different properties of the oxide layer on alternate sides of the oscillation region, and secondly, local cell action along grain boundaries where both hydrogen evolution and anodic dissolution would be expected to proceed most readily. Figure 12 shows a cross section of alloy 44836. This was cut from the sample shown in Figure 9a and serves to illustrate the depth of etching.

The results to date, although they do not provide any conclusive understanding of the mechanism of aluminum oxidation are nevertheless felt to be of value in that recognizable trends in behavior are identifiable.

In summary, it was shown that the Olin alloys, especially alloy number 44836, was superior to pure aluminum with respect to both reversibility and polarization. Alloy number 44836 was corroding at -2 volt vs. Hg/HgO, even though a cathodic current had to be passed in order to maintain this potential. If this improvement in the reversibility of these electrodes could be coupled with an increase in hydrogen overvoltage, Olin alloy 44836 would become a very useful electrode for primary aluminum/oxygen cells. Unfortunately, no adequate method was found during this program that would increase the overvoltage of hydrogen sufficiently.

3. 2 LOW TEMPERATURE PERFORMANCE

It is one of the requirements that the battery be capable of starting up at -35°F. Three electrode types were tested at that temperature - porous zinc,[1] sheet zinc and sheet aluminum alloy. Porous zinc yielded adequately high current densities as shown in Table III.

----

[1]LML ZA/20AH

FIGURE 11   PHOTOMICROGRAPH OF OLIN MATHIESON ALLOY #44836 POLARIZED
(IN THE REGION OF OSCILLATION) FOR 25 MINUTES.
(MAG 30X).   25

FIGURE 12. CROSS SECTION PHOTOMICROGRAPH OF OLIN MATHIESON #44836 ALLOY POLARIZED AT 1.8 VOLTS FOR 25 MINUTES. (MAG 30X).

26

Table III.   Temperature Dependence of Zn Anode

Temperature °F	Current Obtained at ~ -1300 mV versus Hg/HgO in 30% KOH
-35	160 mA/cm^2
+10	330 mA/cm^2
+77	420 mA/cm^2

Neither sheet zinc nor sheet aluminum alloy yielded anodic current at -35°F. On the other hand, it was shown above that porous zinc did perform at that low temperature. This implies that the poor low temperature performance of aluminum alloys might be overcome if porous electrodes were used instead of sheet metal.

3. 3   OXYGEN CATHODES

The oxygen depolarized cathodes used for the battery development were previously developed as fuel cell electrodes at LML. These cathodes contain Teflon-bonded platinum black catalyst and an expanded nickel current collector. Performance of these cathodes is shown in Figure 13. It can be seen from the above figure that the greatest shortcoming of the oxygen electrode is activation polarization (in the low current density region). In the higher current density region, the polarization curve is quite flat. One of the requirements of the original program was that the 1000 volt battery must vary no more than 10% in voltage from open circuit to full load. This seriously limits the maximum current density at which oxygen cathodes can be used. No catalyst is known which eliminates the form of O_2 electrode polarization at ambient or low temperatures.

Additional data for this project was needed on the low temperature behavior of the oxygen depolarized cathode. Experiments with the oxygen electrode were performed in a low temperature environmental chamber manufactured by the Tenney Engineering Company. As expected, the polarization of the oxygen electrode decreased with increasing temperature. For example, at 100 mA/cm^2 current density, the following temperature/polarization characteristics were observed. The voltages quoted are versus the Hg/HgO reference electrode.
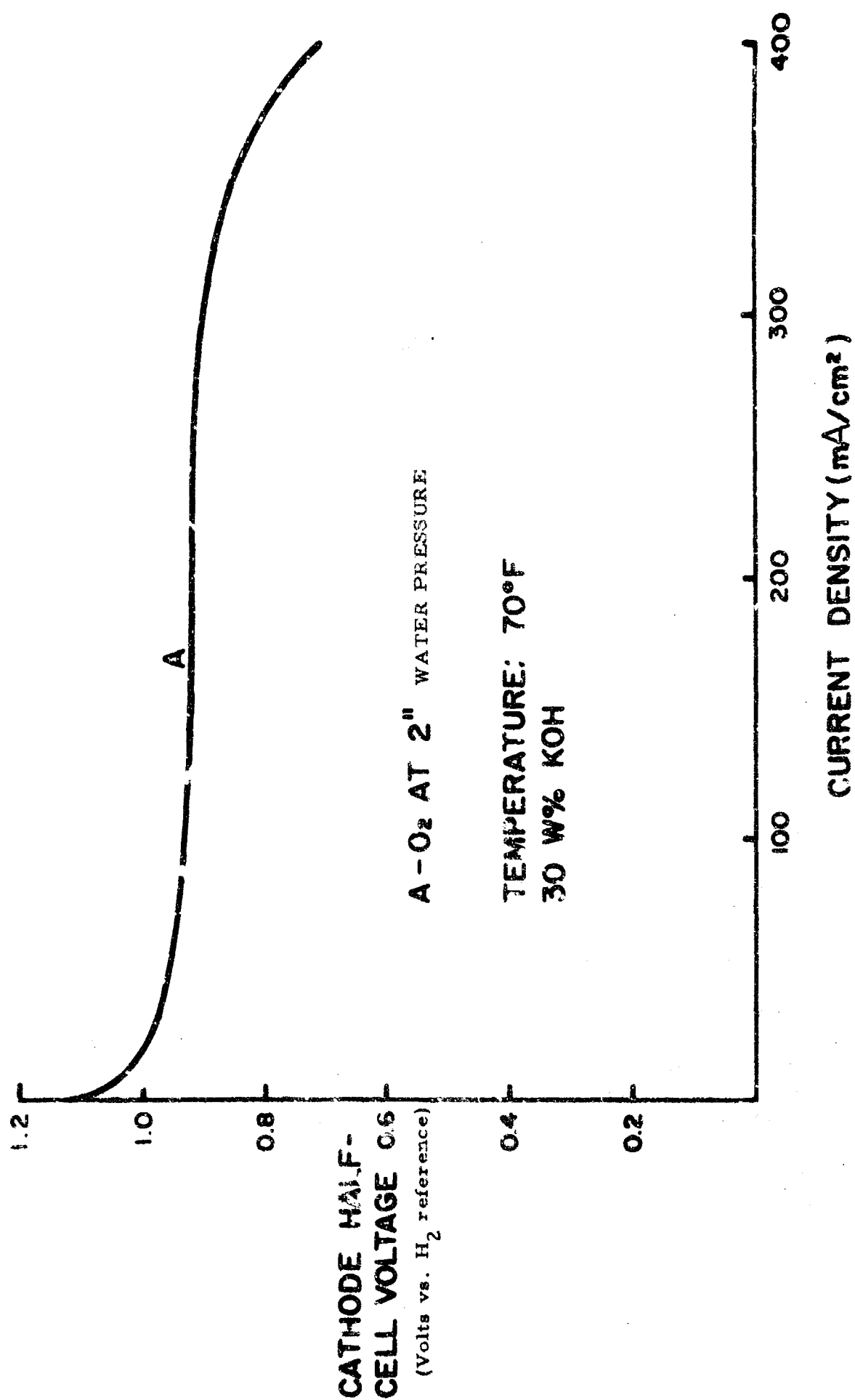
Figure 13. Electrochemical Performance of LML Oxygen Cathode (Type 7Tf/N/Pt)

CATHODE HALF-
CELL VOLTAGE
(Volts vs. H₂ reference)

A - O₂ AT 2" WATER PRESSURE

TEMPERATURE: 70°F
30 W% KOH

CURRENT DENSITY (mA/cm²)

28

Temperature $^{\circ}F$	Potential vs. Hg/HgO at 100 mA/cm^2 Current Density
-35	-0.47
-15	-0.25
+15	-0.215
+50	-0.150
+77	-0.08

In order to minimize the weight of the battery, lighter weight current collectors were needed. The criteria for the selection of the current collector is the following: (a) it has to be inert with respect to the electrolyte and (b) it has to have the highest possible ratio of specific conductivity to specific gravity. Titanium metal fits the above specification well.

A special titanium alloy was purchased to substitute for nickel current collectors. This alloy contained 0.15% palladium, and was supplied in the expanded metal form.

Titanium, as is well known, develops a passive oxide layer at the potential of the oxygen electrode which would preclude its use. However, by electrodepositing small quantity of noble metal on the surface of the titanium, this passivation can be eliminated. Current collectors made from titanium expanded metal were palladium plated and fabricated into diffusion electrodes. The electrochemical characteristics, i.e., polarization, of these oxygen cathodes was identical to those containing nickel expanded metal current collectors.

3.4 CHLORINE DEPOLARIZED CATHODES

When it was realized that the irreversibility of the oxygen cathode is a limitation, the possibility of using chlorine as a depolarizer was investigated briefly. Chlorine has certain inherent disadvantages; for example, its boiling point at one atmosphere is -30.5$^{\circ}F$, which is above the -35$^{\circ}F$ required start-up temperature. Nevertheless, it was felt that if a reversible chlorine electrode could be developed, it would have a significant advantage in terms of lower heat dissipation, the latent heat of vaporization and the smaller storage volume needed for liquid chlorine.

Previously, porous carbon electrodes were used for chlorine depolarized cathodes but for the present application these electrodes would be too heavy. Furthermore, the porous carbon electrodes could not sustain the high current drains that were anticipated in this application. The same platinum black/Teflon cathodes that were used with the oxygen depolarizer were modified by incorporating a Pt screen current collector.

29

In a neutral KCl electrolyte, these electrodes indeed did show apparent reversibility. This can be seen on Figure 14. The data shown were recorded immediately after the electrode was assembled into the testing rig. It was noted that polarization decayed at constant current and that it was time-dependent. Subsequent galvanostatic studies showed that the initial polarization characteristics were probably due to the formation of an unstable chloride intermediate which had been formed prior to the electrochemical test. Thus, the electrode was not behaving as true chlorine electrode and it was apparent that a much longer and detailed study would be needed. This was not within the scope of the project and, hence, the use of a chlorine depolarized electrode was abandoned.

Ambient Temperature
KCl Electrolyte
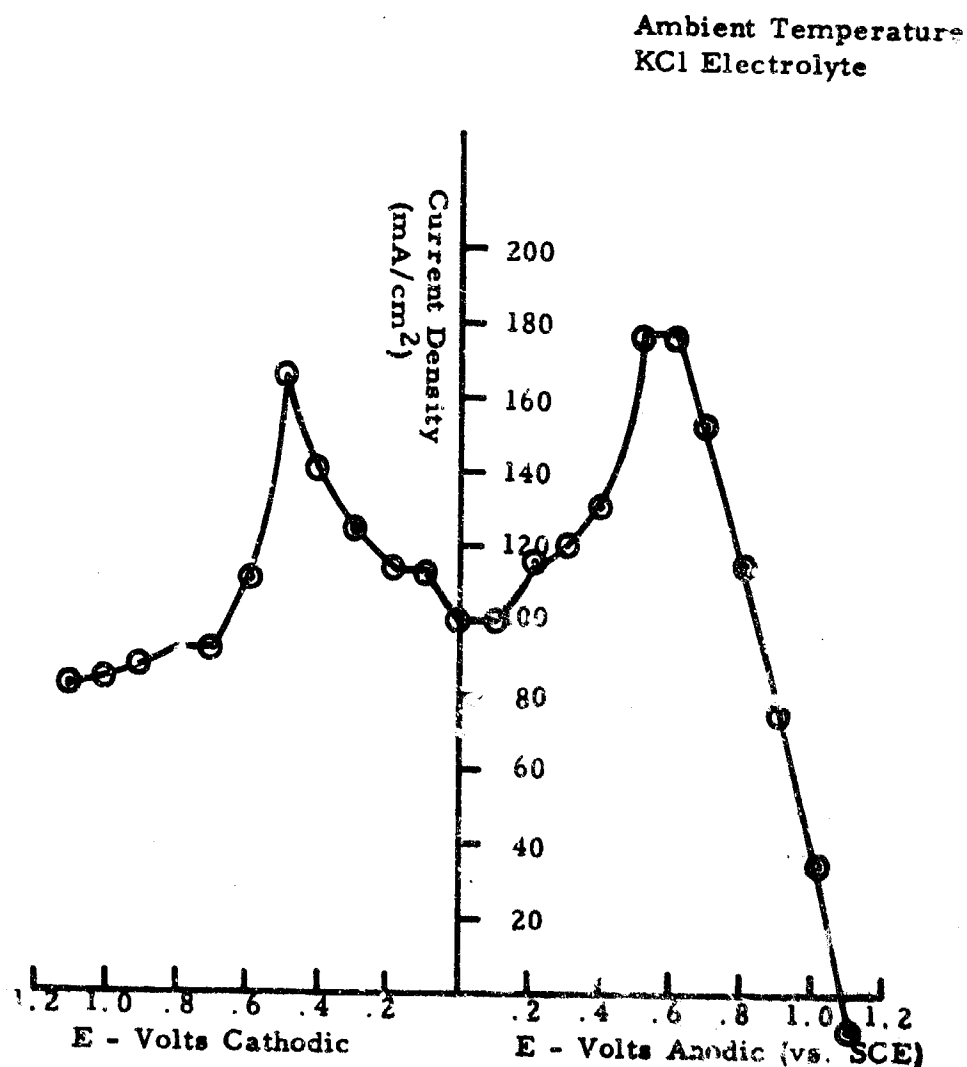
Figure 14.   Representative Potentiostatic Current Voltage
Curve for Chloride Depolarized Anode

SECTION IV

CELL DEVELOPMENT

4.1 BATTERY DESIGN CONCEPT

Although the first phase of the developmental program called for the development of single cells only, a later goal of long term storage life required that the cells to be developed would have to be used in a reserve battery. The conventional reserve approach - injecting the electrolyte into the cells - was the mode decided on. Other schemes, such as inserting the anode into the electrolyte, were also considered but the reliability of such a system using a multiplicity of very thin anodes and narrow electrolyte spacings was considered to be low.

As shown on the accompanying sketch, Figure 15, a battery was visualized, consisting of a number of cells in which the anodes are surrounded on two sides by the cathodes and each cell is separated from the adjacent cell by a woven plastic mesh. The use of two cathodes for each anode permitted the use of half the number of gas spaces. The electrolyte was to be injected from a common manifold after activation. The activation scheme is shown on Figure 16. Unlike conventional activating systems, there is no need for a squib; high pressure oxygen in the storage tank will inject the electrolyte into the cells.

Single cells of the type conceived for the electrolyte injection battery were constructed in the 3.5" x 5" size. Standard LML 7TF/N/Pt cathodes with nickel grid current collector were used, containing approximately 5 mg/cm^2 of Engelhard platinum black. The cells were tested with both zinc and aluminum anodes.

a. Zinc/Oxygen Cells

In order to verify the cell design with anodes having well established electrochemical behavior, several of these cells were studied with zinc anodes. Zinc anodes with silver grid current collector were manufactured in the thickness of approximately 0.010". The anodes had a porosity between 50 and 70%. The separator paper used in these cells was 0.003" thick unplasticized fibrous cellulose membrane manufactured by Union Carbide Food Products Division. The electrolyte was contained partly in this separator and partly in the pores of the zinc anodes.

The discharge of zinc/oxygen cells at various current densities is shown in Figures 17 and 18. At 50 mA/cm^2 the potential is steady; at 100 and 150 mA/cm^2 the voltage increased with time because of increasing temperature: the effect was more pronounced at 150 mA/cm^2. No

ELECTROLYTE MANIFOLD

INTERCELL SEPARATORS

CATHODES

ANODES

ELECTROLYTE INLET

PRESSURE BOUNDARY

O_2 INLET

Figure 15. High-Rate Battery Conceptual Design

32
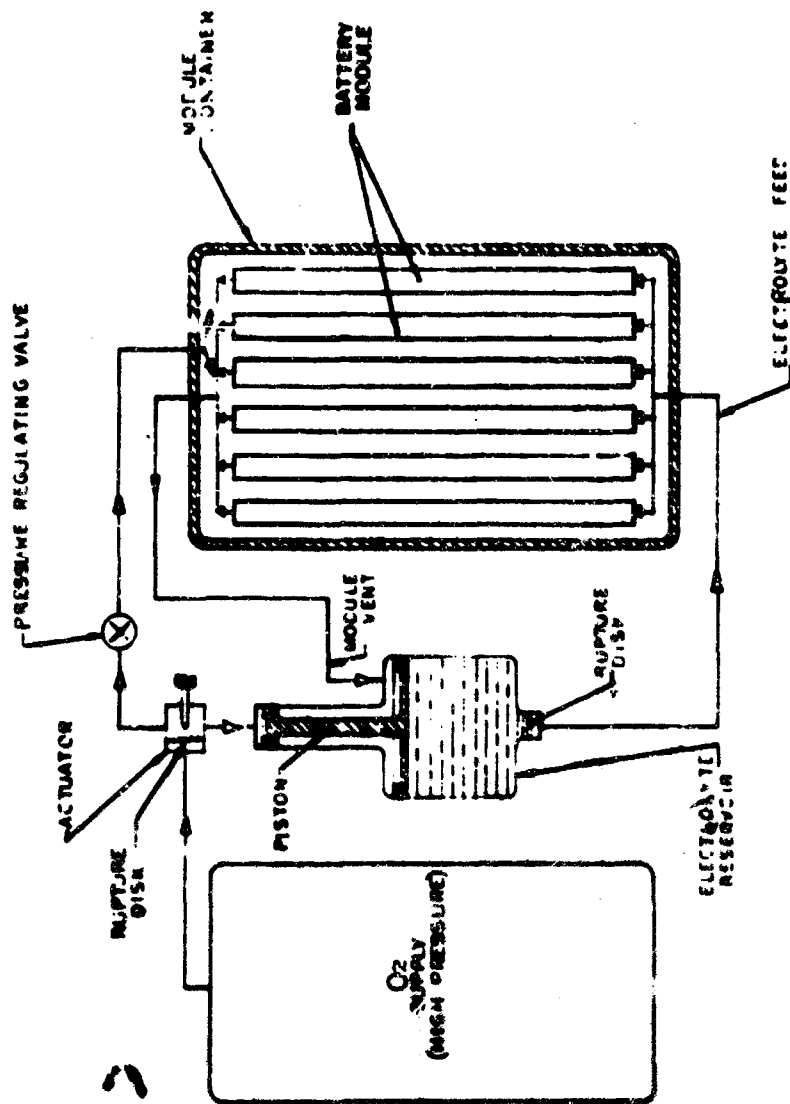
Figure 16.   Metal/O$_2$ Battery Activation System Schematic
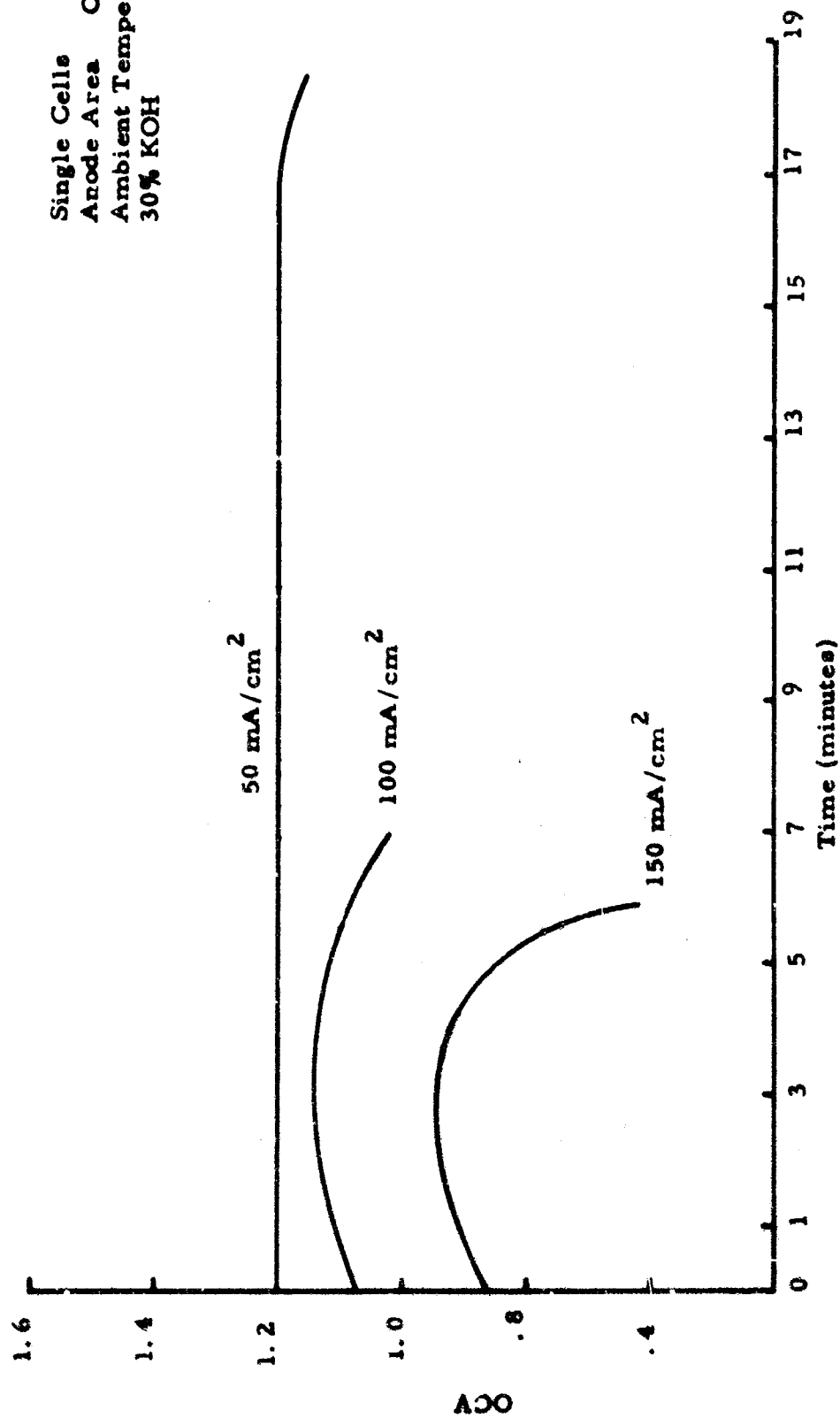
Figure 17. Discharge Voltage vs. Time (Zn/O₂ cell)

Single Cells
Anode Area   Cathode Area
Ambient Temperature
30% KOH

50 mA/cm²

100 mA/cm²

150 mA/cm²

Time (minutes)

OCV

34

3-Cell Battery No. 2
30% KOH
Ambient Temperature
Oxidant O_2 100%

OCV 4.154

100 mA/cm^2

Time (minutes)
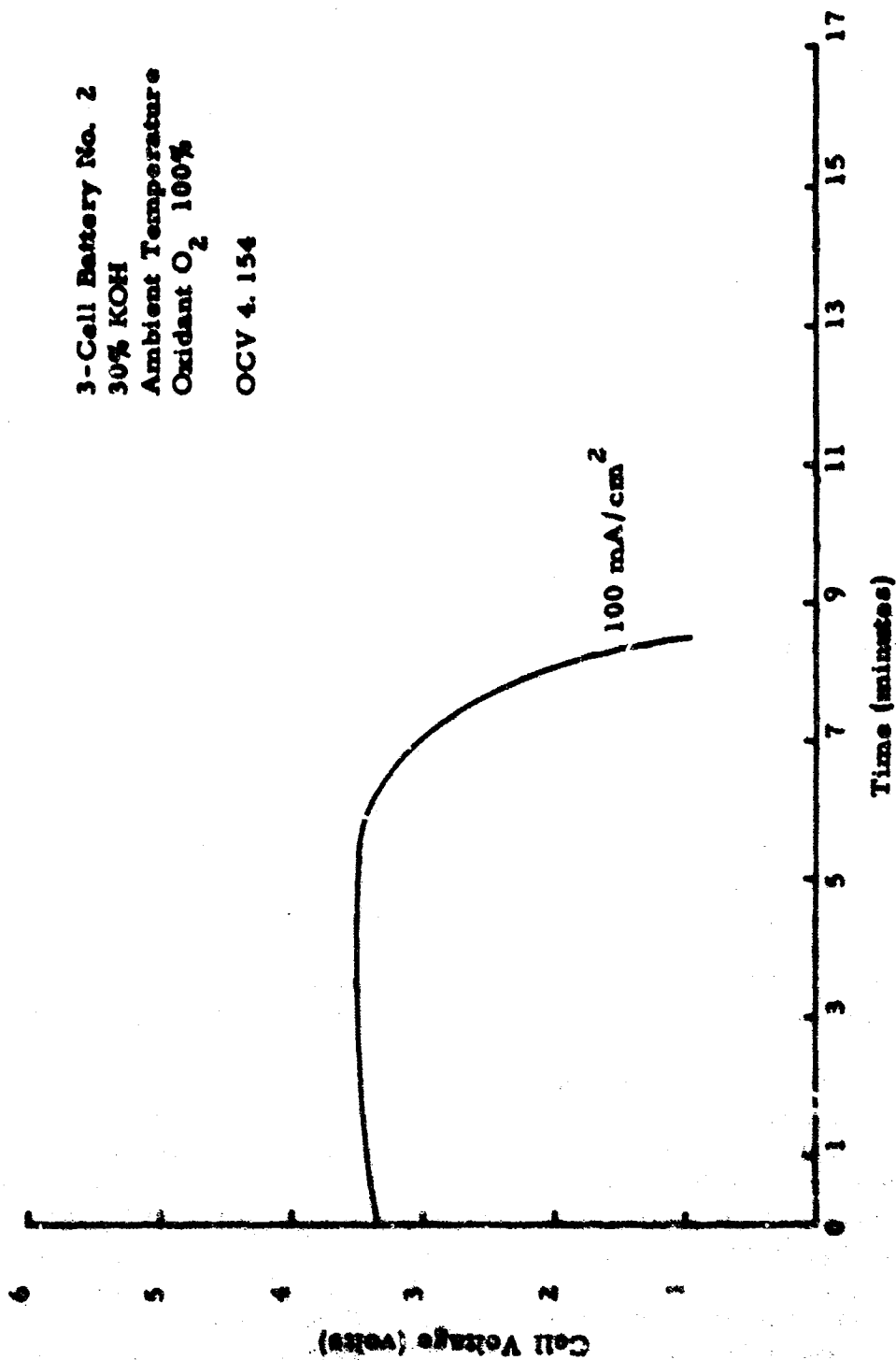
Cell Voltage (volts)

Figure 18. Discharge Voltage vs. Time (Zn/O_2 3-cell Stack)

35

precautions were taken in these experiments to limit convection in the oxygen, thus the amount of heat removed from the cells by this process was not known. This process could not, of course, contribute to heat transfer under zero-G conditions.

To test the reproducibility of the cell performance and to observe the operation of the multiple cell stack, a three-cell unit was discharged at a current density of 100 mA/cm². The three cells were connected in series and separated from each other by a 1/16" thick woven nylon screen. The voltage vs. time relationship of this unit is shown in Figure 18. The recorded voltage was approximately three times that of a single cell discharged at the same current density and the voltage vs. time dependence is very similar. There appeared to be no major problem in individual cell reproducibility and no major interaction in small stacks of cells.

b. Aluminum/Oxygen Cells

As reported earlier, a major problem with aluminum anodes is the evolution of hydrogen, particularly on open circuit stand. As a result, cells could not be tested in the same manner as the zinc/oxygen cells. It was found that when the aluminum anode sheets were separated from the cathodes by an unplasticized cellulose separator (as in the zinc/oxygen cells), the anode gassing separated the cellulose sheet from contact with the aluminum and the energy output was very erratic. Furthermore, the thin separator did not contain sufficient electrolyte to discharge the aluminum anodes completely. To provide sufficient electrolyte in the cells and supply an escape route for the bubbles of hydrogen from the cell, the separator between anode and cathodes was a coarse woven nylon screen.

Difficulties were encountered during the initial testing of these cells because of hydrogen combustion. The initial procedure after cell assembly was to place the cell in an oxygen atmosphere and inject electrolyte into the cells, using a hypodermic syringe. Violent gassing was observed, and some of the electrolyte rejected from the cell. Hydrogen bubbles contacting the oxygen on the surface of the Pt black catalyst started combustion and destroyed several cells. This caused considerable delay in the experiments.

It was observed that the evolution of hydrogen is much less rapid if the electrodes are etched briefly in potassium hydroxide, presumably due to the formation of a more protective oxide layer. A standard pre-etching procedure was then used: immersion of Al anode in 30(w)% KOH at room temperature for approximately twenty seconds, after which time the initial violent gassing was reduced to a slower rate. When anodes prepared in such a manner were removed from the bath, washed, dried, and subsequently reinserted in KOH, the violent initial gassing was still absent. Test cells were assembled using the pre-etched anodes and filled with electrolyte at room temperature. In several of the cells a thermocouple was inserted to

monitor the cell temperature; during the filling procedure, the temperature rose to 90°F. This temperature rise (15°F) results from the corrosion of aluminum in the electrolyte. The cells were discharged immediately after activation was complete and temperature was noted at the end of the tests. Temperatures in the range of 190 to 200°F were recorded at the end of the discharge. After cooling and disassembly of the cells, it was found that the surface of the aluminum anodes was dry, covered only partially by solidified electrolyte, and a dry white powder: aluminum oxide/potassium aluminate. The water loss is attributable to the excessive temperature rise in the cells. Some water loss was observed visually as a mist leaving the test cells during discharge with subsequent condensation on the walls of the container.

A series of parametric tests were carried out to establish the discharge characteristics of aluminum/oxygen cells. Ideally, the performance should be established on non-gassing cells, but since gassing has not been eliminated, the characteristics obtained must be considered less than the optimum which might be achieved in a non-gassing cell. This less than optimum performance is a direct effect of:

(1) Increased electrolyte resistance from entrapped H_2 bubbles.

(2) Increased heat dissipation from the parasitic corrosion process and H_2 oxidation.

(3) Excessive removal of H_2O from the cell by gas bubbles.

The gassing not only resulted in increased polarization but also caused poor reproducibility. Nevertheless, sufficient tests were performed to establish certain trends. Anodes in three nominal thicknesses (3, 6 and 10 mils) using three different electrolyte spacings (0. 296, 0. 320 and 0. 157 cm) were discharged at three different current densities. Eighteen experiments out of the 27 possible combinations were performed. The results are summarized in Table IV, and the voltage versus time characteristics of cells are shown in Figures 19 through 24. Figures 19, 20, and 21 show voltage-time relationships for cells operating at 50 mA/cm^2; anode thickness and electrode separation are variables. Smaller electrode separations result in shorter discharge times and lower anode efficiencies. However, it can be seen from the data in Table II that anode thickness, electrode separation, and anode efficiency a dependent variables and that there is no separable dependence of anode efficiency and anode thickness. The roles of current density and electrolyte volume are equally important because of their effect on heat dissipation ratio and heat-sink capacity. The effects of discharge current density and electrode thickness at constant electrolyte spacing are shown in Figures 22, 23, and 24.

37

The effect of cell temperature on gassing rate is not known at this time; the magnitude of the activation energy for the hydrogen evolution process is the determining factor. Predictably, the rate of gassing will increase with temperature. Control of temperature by incorporating heat sinks will, of course, tend to minimize temperature rise and gassing.

Table IV.   Al-O$_2$ Cells
Effects of Current Density, Anode Thickness and Electrolyte Spacing
on Faradaic Efficiency

Cell No.	Current Density mA/cm^2	Electrolyte Spacing cm	Nominal Anode Thickness mils	Discharge Time minutes	Faradaic Efficiency %
4	50	.157	3	3.50	13.5
16	50	.157	6	12.50	17.2
2	50	.157	10	20.50	7.55
23	50	.320	6	24.25	34.1
37	50	.320	10	22.50	18.2
10	50	.396	3	16.50	47.1
15	50	.396	6	33.75	45.8
36	50	.396	10	41.25	34.3
11	100	.157	3	8	4.38
17	100	.157	6	6.75	18.4
38	100	.157	10	2.75	4.4
8	100	.320	6	11.50	31.5
34	100	.396	3	5.50	27.9
24	100	.396	6	12.50	36.3
9	100	.396	10	17 50	29.7
28	150	.396	3	3.25	26.8
29	150	.396	6	6.25	25.7
19	150	.396	10	2.50	5.92
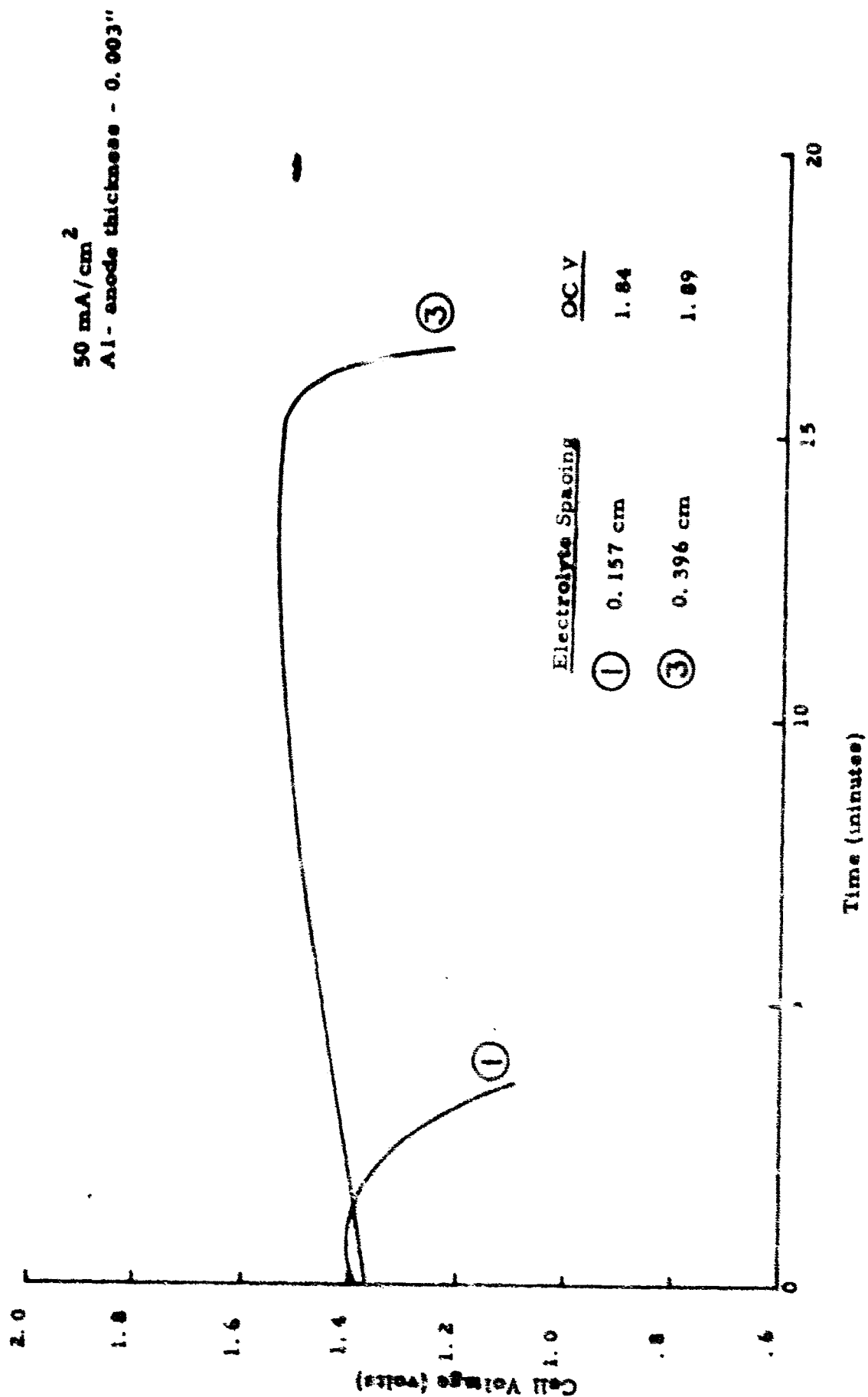
Figure 19. Effect of Electrolyte Spacing (Al/O$_2$ cells)
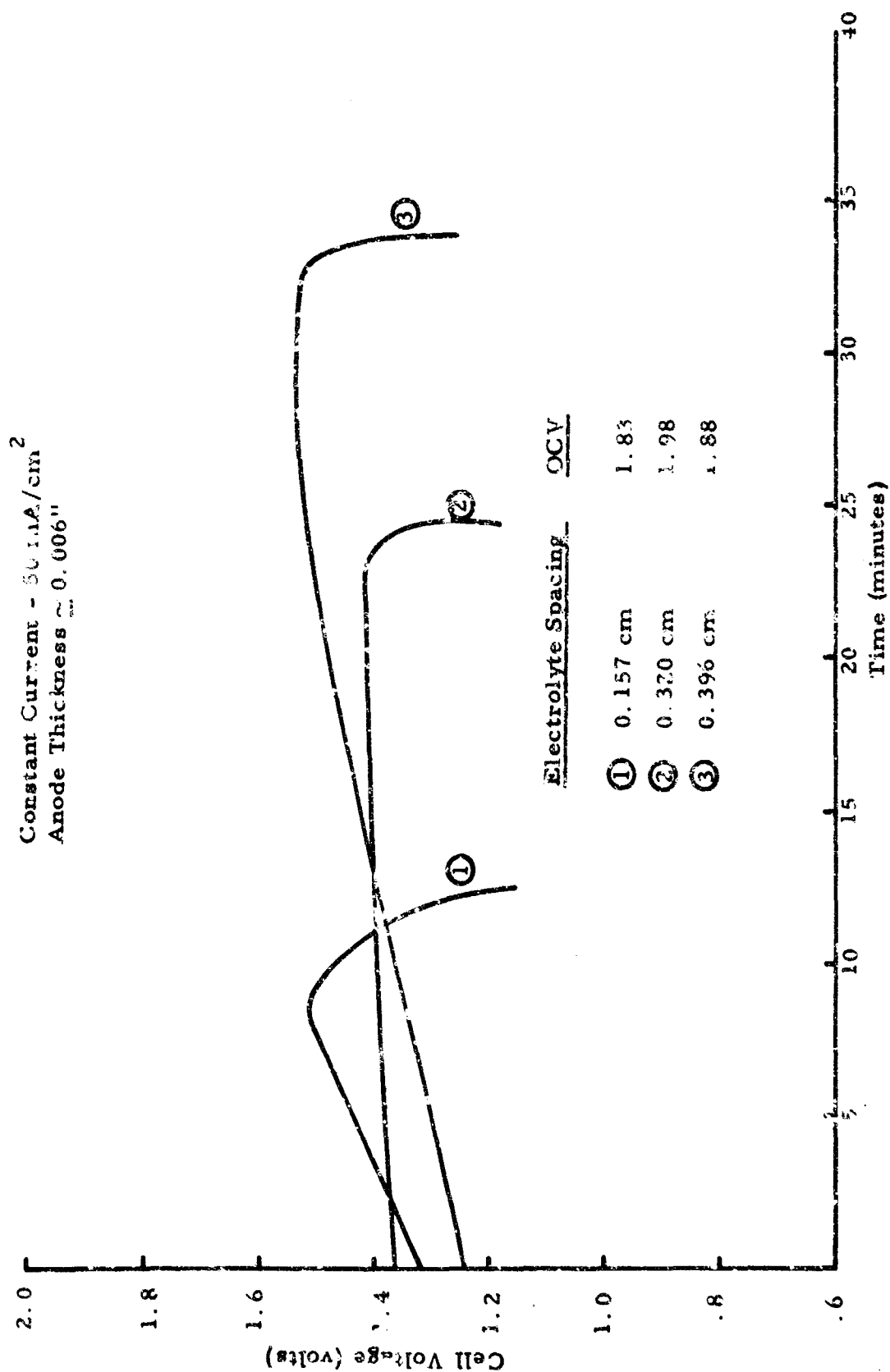
Figure 20. Effect of Electrolyte (Al/O_2 cells)

Constant Current - 50 mA/cm^2
Anode Thickness ≈ 0.006"

Electrolyte Spacing		OCV
①	0.157 cm	1.83
②	0.320 cm	1.98
③	0.396 cm	1.88

Cell Voltage (volts)

Time (minutes)
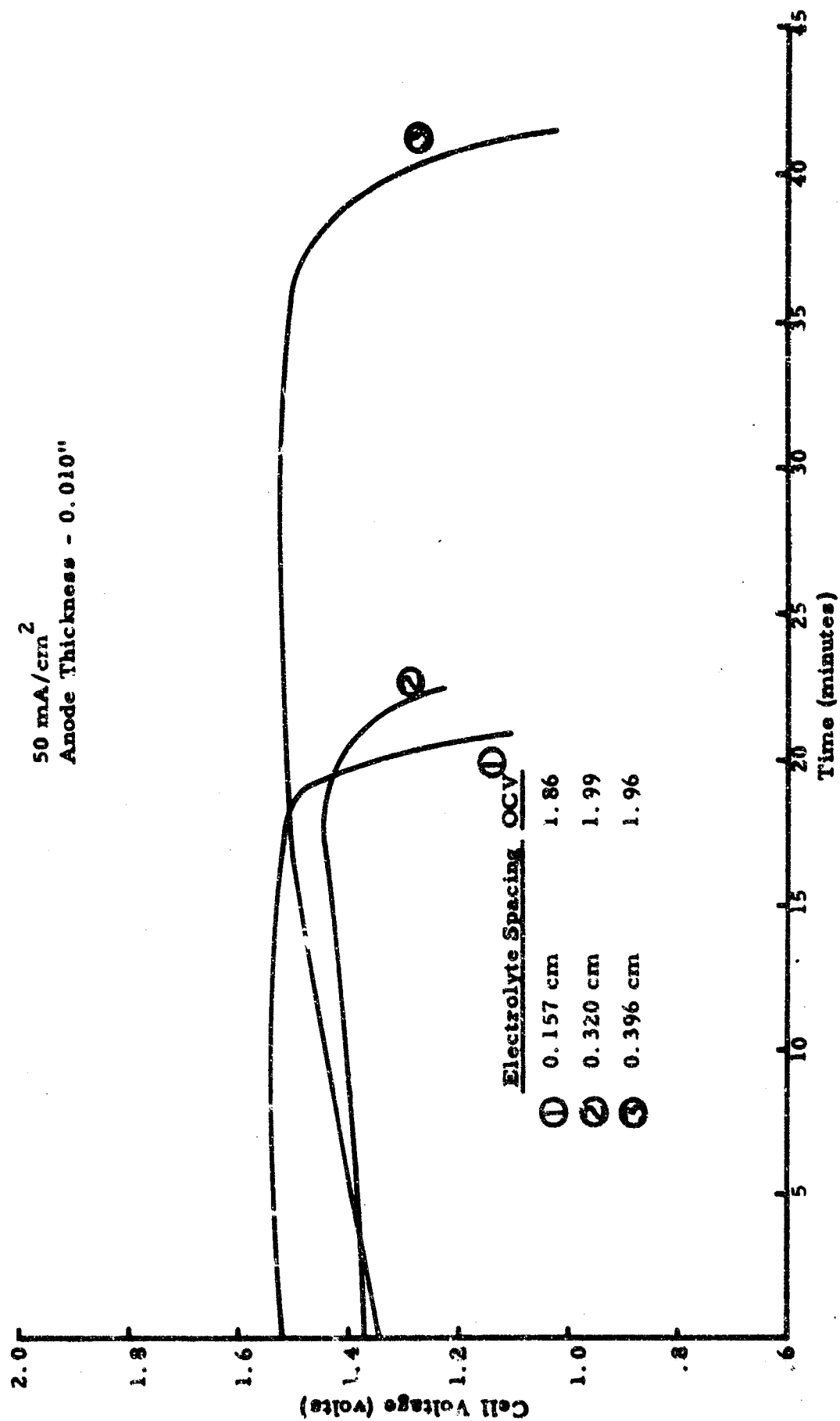
Figure 21.   Effect of Electrolyte Spacing (Al/O$_2$ cells)

50 mA/cm^2
Anode Thickness – 0.010"

Electrolyte Spacing	OCV
① 0.157 cm	1.86
② 0.320 cm	1.99
③ 0.396 cm	1.96

Time (minutes)

Cell Voltage (volts)
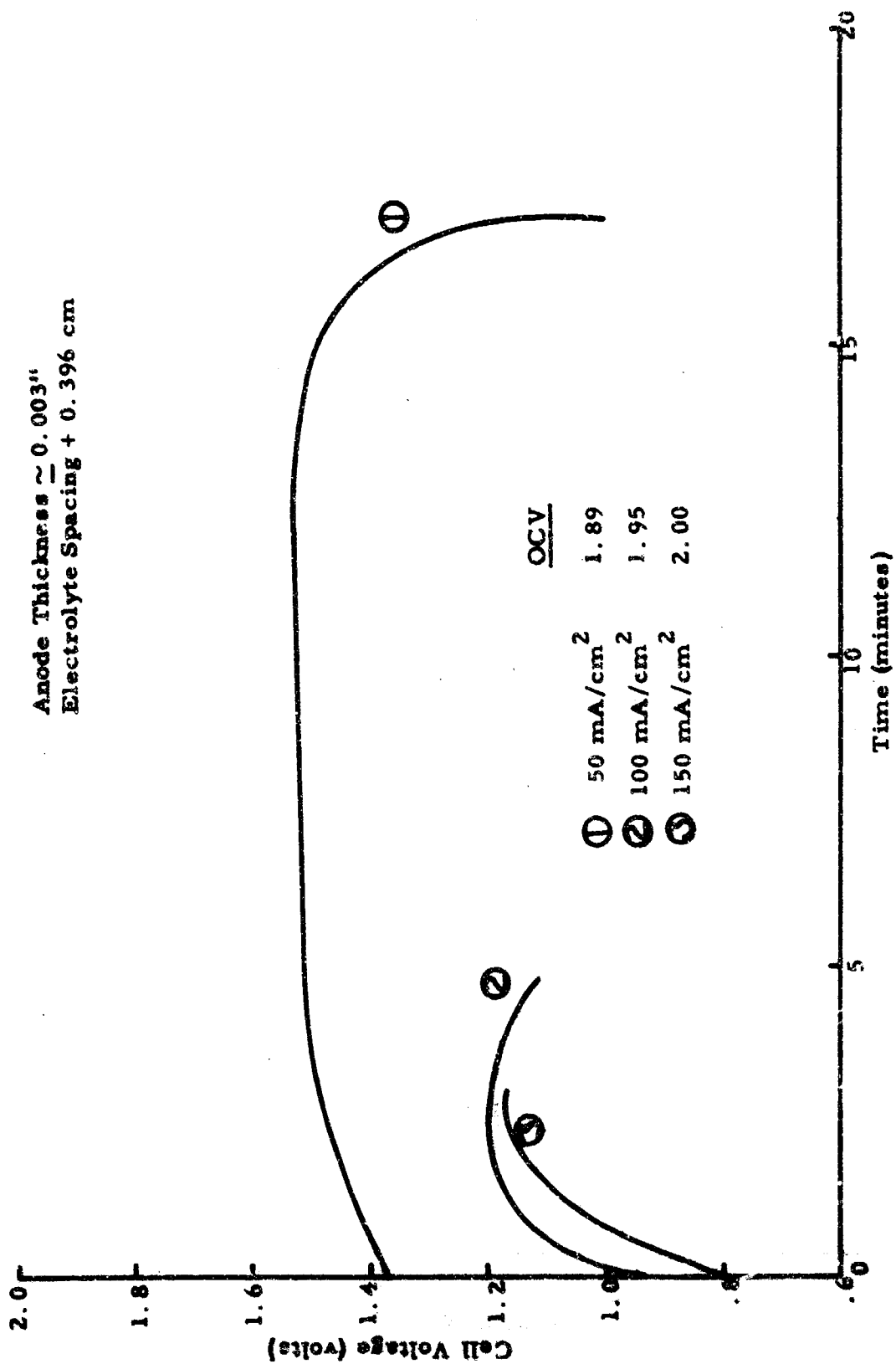
Figure 22.   Effect of Current Density (Al/O_2 cells)

Anode Thickness ≃ 0.003"
Electrolyte Spacing + 0.396 cm

		OCV
①	50 mA/cm^2	1.89
②	100 mA/cm^2	1.95
③	150 mA/cm^2	2.00

Cell Voltage (volts)

Time (minutes)
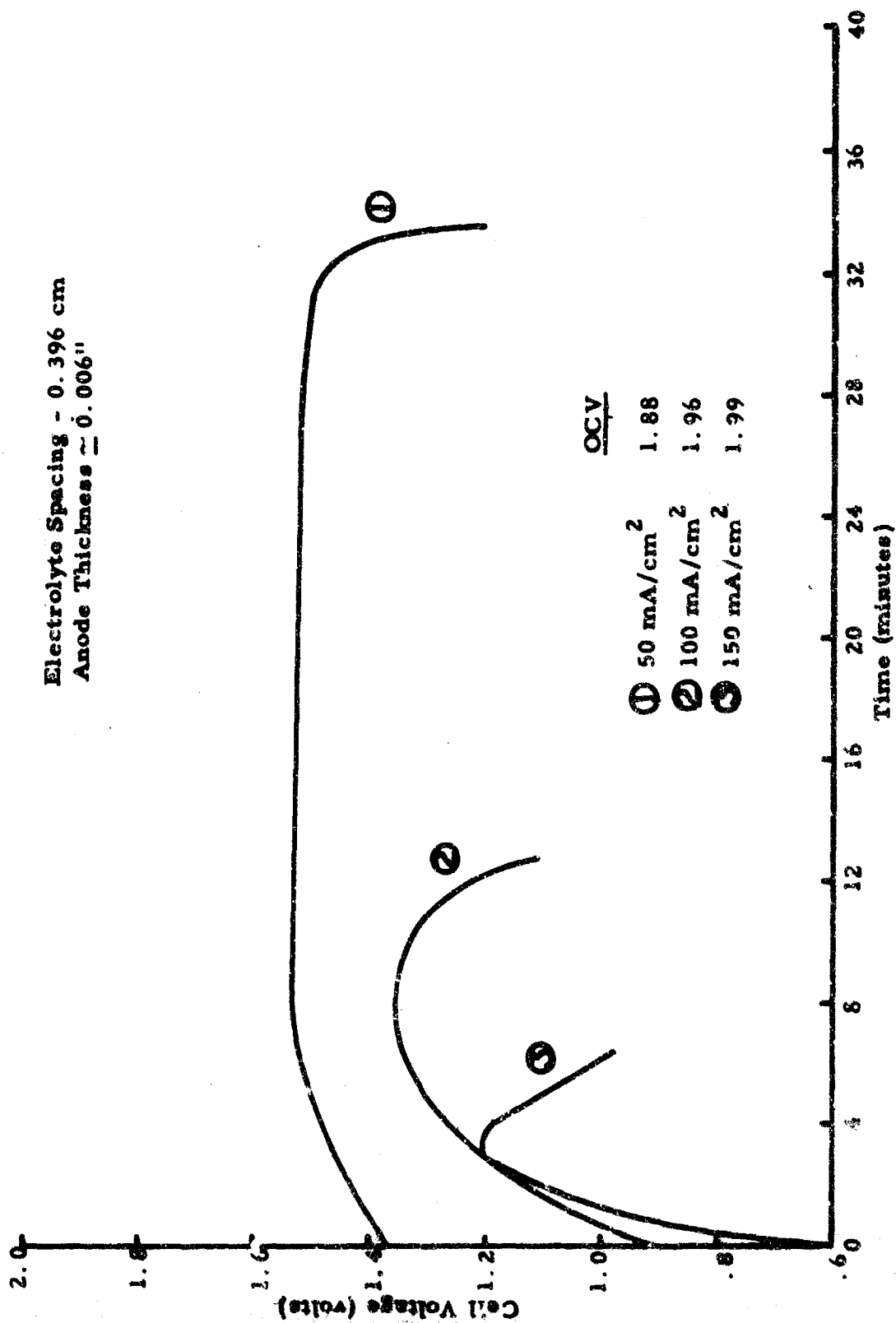
Figure 23. Effect of Current Density (Al/O$_2$ cells,

Electrolyte Spacing - 0.396 cm
Anode Thickness ≃ 0.006"

		OCV
① 50 mA/cm^2		1.88
② 100 mA/cm^2		1.96
③ 150 mA/cm^2		1.99

Time (minutes)

Cell Voltage (volts)

Electrolyte Spacing - 0.396 cm
Anode Thickness ≃ 0.010"

		OCV
① 50 mA/cm²		1.96
② 100 mA/cm²		1.96
③ 150 mA/cm²		1.95

Time (minutes)

Cell Voltage (volts)
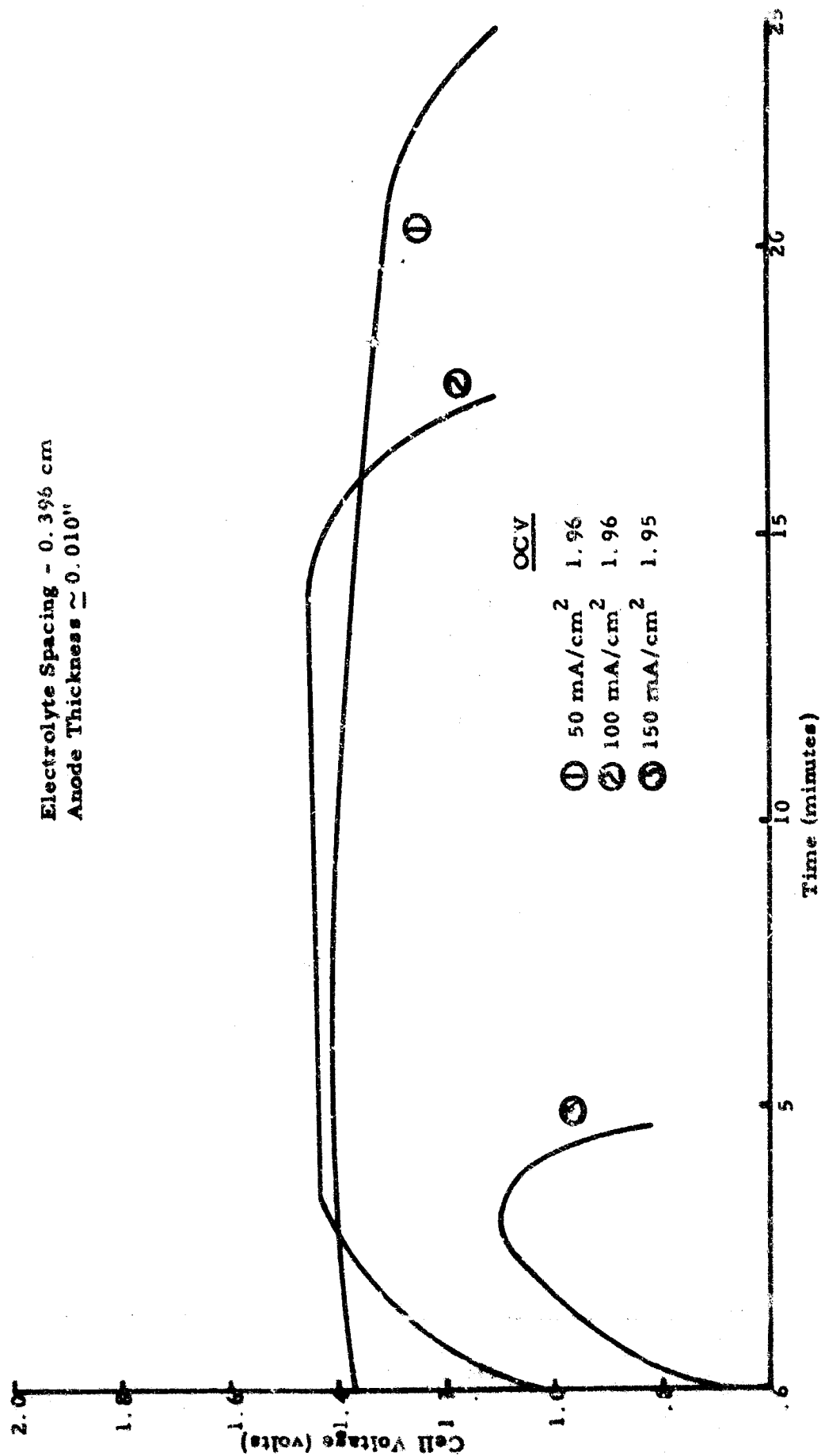
Figure 24.   Effect of Current Density (Al/O₂ cells)

44

SECTION V

SYSTEM ANALYSIS

5.1 THERMAL ANALYSIS

a. Thermal Analysis of the Zn/Oxygen System

The thermal analysis of the Zn/oxygen system consisted of two steps: (1) the determination of the battery temperature rise, assuming an adiabatic battery system, having uniform temperature distribution, and (2) calculating the amount of heat dissipated from the battery case to the surroundings.

To perform the first of these steps it was necessary to determine the battery weight, specific heat and internal heat generation. The specific heat of the battery was calculated to be .28 BTU/lb°F. The operating voltage of the cell versus the current density was assumed including the anticipated improvement in the performance of the present Zn/oxygen system. The E-i relationship is illustrated in Figure 25. From the cell terminal voltage the internal heat generation versus current density could be directly calculated (Figure 26). Knowing the specific heat, the battery temperature rise without heat sinks versus current density was calculated and is shown on Figure 27.

This increase in battery temperature is considered too high and the rate at which the battery can dissipate heat to its surroundings was estimated using the following assumptions: 1.0 ft^2 battery surface area, an emissivity of 0.9 and deep space as the heat sink. This approximates the maximum amount of energy that could be dissipated from the battery and assumes that the battery could be exposed to space environment and simultaneously shielded from the sun. As shown in Figure 28, the heat dissipation rate from the battery case even at this most favorable condition is too low to remove all of the waste heat generated. Thus, in order to reduce the upper temperature limit of the battery, the internal heat storage capacity has to be increased or the rate of heat dissipation to surroundings must be improved or an optimum combination of both methods must be used.

The battery heat storage capacity has to be increased substantially to lower the maximum internal operating temperature to an acceptable level. Methods of improving the heat storage capacity which have been considered are:

(1) Using more cell stacks in parallel, thereby increasing battery thermal capacity and decreasing the total internal heat generation.

45
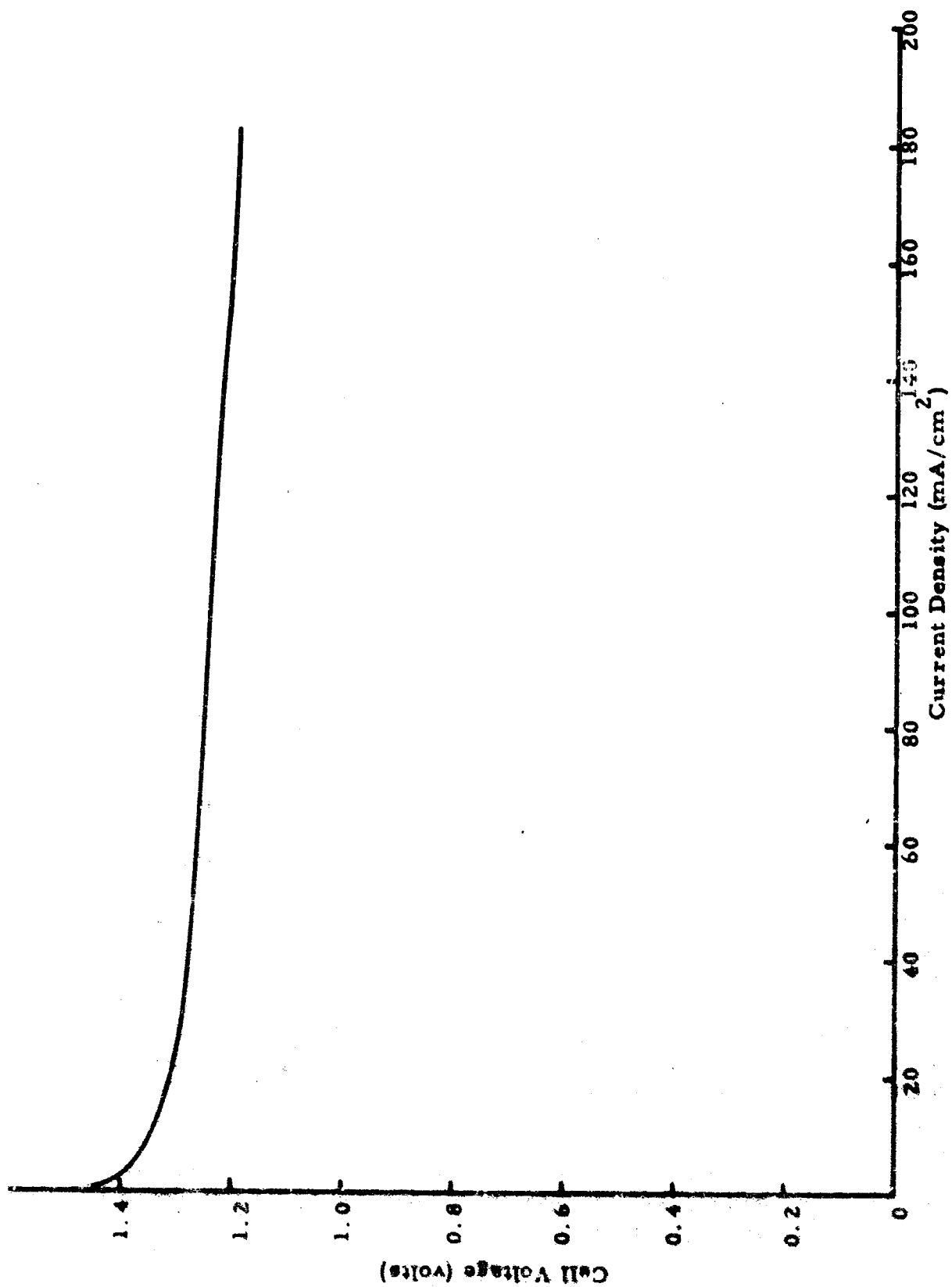
Figure 25. Estimated Zn/O$_2$ Cell Performance

46
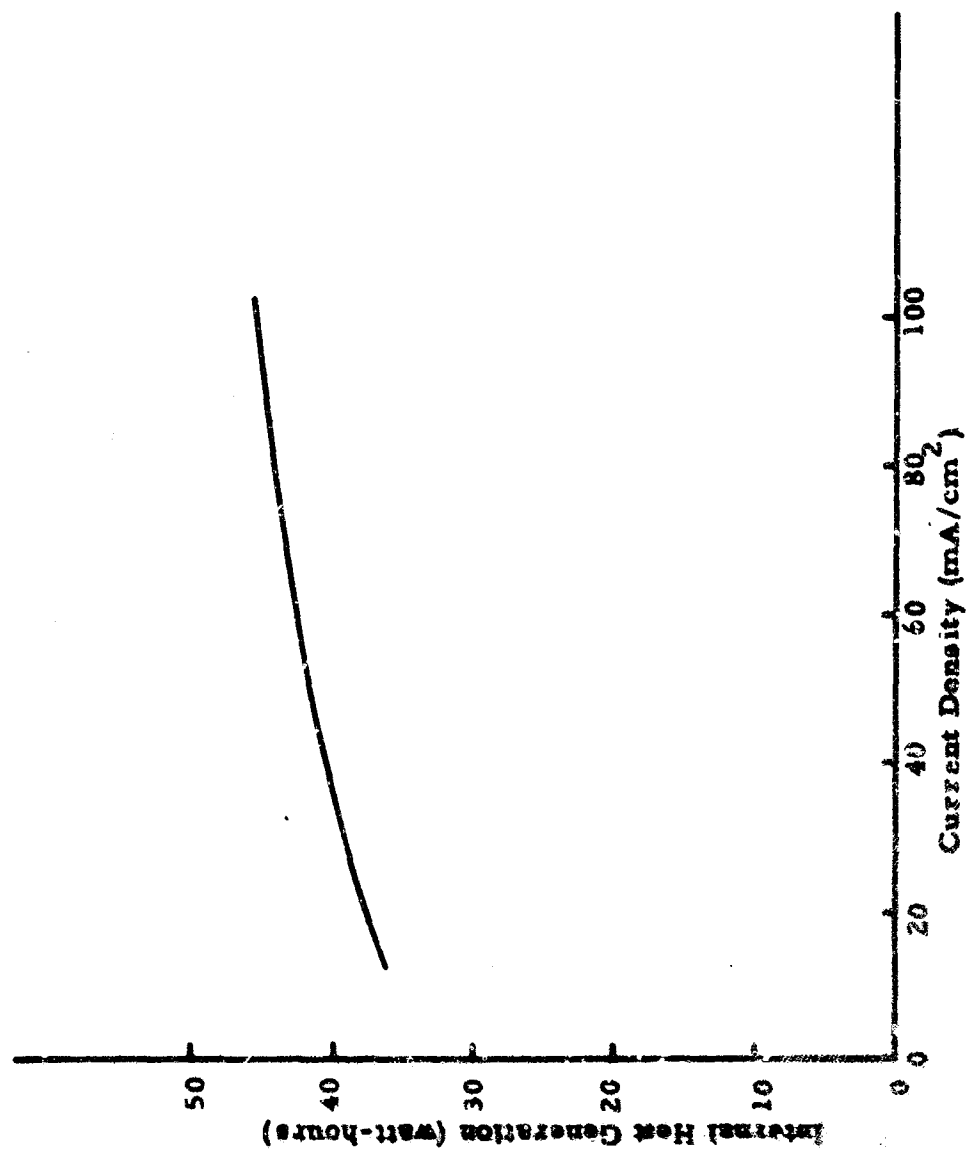
Figure 26. Heat Generation vs. Cell Current Density for a Battery Electrical Energy Output of 100 Watt-Hours

47
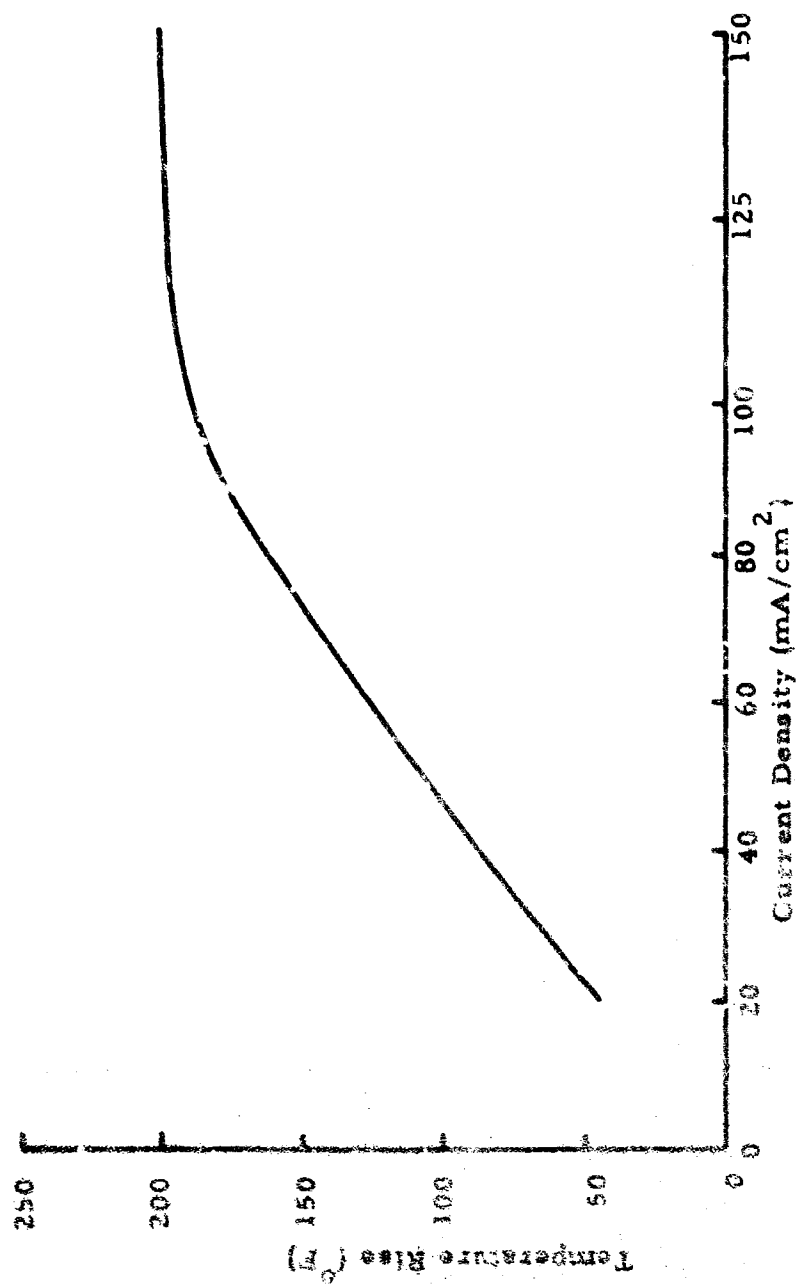
Figure 27. Battery Temperature Rise vs. Cell Current Density (assuming uniform temperature distribution)

48
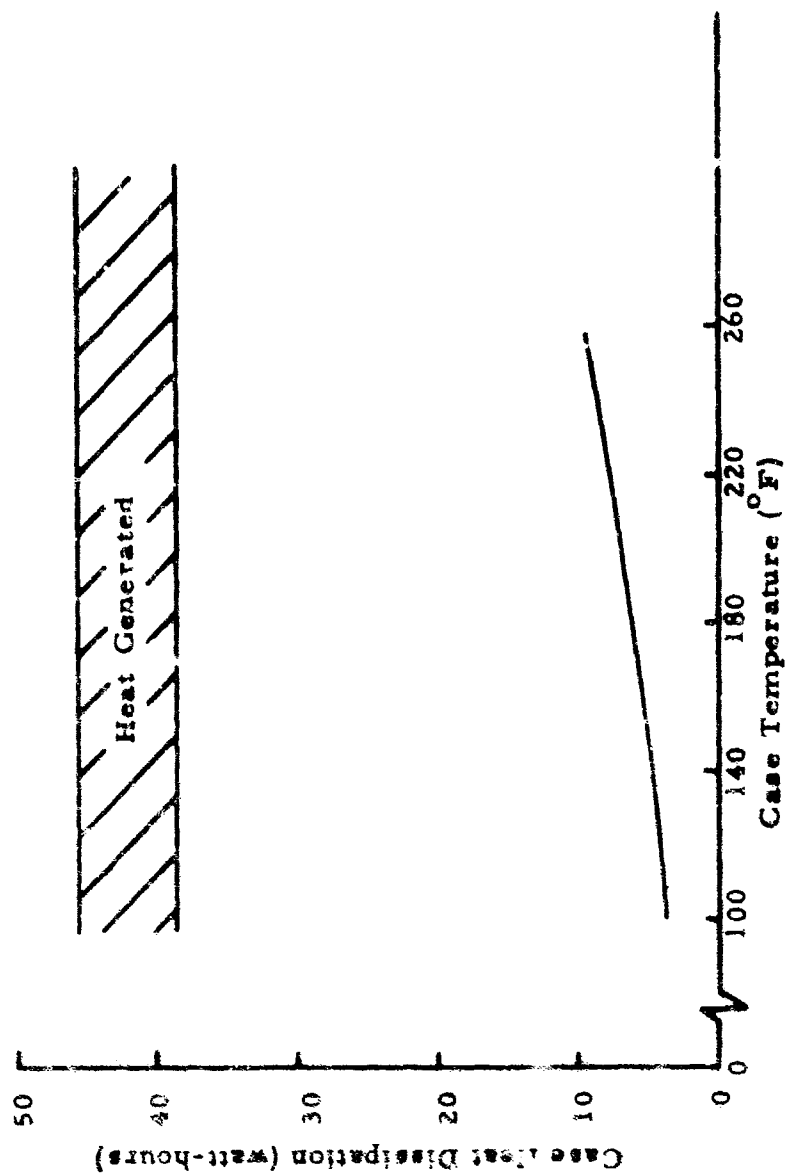
Figure 28. Battery Case Heat Dissipation in 5 Minutes vs. Case Temperature

(2) Incorporation of a high specific heat material in the battery system to increase thermal inertia.

(3) Incorporation of a fusible material with high latent heat of fusion into the battery system, thus permitting substantial heat absorption at the melting temperature.

(4) Incorporation of a subliming material with a high latent heat of sublimation into the battery system.

(5) Use of a vaporizing material with a high latent heat of vaporization to battery system.

These five methods of obtaining increased thermal capacity have been listed above in order of their increasing theoretical heat capacity. Since the latent heat of vaporization is usually higher than latent heats of fusion, the logical choice would be to use an evaporative cooling system.

Although evaporation cooling offers the minimum theoretical weight penalty, this is offset by the practical difficulties of constructing such a thermal sink to operate under zero G conditions. Manifolds, valves and liquid traps would be necessary and since the system would have to operate at atmospheric pressure as well as in high vacuum, a valving arrangement would be needed to release vapor at constant pressure. Furthermore, in the absence of convective heat transfer and at these short discharge times, cooling of the outer shell of the battery case would not suffice and the vaporizing chambers would have to be incorporated within the cells. During boiling of the liquid, the liquid phase would be ejected together with the vapor phase and efficient use of the liquid heat sink would not be possible. This is especially true under zero G conditions. The low weight penalty evaporation cooling is outweighed, therefore, by these practical disadvantages.

Heats of sublimation are usually somewhat less than heats of vaporization of liquids, but are still higher than heats of fusion. "Subliming materials may not be ejected from the vaporizing chambers; however, a complicated manifolding and valving arrangement would still be required." Furthermore, it would have to be designed in such a manner that all components of the manifolding system would be kept at temperatures above the sublimation point of the subliming material: clogging of the lines would occur otherwise which would prevent the operation of this subsystem. This requirement again adds complications and weight to the battery pack, and hence this approach was rejected.

Another alternative was to increase the number of cells and operate them at a lower current density, hence increase the thermal inertia of the system. However, since the specific heat and thermal capacity of the battery components is relatively low, this is not an efficient approach and results in large weight penalties.

50

Incorporation of a fusible material into the cells incurs the least weight penalty, providing that a fusible material can be found which has a sufficiently high latent heat of fusion and which melts within the desired operating temperature limits. Materials meeting these requirements are shown in Table V. The approximate weights of material required to store the waste heat generated with the various methods described is shown in Figure 29.

For the 15-second operation the size of the battery required is large enough so that extra heat sinks are not required. The present analysis was carried out in order to determine the optimum battery weight for the various discharge rates. Obviously, if a battery capable of delivering the required capacity in 15 seconds is discharged at the 5 minute rate, then heat sinks would be unnecessary.

Table V.   Table of Fusible Materials

Compound	Melting Point, °C	Heat of Fusion BTU/#	Specific Heat BTU/# °F
Magnesium Nitrate	90	68	0.887
Orthophosphorous Acid	73.6	67	--
Azobenzene	68	58.4	0.36
P. Chloroaniline	70	67	0.43
Naphthalene	80	64	0.67
α -Naphthol	95	70	0.365
Hydrazine Monochloride	89	95	0.3 ~
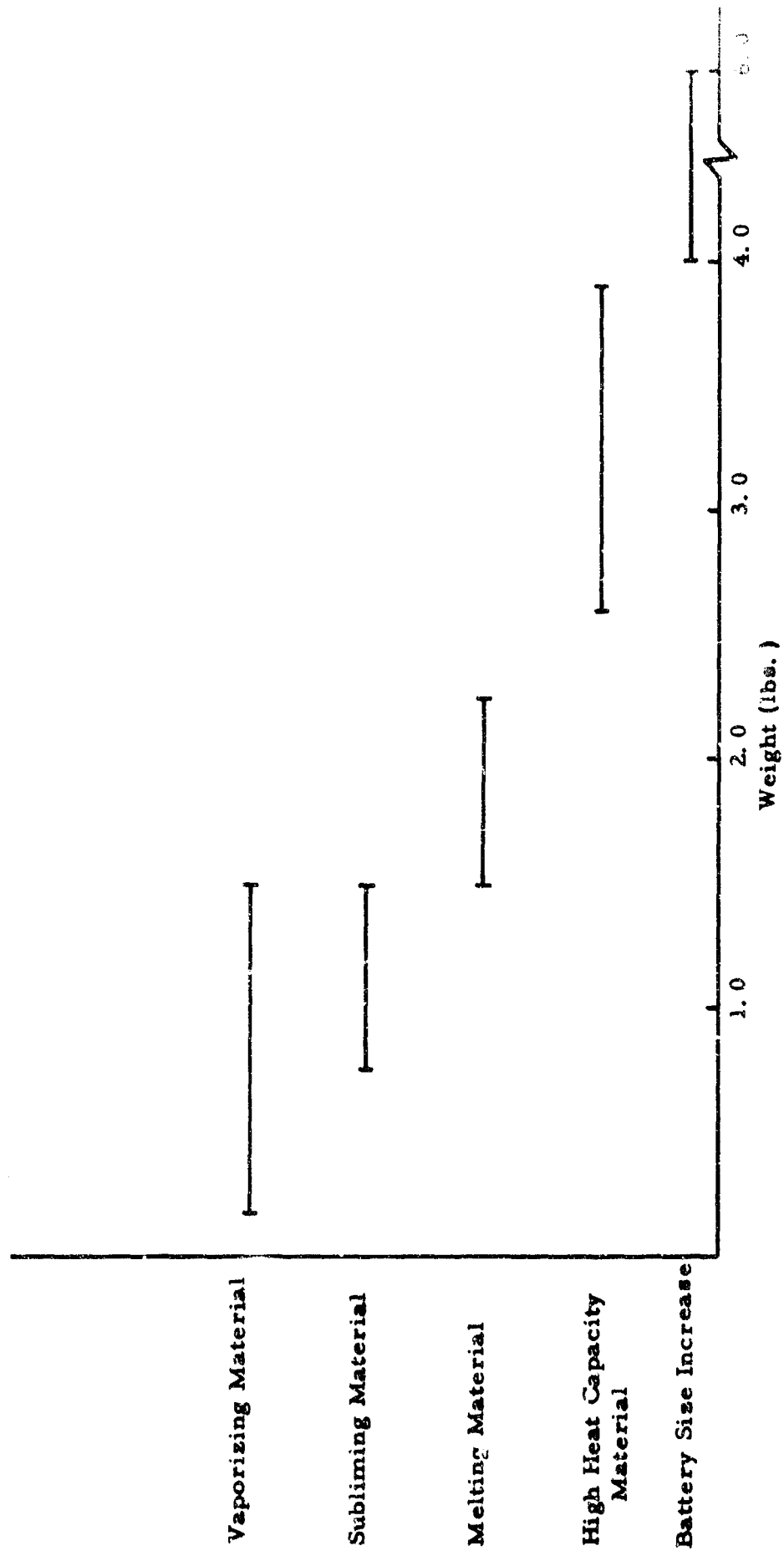
Figure 29. Material Weight Required to Store 45 Watt-Hours of Internally Generated Heat Without Exceeding the Battery Operating Temperature Limit

b.   Thermal Analysis of Al/Oxygen System

Using the same methods described in the previous section, the thermal analysis of the 5 minute rate of the Al/oxygen system was performed.   The single-cell current/voltage curve is shown in Figure 30 and the resultant heat generation versus current density curve is shown in Figure 31.   Figure 32 shows the estimated weight of the battery required dependent on the current density of operation.

In Figure 33 the temperature rise of a battery without heat sinks is shown as a function of current density: obviously such temperatures could not be tolerated.

Incorporation of the fusible materials (listed in Table V) into env:lope-type anodes was considered, and the temperature gradient in :he cell was calculated assuming conduction as the only means of `·`at transfer. (This a·:sumption has to be made, since u   :r zero-G conditions there is no convective heat transfer.)   The temperature gradients between cathode surface and   iter of heat sink versus current density are shown in Figure 34. The magnesium nitrate material offers a distinct advantage because of its higher heat conductivity.

As in the case of the zinc/oxygen system, at the 15-second rate, other components of the battery have sufficient thermal inertia and no extra heat sink would be necessary.

5.2   SCALE-UP CONSIDERATIONS

In a battery electrode, current is generated on the entire surface of the electrode and conducted through the electrode to a current collector. In order to make a lightweight battery system, the current collector weight must be optimized with respect to the ohmic losses within the electrode. Because of the contribution of the ohmic loss, the local current density near the point of current collection is higher than that at the extreme areas of the collector.   Thus, on large electrodes, the current density can vary con- siderably across the profile.[2]   The variation in current density is dependent on many factors such as electrode and electrolyte resistances and the reversibility of the electrode process.   Obviously, for high-rate electrodes of lightest possible weight, this effect must be calculated and the design optimized.   The resulting ohmic inefficiency (ratio of the current generated at a given potential by an electrode to the amount of current generated at

---

[2]Conway, B. E., Gileadi, E., and Oswin, H. G.; The Theory of Current Distribution and Potential Profile at an Electrode of Significant Ohmic Re!   ance, Canadian Journal of Chemistry, Volume 41 (1963).
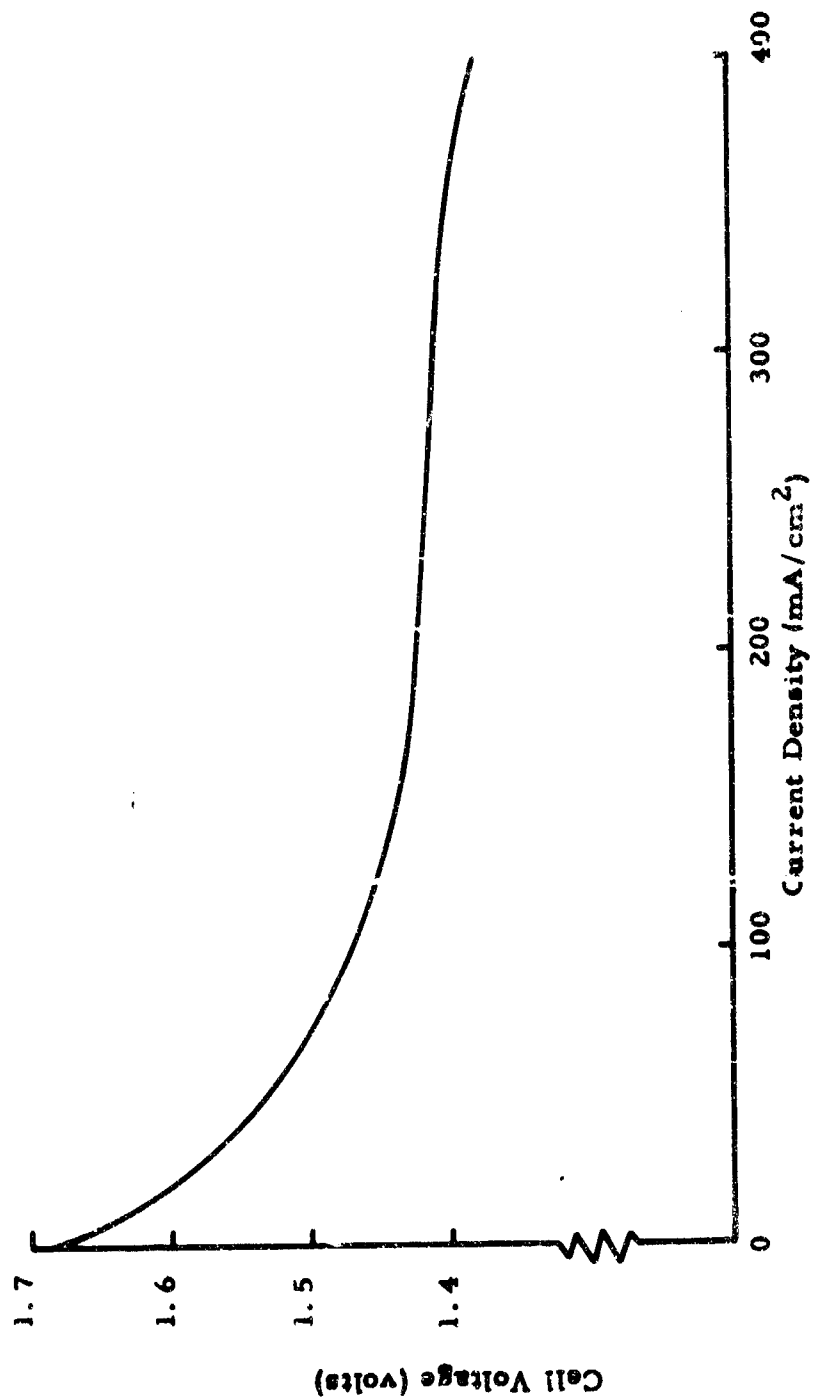
Figure 30. Estimated Performance O_2 Cells (in the absence of anode gassing)

54
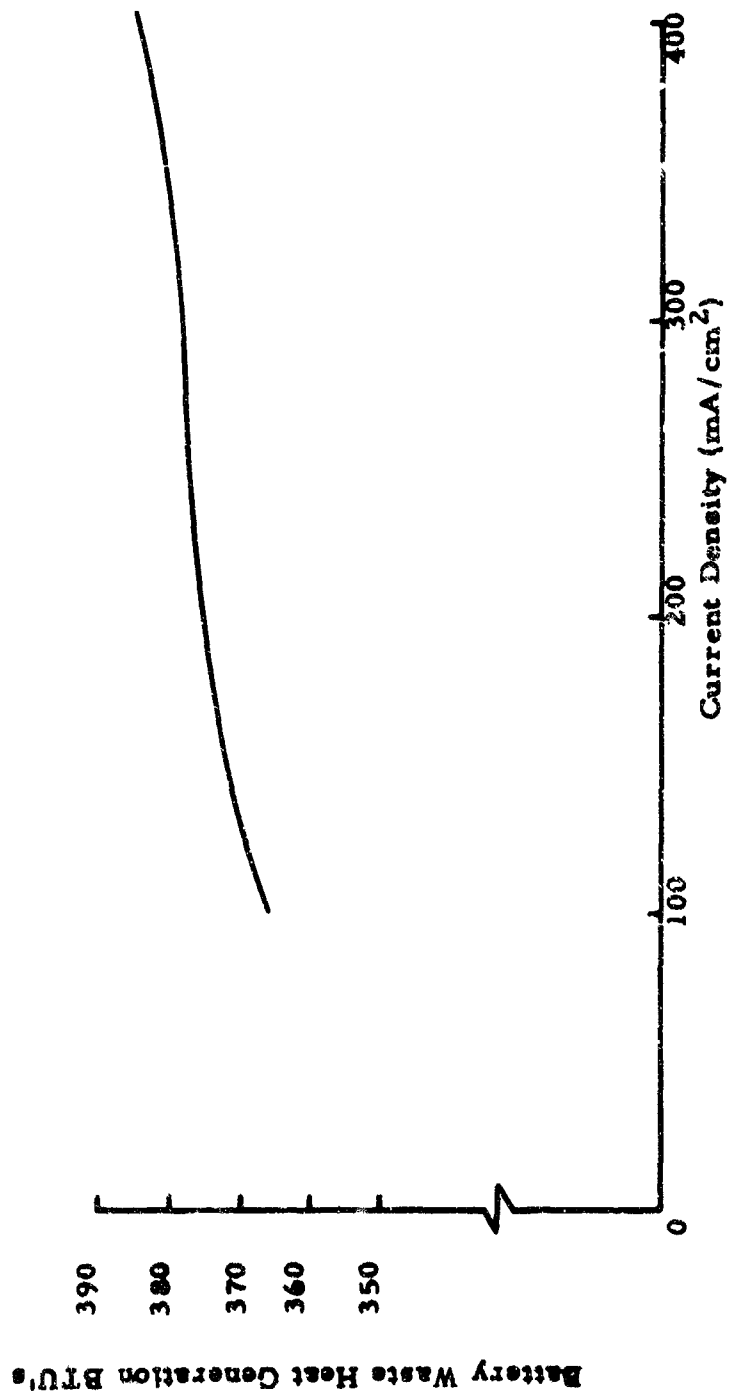
Figure 31. Thermal Energy Generation vs. Current Density (Al/O$_2$)
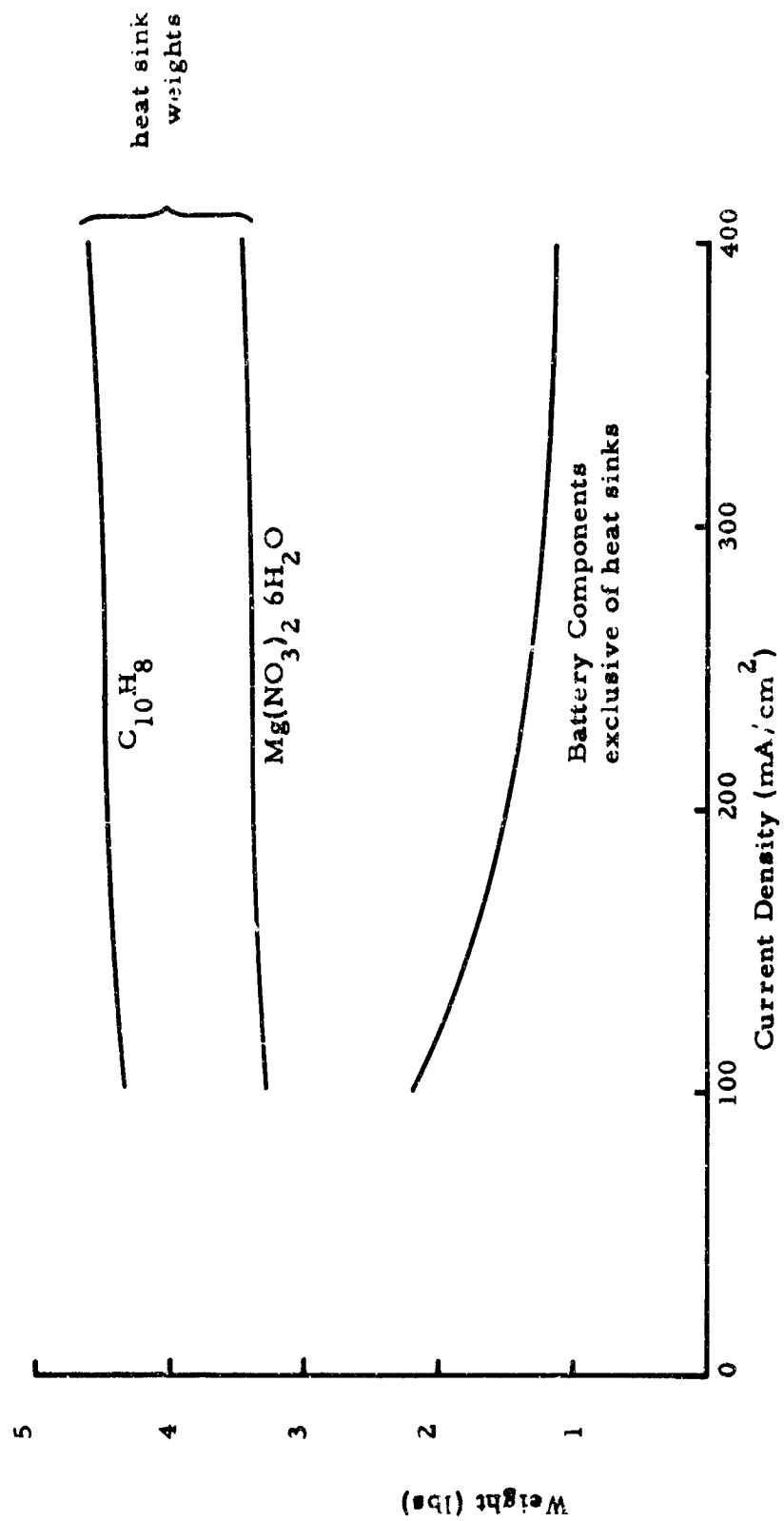
Figure 32.   Battery and Heat Sink Weights (Al/O_2)

56
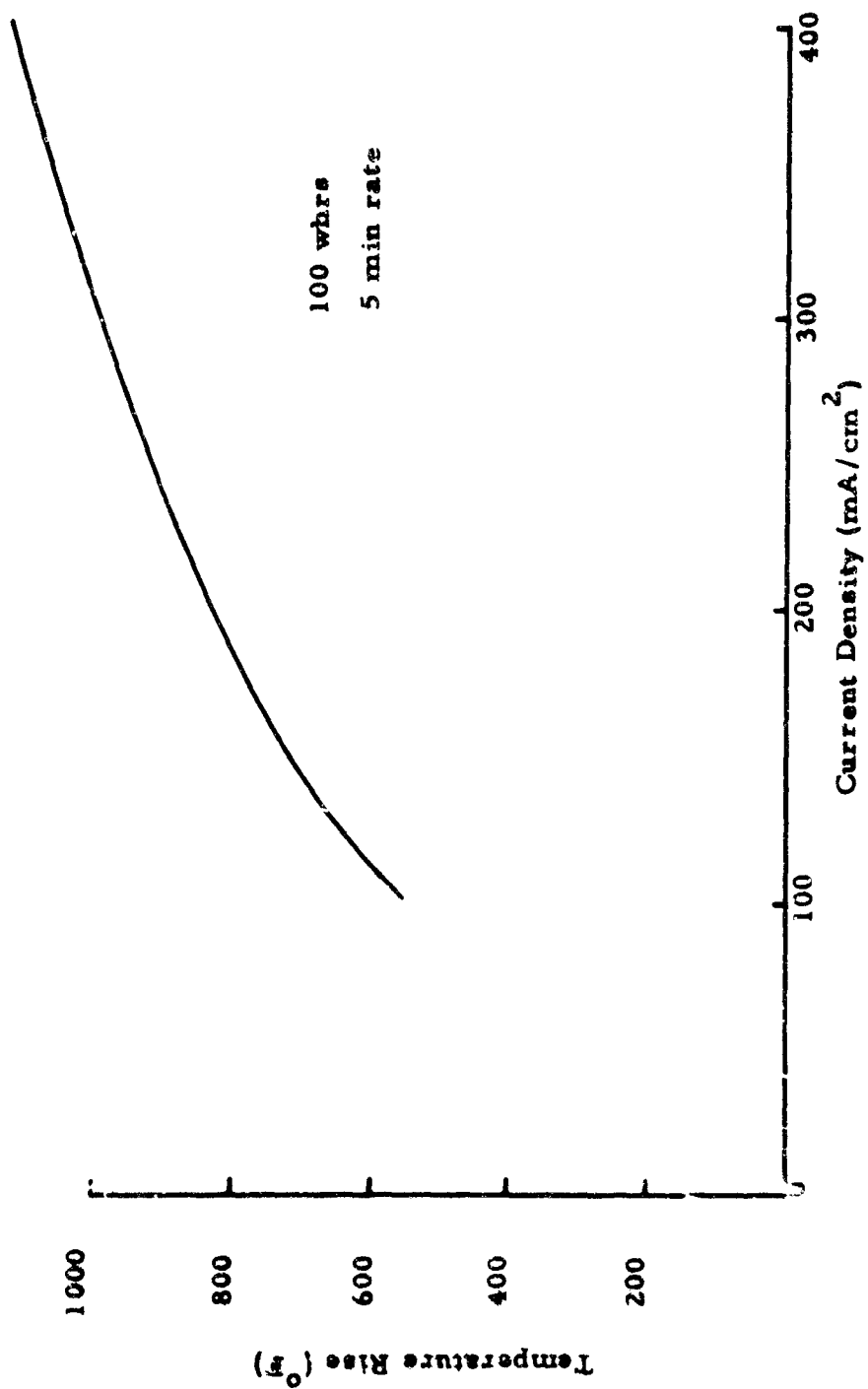
Figure 33.   Battery Adiabatic Temperature Rise vs. Current Density
(Al/O$_2$)

100 whrs

5 min rate

Current Density (mA/cm^2)
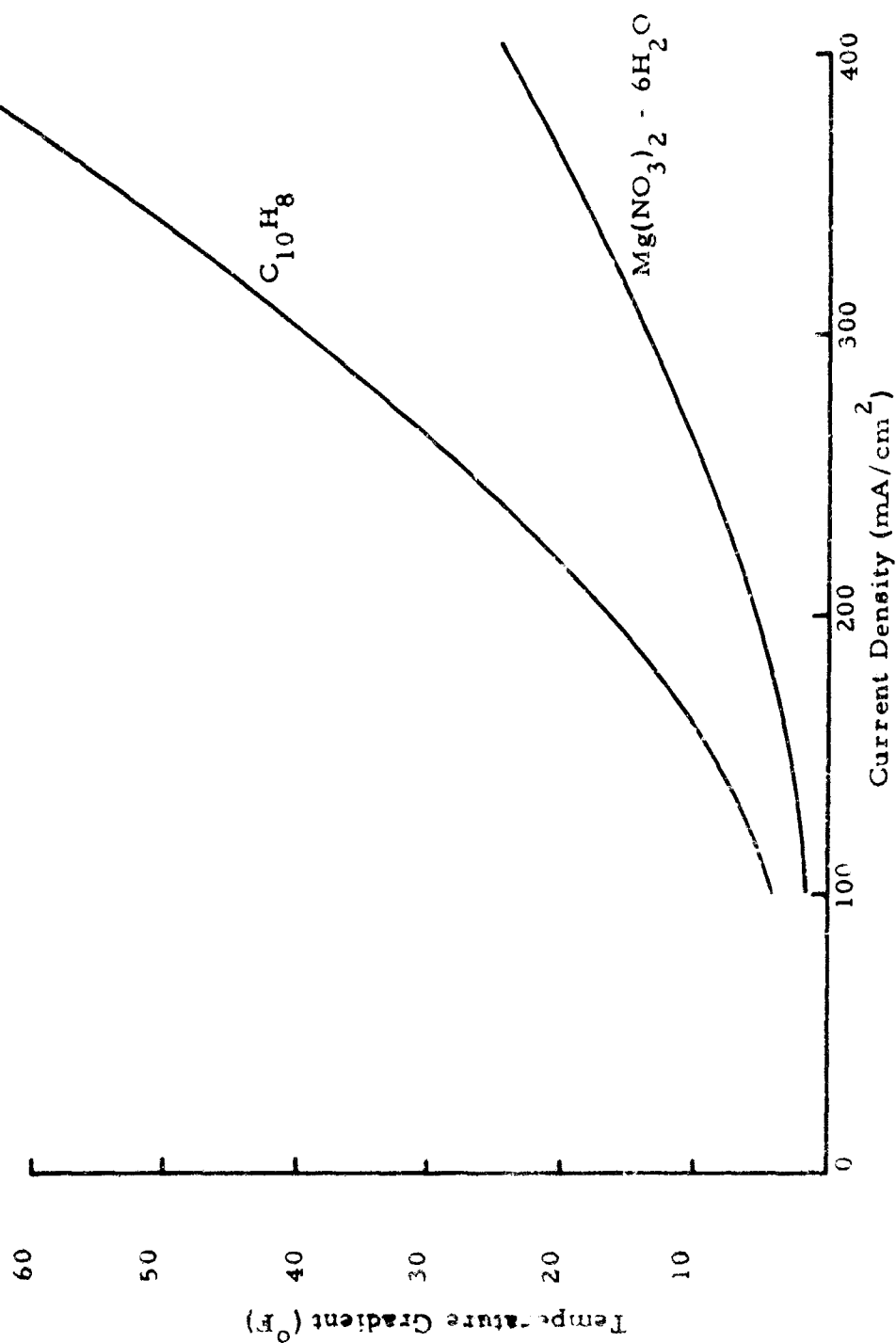
Temperature Rise ($^\circ$F)

Figure 34. Cell Steady-State Temperature Gradient vs. Current Density

58

the same potential had infinitely conductive current collectors been used in the electrode) can be calculated for rectangular electrodes where current is collected along the electrode from the relationship:

$$E = \frac{\tanh\left[\left(\frac{c\rho}{t}\right)^{\frac{1}{2}} w\right]}{\left(\frac{c\rho}{t}\right)^{\frac{1}{2}} w}$$

Using the method of R. Brown[3] the derivation of the above relationship is shown in Appendix I. The application of the above relationship to design of cells is also presented in Appendix I.

5.3   WEIGHT ESTIMATES

The weight estimates presented below depend on one major assumption in the aluminum/oxygen system it is assumed that polarization will not change when the hydrogen evolution is eliminated. Data for the aluminum/oxygen system is based on half cell measurements. The estimates presented below are for the case of no hydrogen evolution in the battery: i.e., no waste heat generation due to parasitic conversion.

The components used for the design on which the weight estimates are based are at present available from commercial sources or could be manufactured without any anticipated difficulty. For example, the current collectors in these cells are expanded metal mesh which is commercially available. Changing of the mesh size, which would involve major retooling, was not anticipated. Similarly, all the other components such as the separators, etc., are all commercially available materials; the gas regulator is also a catalog item (Scott Aviation Corporation, Lancaster, New York, Part No. 15575).

The weights of the oxygen storage tank, the activation system, and the battery case, on the other hand, are estimates derived standard design calculations.

a.   Method of Weight Estimation

The design of a 28 volt missile battery was programmed for computation to certain parametric studies. The program in its present form can evaluate the effect of incremental changes

_____

[3] Brown, R. J.; J. Electrochem. Soc. 112, 1228 (Dec. 1965).

in current density, capacity, and discharge rate on the battery design and optimum system weight. This was done for both the zinc/oxygen and aluminum/oxygen system. Flexibility is achieved by incorporating into the computer program the design method only and the data on cell performance and component properties are supplied for the specific case. The computer output is the battery weight, its energy density, and a detailed breakdown of the weights of the various components.

(1) Assumptions

(a) Steady state operation is implicit in the structure of the program. Cell performance and component properties in the input data are steady state values. In other words, this implies that thermal equilibrium is attained instantaneously and that the depth of discharge has no appreciable effect on the cell performance. This assumption is not expected to cause any significant error due to the fact that very thin cells are used for the high discharge rates.

(b) Polarization vs. current density curves for both half cell and full cell reactions have been linearized from 0.050 to 0.200 amps/cm^2.

(c) Temperature gradients were ignored in this study: it is estimated that in general they are small enough to be neglected. In addition, any errors resulting from this assumption will always be conservative, i. e. , would tend to generate higher system rates.

b. Cell Design

In Figure 15, a battery concept was shown where the cathodes were folded around the anode. In order to minimize the length of the electrolyte path upon activation it was desirable that the electrolyte be injected in the center of the cells. Hence, a folded arrangement was conceived which is illustrated in the sketch of Figure 35. The anodes, cathodes and inner-cell separators are sealed into epoxy at each edge. The width this sealing compound is approximately 1/8 of an inch. The current collec grid of the ca le exte beyond the length of the seal at one end of the module and that o e anode the other end of the module. This way, they form the two terminals of the cells on opposite sides. In order to connect t single cells in series, the ends of the cells are to be contacted. To facilitate this, a 1 mil thick silver foil would be attached on each side to the anode and cathode grids to provide for a smooth contact surface.

As has been described in Section 5. 2, the actual electrode area required depends on the polarization of the cells and the ohmic drops (which are a function of the length of the current path). The direction and length of the current path are indicated on Figure 35 with the notation W. The longer this dimension is, the great the ohmic losses are, hence, the larger

60

Ag Foil
Terminal
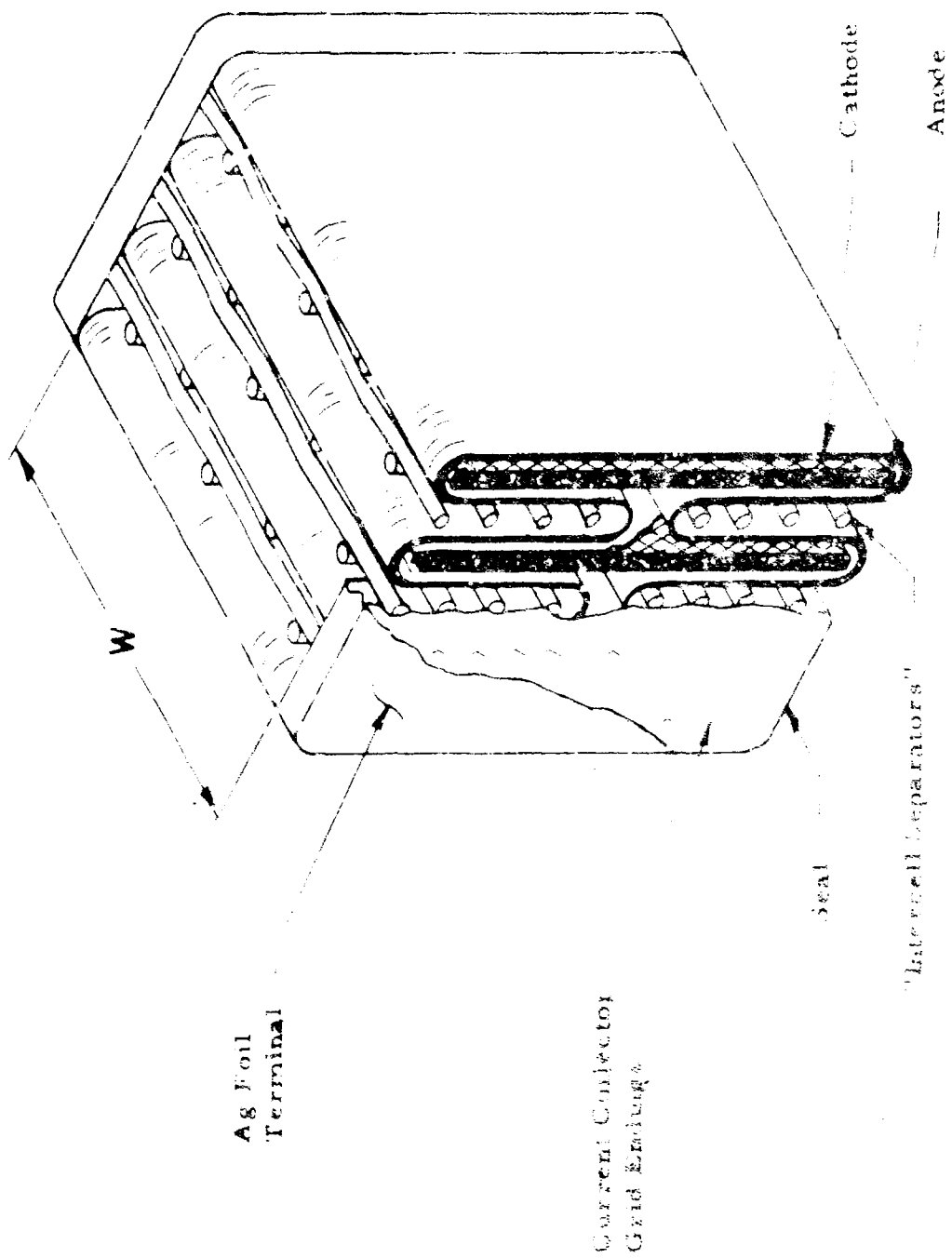
Current Collector
Grid Endings

W

Cathode

Anode

Seal

"Intercell Separators"

the area required resulting in increased battery weight. Counter to this trend, the longer this dimension is, the less seals are required at the terminals, hence decreasing the overall battery weight. There is an optimum width, then, at which battery weight is at a minimum, and this was determined with the computer as described below.

c. Computer Program Logic

After the fixed input data has been read into the computer, the program sets the increment of variables and minimum values and computes the corresponding current and area requirements based on the nominal battery voltage. The electrolyte voltage drop is then calculated and the actual cell voltage neglecting terminal losses is determined. The cell area and current requirement are then adjusted and the number of cells required are computed.

With the cell area established, selection of a particular electrode width must be made. As mentioned above, the smaller the width selected, the greater the electrode efficiency becomes, and the weight of the overall system would tend to decrease. Counterbalancing this trend is the weight of seals, which increases with decreasing electrode width. An optimization loop was set up in the computer program in order to determine the particular electrode width at which the battery system weight is at a minimum. A suitable maximum width was selected which, in our estimation, would not cause any manufacturing difficulties, and was incrementally decreased with each pass through the loop. For a specified cathode current collector, the cathode efficiency can be evaluated at each incremental width.

Because of the similarity of current densities in anodes and cathodes, the calculation of the cathode ohmic efficiency would establish the required anode ohmic efficiency. This, in turn, establishes the required thickness of the current collector in the anodes. For this analysis, amalgamated silver current collectors were used for the zinc anodes. For the aluminum anodes, uniform surface corrosion was assumed and the thickness of the aluminum anodes was increased correspondingly so that part of the anode would act as current collector, even when all the required energy is discharged.

The anode and cathode area is again readjusted after the ohmic efficiency calculation and then the length and the number of folds are determined (see Figure 34). The computer is now able to evaluate the weight of all of the active and non-active cell components, the magnitude and weight of the heat sink required, and the weights of ancillary hardware. This calculation is performed for each increment of width and when the minimum system weight is found it is printed in the output data together with the volume and then the next set of data is evaluated.

This computer logic is shown in Figure 36. In order to avoid over-crowding, several abbreviations were used. A list of symbols used in Figure 36 is shown on page 65. The required input data list is presented as Appendix II. Each of these values can be varied to evaluate the optimum battery weight for a given condition. The complete Fortran program for the IBM 1620 computer is also included in the report as Appendix III.

(1) Fifteen Second to Five Minute Rate

To illustrate the type of information obtainable from the computer program, the output data for the fifteen second - five minute rate at a total capacity of 100 watt-hours is included on Tables VI and VII for the aluminum/oxygen and zinc/oxygen systems operating at 100 mA/cm^2 current density. The single cell nominal operating voltage was 1.4 volts for the aluminum/oxygen system and 1.2 volts for the zinc/oxygen system.

The computer program permitted the rapid estimation of the battery energy density as a function of various operating parameters. Such correlations are shown on Figures 37 through 40. The total battery capacity was varied between 100 and 600 watt-hours, and at operating current densities of 50, 100 and 200 mA/cm^2. On Figure 37, the energy density of the zinc/oxygen system operating at 1.2 volts single cell voltage is illustrated. On Figure 38, the aluminum/oxygen system operating at 1.44 volts single cell voltage is shown.

On Figures 39 and 40, energy densities for the aluminum/oxygen system operating at 1.75 and 2.05 volts single cell voltage are shown. These values were computed to determine what could be expected if improvements in anode reversibility could be achieved.

The reader's attention is called to Tables VI and VII in which the computer output is listed (output format for these tables are shown on page 72), especially to the column where the percentage weights are shown. It should be noted that at the rates longer than 15 seconds, a significant portion (up to 53% in the aluminum/oxygen system) is the heat sink. Attention should be called to the fact that for this small 100 watt-hour capacity battery, the means of heat removal were melting heat sinks. With larger batteries this method may not be the optimum and the weight penalty may be less severe for heat removal. This statement is especially true for longer rates.

63
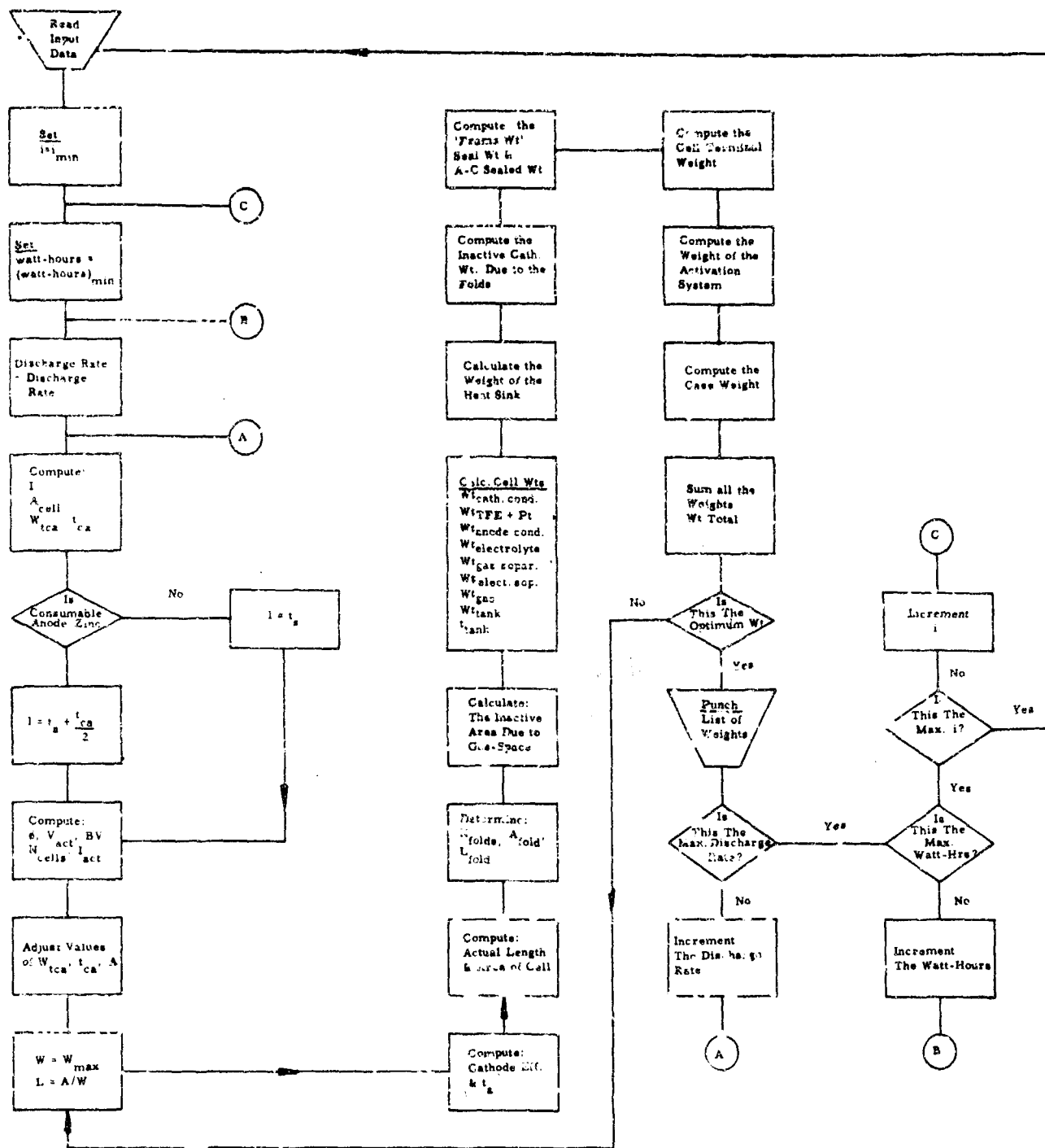
Figure 36.   Computer Logic Flow Chart

COMPUTER LOGIC FLOW CHART SYMBOLS FOR FIGURE 36

A	Cell area based on Iact
A_{CELL}	Cell area, cm^2
Afold	Area of folds
BV	Battery voltage
i	Current density; amps/cm^2
I	Total current; amps
Iact	Total current based on Vact
l	Length of ionic path: cm
L	Electrode length
Lfold	Length of folds
Ncells	Number of cells required
Nfold	Number of folds
0	Electrolyte ohmic loss; volts
ta	Anode conductor thickness
tca	Thickness of consumable anode; cm
ts	Thickness of electrolyte matrix; cm
Vact	Actual cell voltage; volts
W	Electrode width
Wtca	Weight of consumable anode; gms
$Wt_{cath.\ cond.}$	Weight of cathode conductor
$Wt_{elect.\ sep.}$	Weight of electrolyte separator
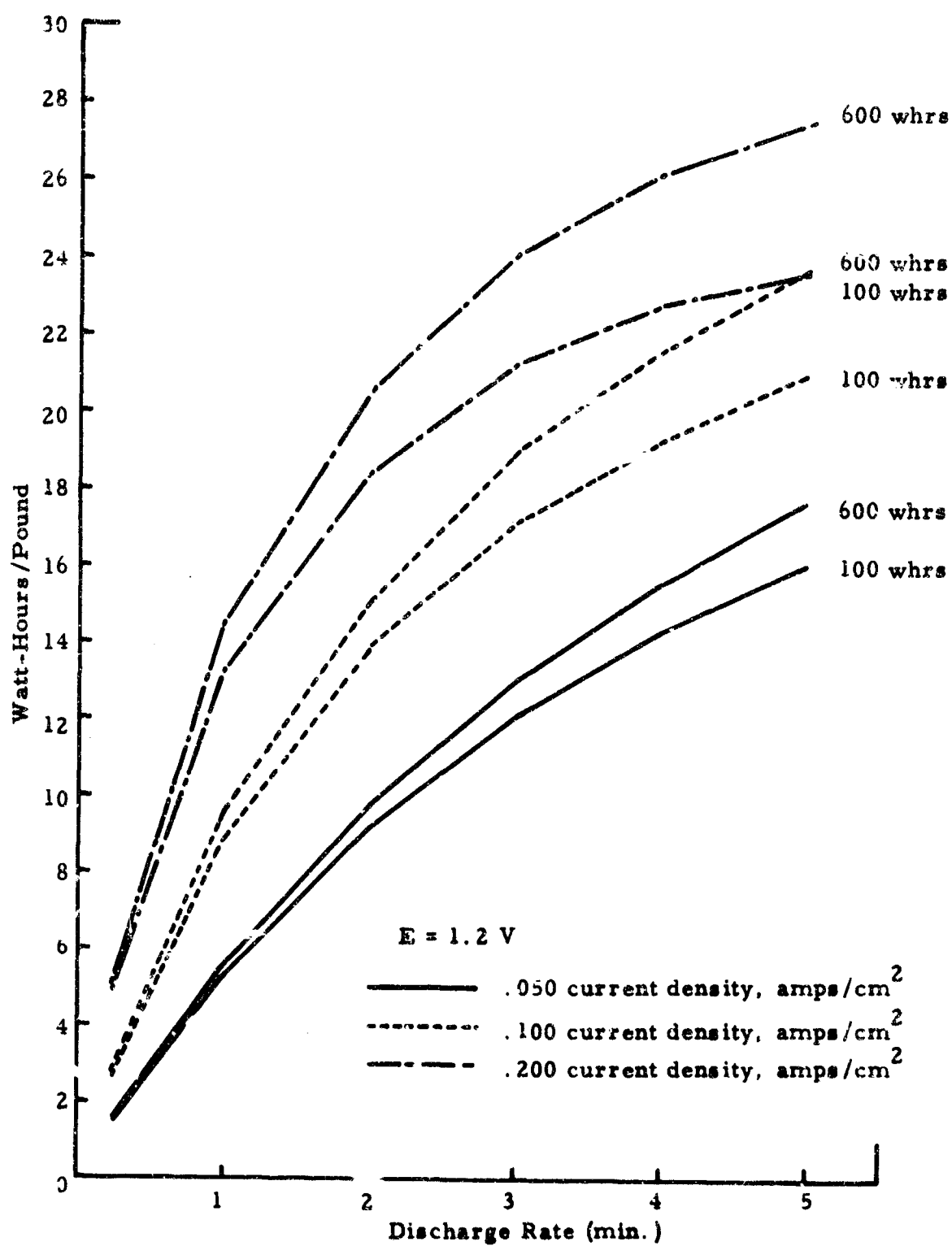
Figure 37.   Zinc/Oxygen Watt-Hours/Pound vs. Discharge Rate

66
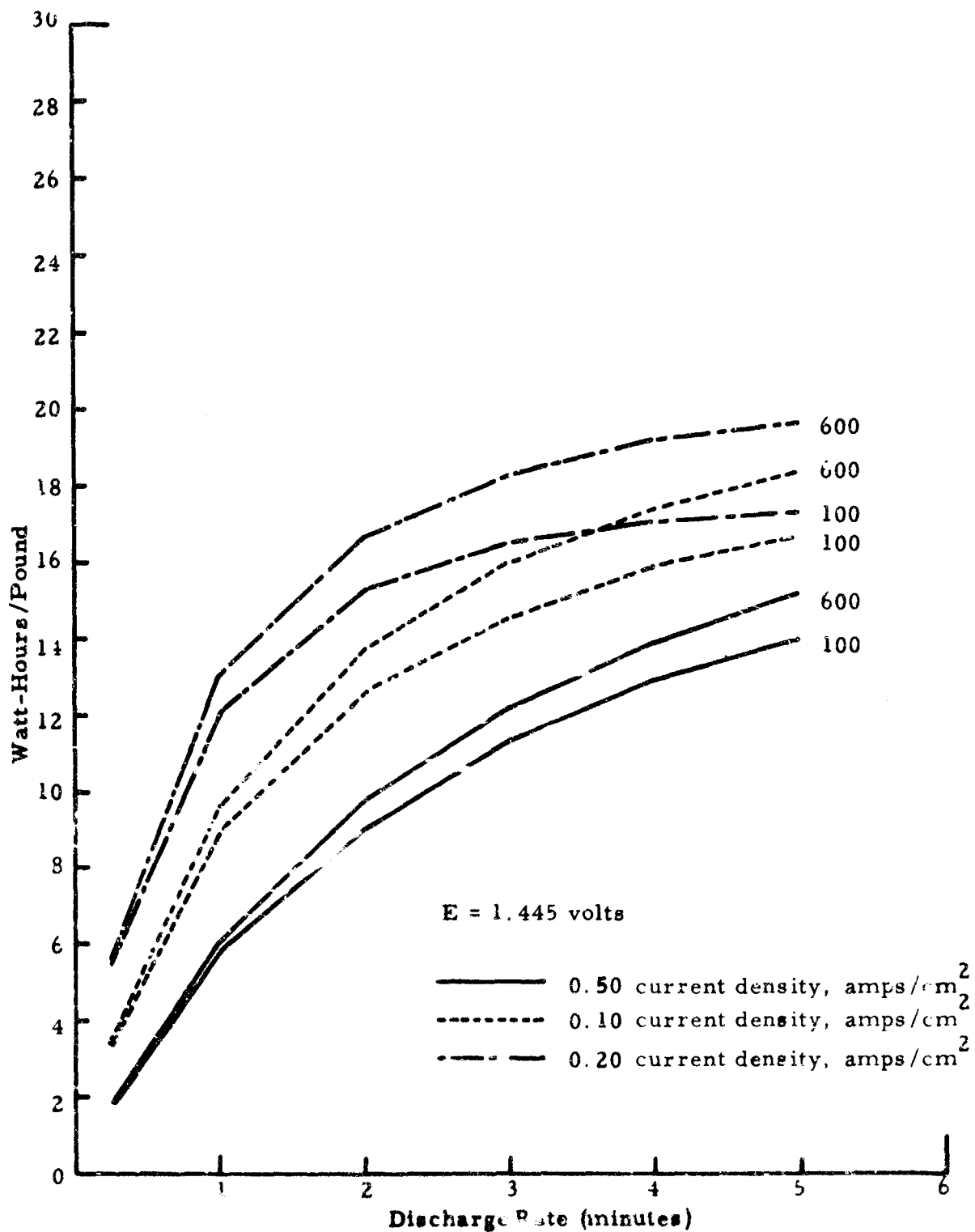
Figure 38.   Al/O$_2$ Watt-Hours/Pound vs. Discharge Rate

67
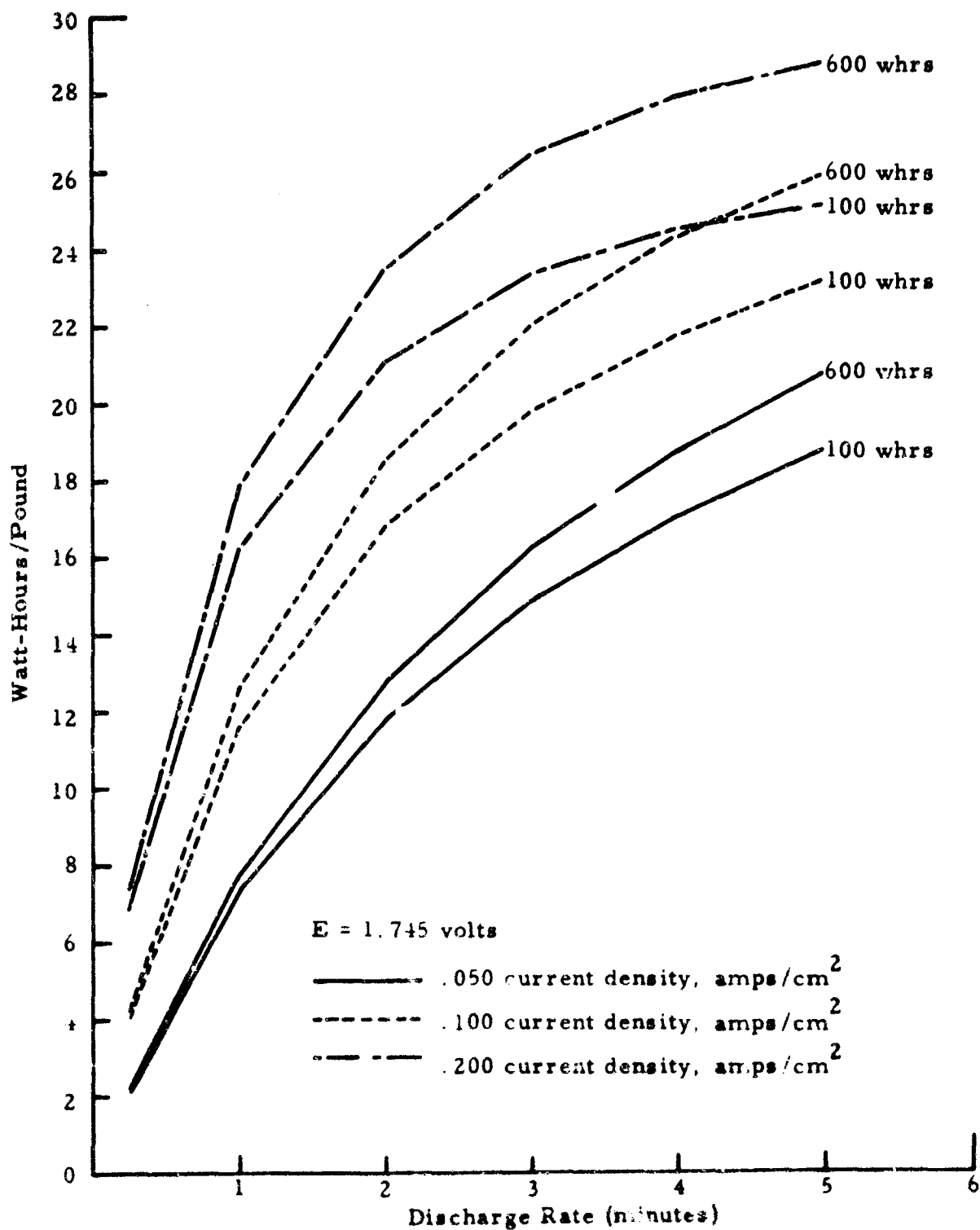
Figure 39.   Aluminum/Oxygen Watt-Hours/Pound vs. Discharge Rate

68
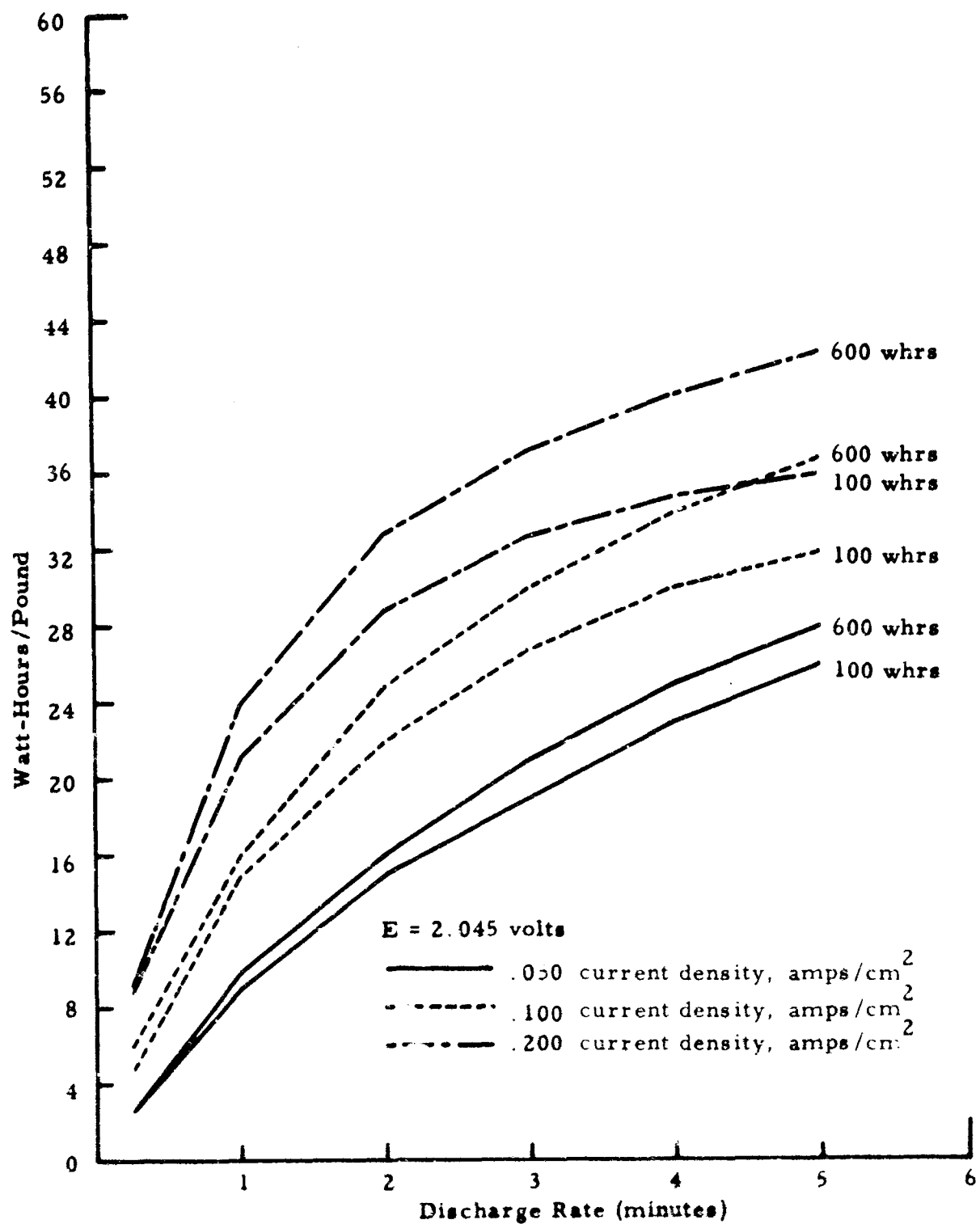
Figure 40.   Aluminum/Oxygen Watt-Hours/Pound vs. Discharge Rate

o9

Table VL Computer Output Data for Zinc/Oxygen System Operating at 1.2 Volts (refer also to Figure 36)

CURRENT DENSITY = .1000
WATT-HOURS = 100.0000
DISCHARGE RATE = 1.0000
WIDTH = 10.8000
TOTAL VOLUME = 258.6864
ENERGY DENSITY = .3865
TOTAL WEIGHT = 11.1829

WATT-HOURS/LB = 8.9421

1	197.14	3.88
2	387.83	7.64
3	1095.94	21.60
4	558.80	11.01
5	571.87	11.27
5	388.49	7.65
7	494.93	9.75
8	30.10	.59
9	32.54	.64
10	70.00	1.37
11	193.12	3.80
12	604.03	11.90
13	9.34	.18
14	89.06	1.75
15	349.25	6.88
	5072.52	100.00

8.9421475E+00   1.0000200E+00

CURRENT DENSITY = .1000
WATT-HOURS = 100.0000
DISCHARGE RATE = 2.0000
WIDTH = 10.1500
TOTAL VOLUME = 153.0851
ENERGY DENSITY = .6532
TOTAL WEIGHT = 7.1721
WATT-HOURS/LB = 13.9427

1	197.16	6.06
2	202.97	6.23
3	573.55	17.63
4	276.29	8.49
5	370.10	11.37
6	192.09	5.90
7	271.91	8.35
8	30.10	.92
9	32.54	1.00
10	70.00	2.15
11	379.86	11.67
12	338.11	10.39
13	5.70	.17
14	66.63	2.04
15	246.17	7.56
	3253.25	100.00

1.3942746E+01   2.0000400E+00

CURRENT DENSITY = .1000
WATT-HOURS = 100.0000
DISCHARGE RATE = 3.0000
WIDTH = 10.1500
TOTAL VOLUME = 118.3839
ENERGY DENSITY = .8447
TOTAL WEIGHT = 5.8216
WATT-HOURS/LB = 17.1772

1	197.17	7.45
2	141.55	5.36
3	400.00	15.14
4	184.21	6.97
5	304.33	11.52
6	125.07	4.84
7	203.94	7.72
8	30.11	1.14
9	32.54	1.23
10	70.00	2.65
11	439.70	16.65
12	238.76	9.04
13	4.32	.16
14	58.48	2.21
15	207.40	7.85
	2640.66	100.00

1.7177221E+01   3.0000600E+00

CURRENT DENSITY = .1000
WATT-HOURS = 100.0000
DISCHARGE RATE = 4.0000
WIDTH = 12.7500
TOTAL VOLUME = 102.5953
ENERGY DENSITY = .9746
TOTAL WEIGHT = 5.1662
WATT-HOURS/LB = 19.3564

1	197.18	8.41
2	110.86	4.73
3	313.26	13.36
4	145.17	6.19
5	276.46	11.79
6	100.93	4.30
7	214.31	9.14
8	30.11	1.28
9	32.54	1.38
10	70.00	2.98
11	450.17	19.21
12	155.98	6.65
13	2.95	.12
14	54.85	2.34
15	188.53	8.04
	2343.36	100.00

1.9356465E+01   4.0000800E+00

CURRENT DENSITY = .1000
WATT-HOURS = 100.0000
DISCHARGE RATE = 5.0001
WIDTH = 10.8000
TOTAL VOLUME = 90.7193
ENERGY DENSITY = 1.1023
TOTAL WEIGHT = 4.7319
WATT-HOURS/LB = 21.1330

1	197.20	9.18
2	90.61	4.22
3	256.05	11.92
4	111.79	5.20
5	252.63	11.77
6	77.72	3.62
7	165.02	7.68
8	30.11	1.40
9	32.54	1.51
10	70.00	3.26
11	483.43	22.52
12	150.82	7.02
13	3.03	.14
14	51.65	2.40
15	173.68	8.09
	2146.36	100.00

CURRENT DENSITY = .1000
WATT-HOURS = 100.0000
DISCHARGE RATE = .2496
WIDTH = 10.1500
TOTAL VOLUME = 919.7438
ENERGY DENSITY = .1087
TOTAL WEIGHT = 37.1136
WATT-HOURS/LB = 2.6944

1	197.13	1.17
2	1511.92	8.98
3	4272.35	25.37
4	2213.71	13.14
5	1753.95	10.41
6	1539.05	9.14
7	1704.97	10.12
8	30.10	.17
9	32.53	.19
10	70.00	.41
11	.00	.00
12	2470.63	14.67
13	36.47	.21
14	188.00	1.11
15	813.59	4.83
	16834.46	100.00

```
CURRENT DENSITY  =        .1000        CURRENT DENSITY =         .1000
WATT-HOURS       =     100.0000        WATT-HOURS       =     100.0000
DISCHARGE RATE   =       1.0000        DISCHARGE RATE   =       4.0000
WIDTH            =      10.8000        WIDTH            =      12.7500
TOTAL VOLUME     =     271.6132        TOTAL VOLUME     =     122.8036
ENERGY DENSITY   =        .3681        ENERGY DENSITY   =        .8143
TOTAL WEIGHT     =      11.1304        TOTAL WEIGHT     =       6.2861

WATT-HOURS/LB    =       8.9843        WATT-HOURS/LB    =      15.9080
    1        47.24       .93               1        47.24      1.65
    2       352.75      6.98               2       108.79      3.81
    3       996.79     19.74               3       307.43     10.78
    4       188.48      3.73               4        48.95      1.71
    5       592.52     11.73               5       153.90      5.39
    6       158.47      3.13               6        41.16      1.44
    7       432.19      8.56               7       187.10      6.56
    8        26.29       .52               8        26.29       .92
    9        28.41       .56               9        28.41       .99
   10        70.00      1.38              10        70.00      2.45
   11      1138.31     22.54              11      1413.12     49.56
   12       562.64     11.14              12       168.20      5.89
   13         2.55       .05              13         1.00       .03
   14        91.19      1.80              14        37.12       .30
   15       360.79      7.14              15       212.53      7.45
           5048.68    100.00                      2851.33    100.00
  8.9843699E+00  1.0000200E+00          1.5908096E+01  4.0000800E+00
CURRENT DENSITY  =        .1000        CURRENT DENSITY =         .1000
WATT-HOURS       =     100.0000        WATT-HOURS       =     100.0000
DISCHARGE RATE   =       2.0000        DISCHARGE RATE   =       5.0001
WIDTH            =      12.7500        WIDTH            =      11.4500
TOTAL VOLUME     =     174.6984        TOTAL VOLUME     =     111.9571
ENERGY DENSITY   =        .5724        ENERGY DENSITY   =        .8931
TOTAL WEIGHT     =       7.9331        TOTAL WEIGHT     =       5.9614
WATT-HOURS/LB    =      12.6052        WATT-HOURS/LB    =      16.7743
    1        47.24      1.31               1        47.24      1.74
    2       193.19      5.36               2        94.71      3.48
    3       545.92     15.17               3       266.50      9.85
    4        97.91      2.72               4        38.15      1.41
    5       307.81      8.55               5       119.93      4.43
    6        82.32      2.28               6        32.07      1.18
    7       280.65      7.79               7       145.80      5.39
    8        26.29       .73               8        26.29       .97
    9        28.41       .78               9        28.41      1.05
   10        70.00      1.94
   11      1313.18     36.49              10        70.00      2.58
   12       276.28      7.67              11      1442.02     53.32
   13         1.41       .03              12       161.03      5.95
   14        58.93      1.63              13         1.02       .03
   15       268.83      7.47              14        31.43      1.16
           3593.43    100.00              15       199.83      7.38
  1.2605262E+01  2.0000400E+00                   2704.07    100.00
CURRENT DENSITY  =        .1000        CURRENT DENSITY =         .1000
WATT-HOURS       =     100.0000        WATT-HOURS       =     100.0000
DISCHARGE RATE   =       3.0000        DISCHARGE RATE   =        .2496
WIDTH            =      10.1500        WIDTH            =      10.1500
TOTAL VOLUME     =     137.9648        TOTAL VOLUME     =     866.0465
ENERGY DENSITY   =        .7248        ENERGY DENSITY   =        .1154
TOTAL WEIGHT     =       6.8625        TOTAL WEIGHT     =      30.0059
WATT-HOURS/LB    =      14.5719        WATT-HOURS/LB    =       3.3326
    1        47.24      1.51               1        47.24       .34
    2       138.72      4.43               2      1322.04      9.71
    3       391.99     12.59               3      3738.04     27.46
    4        62.12      1.99               4       746.73      5.48
                                           5      2347.45     17.24
    5       195.30      6.27               6       627.82      4.61
    6        52.23      1.67               7      1485.92     10.93
    7       178.07      5.72               8        26.29       .19
    8        26.29       .84               9        28.41       .20
    9        28.41       .91              10        70.00       .51
   10        70.00      2.24              11         1.49       .01
   11      1399.32     44.95              12      2146.78     15.77
   12       248.44      7.98              13         8.50       .06
   13         1.40       .04              14       228.32      1.67
   14        43.51      1.39              15       781.60      5.74
   15       229.68      7.37                     13610.49    100.00
           3112.78    100.00
  1.4571920E+01  3.0000600E+00
```

OUTPUT FORMAT FOR TABLES VI AND VII

Current Density $=$ (amps/cm^2)

Watt-Hours $=$

Discharge Rate $=$ (minutes)

Width (optimum) $=$ (centimeters)

Total Volume $=$ (cubic inches)

Energy Density $=$ (watt-hours/in^3)

Total Weight $=$ (pounds)

Watt-Hours/Lb. $=$

	Component	Weight (gms)	% of Total
1.	Consumable Anode		
2.	Cathode Conductor		
3.	TFE + Pt		
4.	Anode Conductor		
5.	Electrolyte		
6.	Electrolyte Matrix		
7.	Gas Separator		
8.	Oxygen		
9.	Storage Tank (O_2)		
10.	Regulator		
11.	Heat Sink		
12.	Seal		
13.	Terminals		
14.	Activation System		
15.	Case		
	Total		

d. Twenty Minute Zinc/Oxygen Battery System

Since the computer program was now available for this work and the design methods already worked out for the five minute rate, at the request of AFAPL, a brief look was taken at the twenty minute rate operation of the zinc/oxygen system. Two estimation methods were used; namely the computer program described above was run with the new input data and also hand calculations were performed using a method similar to the one presently used with zinc/oxygen batteries at LML. In the appendix the hand calculations are shown. In Figure 41 the output of the computer design is illustrated for three capacities, namely 400, 1000 and 5000 watt-hours. The energy density is shown as a function of the current density of operation. Note on Figure 40 that the optimum operating current density is approximately 100 mA/cm^2. This optimum is a result of the fact that the savings in electrode weight at the higher current densities of operation is outweighed by the additional heat sink requirement. It can also be seen that there is an improvement in energy density when larger systems, i. e. , high capacities are used; however, this improvement is not linear and diminishes with increasing capacity.

In Table VIII the battery weights as estimated by the hand calculation and by the computer are shown along with the resulting energy density figures. It can be seen that the hand calculation and the computer design only differ by 9. 4%, which is considered very good agreement, considering that two different basic designs were assumed. Of the total battery weight, about 45% is the contribution of the heat sinks. Again, it must be mentioned that the use of melting heat sinks may not be the optimum for this battery, especially for the larger capacity batteries and some weight saving may be achieved if a better method is found.

Table VIII. Estimated Battery Weights

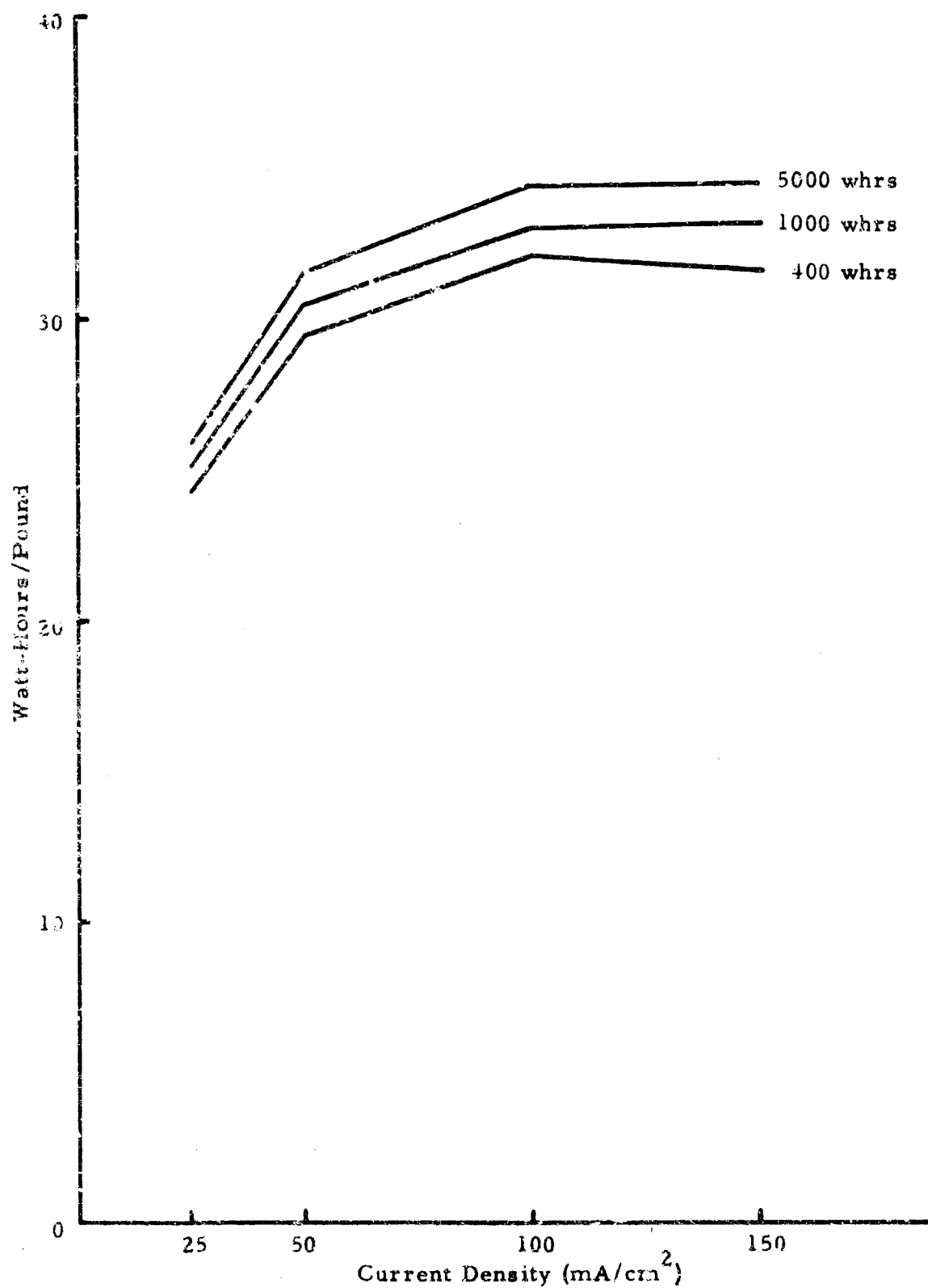| Design Mode	Without Heat Sinks		With Heat Sinks	
	Battery Weight lbs.	Energy Density watt-hours/lb.	Battery Weight lbs.	Energy Density watt-hours/lb.
Computer Design	7. 22	55. 5	12. 44	42. 15
Hand Calculation	7. 3	54. 8	14. 7	32. 2

Figure 41.   Zinc/Oxygen Watt-Hours/Pound vs. Current Density
at 20 Minute Rate

74

SECTION VI

DISCUSSION

The analyses and conclusion presented here refer to the particular requirements and goals of this contract. They are not necessarily applicable to all high-rate applications.

6.1 CONCLUSIONS ON HIGH-RATE BATTERIES WITH AQUEOUS ELECTROLYTES

At the beginning of this report, in Section II, it was shown that for batteries operating in the ambient temperature range, aqueous electrolytes have to be used for reasons of their higher conductivity. This statement is especially true if no external energy can be supplied in order to start up the battery. Electrolyte conductivity is a prime requirement for higher power densities: although no firm value can be attached to this parameter, conductivities in excess of $C. 2 \Omega^{-1}$ cm^{-1} are desirable to permit the use of current densities at or above 100 mA/cm^2. Only concentrated aqueous electrolytes are capable of meeting this requirement. The use of lower-conductivity, non-aqueous electrolytes necessitates lower current densities which also results in increased cell size and battery weight. Only couples which are operable in the aqueous media can therefore be considered.

The battery-weight-controlling parameters vary in importance depending on the type of battery construction used; conventional or pile. In a conventional battery, the electrodes are supplied with current collectors. The current is transferred to the cell terminal at the ending of such a collector. Hence, the current is transferred from each cell to the next via external connectors. In a bipolar- or pile-construction battery, the current generated in each cell is not collected and conducted to the parameter of the cell; instead, it is conducted through a thin, conducting, support layer into the next cell. Because of this difference in their construction, the conductors in the conventional battery have to be considerably heavier than in the pile type battery. Hence, for a conventional battery the operating voltage of a cell is a major weight-controlling parameter. With higher operating cell voltages and thus less cells, fewer current collectors are required and weight is saved. Whereas this statement is also true for the pile construction battery, the effect of current collectors is considerably less, and although there are common weight-controlling parameters, their order of importance is different. These two battery types are discussed separately.

a. Conventional Construction Batteries

On the basis of data generated so far, weight-controlling factors, in order of importance, are: (1) terminal voltage under load, (2) couple reversibility, (3) magnitude of the entropy change, and (4) theoretical energy density.

75.

Cell operating voltage alone determines the number of cells in a stack, the number required to achieve a battery voltage being inversely proportion_l to individual cell voltage. The relative difference of theoretical energy density and operating voltage at very high rates is best shown by an example. In Table VI, page 70, the weights of the zinc/oxygen battery components at the 2 minute rate, operating at a voltage of 1.2 volts/cell are shown. Assume now a cell, the couples in which have an energy density equal to only 25% that of the zinc/oxygen system but in turn are able to operate at 2.4 volts (i.e., double that of the zinc/oxygen system) at a similar[4] level of reversibility. The weight analysis shows that the percentage of consumable zinc and oxygen is 6.98%; the nonvariants (regulator, gas storage, battery case, heat sinks) is 22.38%; and the weight of the remaining components is 71.56%. This last figure varies almost linearly with the number of cells.

Substituting the low energy density, high voltage couple for zinc/oxygen, it is apparent that for every 100 gms of the zinc/oxygen battery the new components would weigh as follows:

	Zinc/Oxygen 1.2 V	"New Couple" 2.4 V
Consumables	6.98	27.92
Non-Variants	22.38	22.38
Balance	70.64	35.32
Total	100.00	85.62

Hence, a 14.4% weight saving or, 17% increase in energy density is achieved. This was accomplished even thoug' the couples used had only 1/4 the energy density of zinc/oxygen. Obviously, an even more significant improvement can be made if the couple had an energy density equal to as much as 50% that of zinc/oxygen.

Two aspects of couple reversibility have to be considered. Firstly, the deviation between theoretical open circuit voltage and operating cell voltage which reflects that portion of the free energy change which is dissipated as heat. This heat must be either absorbed in the battery or ejected to the surroundings - in either case this means a weight penalty. Secondly, the difference between the observed OCV of the battery and the operating battery voltage: this determines the voltage control attainable at various current densities and, therefore, power densities. The significance of this can be only evaluated in terms of a specific requirement. It was noted earlier

---

[4] expressed as (operating voltage) $\times \left(\dfrac{nF}{-\Delta H} \right)$

that the oxygen depolarized electrode is very limited by the requirement of a maximum 10% variation between open circuit voltage and full load voltage in the high voltage battery.

Negative entropy changes in the overall redox process also result in waste heat generation. It can be argued that a positive entropy change (resulting in the net absorption of heat) is desirable for very high rate applications but no such system is known at present. Overall negative entropy changes should be as small as possible, however, to minimize heat generation. In this respect it must be noted that all gas-depolarized cathodes are not nearly as efficient as the secondary type of electrode (oxides, chlorides, etc.).

Both free energy losses and the negative entropy change result in waste heat generation which must be either absorbed in the battery or removed, resulting in a weight penalty. Considering waste heat generation as the primary source of the increase in the battery weight, it is entirely possible that couples with a lower energy density which generate less waste heat would be more suitable for a high rate application than those having higher energy densities. This statement is especially true at the 20 minute rates where the fusible heat sinks account for approximately 45% of the overall battery weight, simply because the total heat dissipation is increased at the 20 minute rate.

b. Pile Type Battery

The controlling factors in addition to the energy density of the couples in order of estimated importance are: (1) couple reversibility, (2) couple combinations which permit easy bipolar electrode design, (3) wet shelf life, (4) magnitude of the entropy change, and (5) high operating cell voltage.

The arguments put forward with respect to couple reversibility and the magnitude of the entropy change in the previous section are valid also for a pile type battery. In addition, it should be noted that because the weight of the ancillaries, such as current collectors, is less in a pile-type battery, the influence of couple irreversibility (i. e. , waste heat generation) is relatively larger with this battery type than with a conventional battery.

A couple combination which permits easy bipolar electrode fabrication is essential for this application; the gas depolarized electrodes that were proposed for the aluminum/oxygen system are not well suited to this type of battery construction. The reason is simple: it is implicit in the gas depolarized electrode that access space for gas distribution be provided behind each electrode; hence, it is almost impossible to manufacture simple bipolar electrodes with these systems.

So far, wet shelf life has not been mentioned as a major weight-controlling parameter because in a conventional battery the electrolyte storage and activation system, if properly designed, should only comprise a relatively small percentage of the overall battery weight. With the relatively few cells connected in series, a manifolding system can be used which, when filling the cells, is so designed that the parasitic shunt currents between each cell are small and last only during the time of activation, after which time the ionic path between the cells is disrupted. For a high voltage battery pile with multiplicity of cells (in the hundreds), this is an almost impossible task. In order to achieve high energy densities for the short duration discharge rates, the thickness of the cells must be very small. Hence, with a common manifolding system, especially one designed for rapid activation, there would be a relatively short ionic path between each of the cells, which would result in large shunt currents. This is especially true when one considers the high voltage differential between points located relatively close to one another. Because of the thinness of the cells and narrow inlet ports, activation time could be considerable, causing extensive self-discharge. This would, of course, lower the energy density but a more important problem would be the hydrogen/oxygen gas bubble formation leading to infinite impedance in zero-G environment which would render the battery inoperable. Hence, a complicated manifolding arrangement is required to provide separate electrolyte injection for each of the cells. This latter approach would involve a severe weight penalty in addition to the inherent slowness of the activation procedure.

In all cases the reliability of any electrolyte injection system involving hundreds of cells would be very low.

It would, therefore, be more advantageous if the battery could be activated before installation and had a long wet stand life. Such a battery could be tested prior to installation and would not have to depend on the statistical probability that the activation system would work for each of the many hundreds of cells.

Lastly, it must be pointed out that whereas the theoretical energy density of the couples was not a significant weight-controlling factor with the conventional 28 volt battery, it might be more significant with the pile construction battery. As mentioned earlier, the thinness of the cell separator/current collector layers are limited only by mechanical design considerations since they are no longer required to act as current collectors. For this reason, high operating cell voltage is not as important as with a conventional battery (from the weight standpoint); it is, however, important to reliability.

6.2 SUMMARY OF FINDINGS WITH THE ALUMINUM/OXYGEN SYSTEM

The results of the parametric studies, conceptual design studies, and thermal analysis to date have shown that the weights of the aluminum/ oxygen and zinc/oxygen batteries are penalized to a major extent by the need for heat sinks at rates longer than fifteen seconds. This is the result of irreversible thermodynamic losses which appear as waste heat during discharge of the cell.

In all cases, the most reversible aluminum anodes found have been the materials supplied by Olin. These alloys have demonstrated consistent superiority over and above high purity and commercial purity aluminum. These alloys provide superior cell voltages to zinc in potassium hydroxide but this advantage is lost because of the greater % irreversibility.

Part of the waste heat released in the aluminum/oxygen (and zinc/ oxygen) cells is the contribution of a significant negative entropy change which occurs during the oxidation process. In the case of lower-energy-density couple combinations such as silver oxide/zinc, NiOOH/Cd, and zinc/ manganese dioxide, where the oxidant species, O or OH, is transferred from one atom to another, the entropy change involved is very small and contributes less to the overall heat of reaction. In the case of the aluminum couple, the entropy change is probably magnified by the degree of hydration of the aluminum ion.

Studies on pure aluminum and selected alloys have shown that in the case of certain alloys, anodic oxidation is occurring at potentials more cathodic than the observed open circuit potential. This oxidation process is masked, however, by the simultaneous evolution of hydrogen which is preventing useful current and energy from being released at more negative potentials. The real current density of the anodic process is, however, quite small.

The overall improvement in reversibility of Al alloys over 99.999% aluminum is clearly shown in Table IX. The improvement is more marked in chloride electrolyte: in KOH the improvement is still significant. The greater reversibility of the A6 alloy in chloride electrolytes unfortunately cannot be used to advantage since it was shown that the oxygen electrode is more irreversible in this electrolyte. Further, very low limiting currents were observed on the oxygen-depolarized cathode - 20 mA/cm^2. Thus, improved anode reversibility is balanced by poor cathode behavior and KOH remains the preferred electrolyte for Al alloy/O_2 cells.

Hydrogen gassing is a major problem although the actual rate ($\approx$ 5 mA/cm^2) is small. The gassing results in added heat generation, loss of electrolyte from test cells, combustion with positive depolarizer and would be unacceptable in zero-G environment since it would cause infinite cell impedance.

In KOH, gassing was worst at OCV and was minimized by pre-anodization. The rate of gassing diminished when the alloy was polarized. The reverse is true in KCl or $AlCl_3$.

Table 1. Comparison of Alloys and Pure Aluminum

Alloy Number	Electrolyte	Reference	Reversible (Eo) OCV (V)	Attained OCV (V)	Difference from Eo(V)	Voltage @ 100 mA/cm^2
99.999%	KOH	Hg/HgO	-2.42	-1.56	0.86	-0.88
44836	KOH	Hg/HgO	-2.42	-1.84	0.58	-1.54
99.999%	KCl	Calomel	-1.93	-0.77	1.16	-0.76
A6	KCl	Calomel	-1.93	-1.53	0.40	-1.55*

*due to negative difference effect

6.3 RECOMMENDATIONS

As a result of the studies performed, it is concluded that for the required high rate, high energy density batteries, the theoretical energy density of the couple combination is a minor, rather than a major, weight-controlling factor. This is shown clearly in Tables VI and VII on pages 70 and 71 where the percentage weights of zinc and aluminum in the overall battery system are shown.

In a simplified form, the conclusions regarding the aluminum/oxygen system for the high rate application are as follows:

- Because of the low hydrogen overvoltage and consequent gassing, the aluminum/oxygen system is not ready for battery development.

- If the hydrogen overvoltage is increased and reliable cells could be constructed, waste heat dissipation is still a problem and no major weight saving over presently available silver peroxide/zinc batteries is foreseen.

80

- If both the aluminum alloy reversibility and hydrogen over-voltage are improved simultaneously, the aluminum/oxygen system will offer considerable weight saving over the silver peroxide/zinc system.

- For high-voltage, pile-construction batteries, gas-depolarized electrodes, and hence, the aluminum/oxygen system are unsuitable.

It is recommended that in order to modify the aluminum characteristics to the point where major improvements in reversibility and H_2 over-voltage could be realized, a long-range research program should be established. A better fundamental understanding of the ionic and electronic conduction processes in the surface oxide, the composition of the oxide (and in particular, the concentration of Sn^{++++} ions) is needed before improvement can be sought.

APPENDIX I

DETERMINATION OF OHMIC INEFFICIENCY AS A FUNCTION OF ELECTRODE AND ELECTROLYTE RESISTANCES AND THE REVERSIBILITY OF THE ELECTRODE PROCESS

For rectangular electrodes with current being collected at one end, the following relationship for ohmic losses has been derived:

$$V_r = \eta \left[1 - \cosh \left[\left(\frac{c\rho}{t} \right)^{\frac{1}{2}} w \right] + \tanh \left[\left(\frac{c\rho}{t} \right)^{\frac{1}{2}} W \right] \sinh \left(\frac{c\rho}{t} \right)^{\frac{1}{2}} w \right]$$

where:

V_r = ohmic component in volts

η = electrode polarization in volts

c = a constant equal to current density (i) divided by polarization voltage (η)

ρ = electrode resistivity in ohm-cm

t = thickness of electrode-cm

W = total electrode length-cm

w = distance from current collector-cm

The assumptions made in this derivation are:

1. The polarization-current density curve is linear.

2. Uniform electrode.

3. No axial iR losses

Let us consider a flat rectangular electrode of length W as shown below:
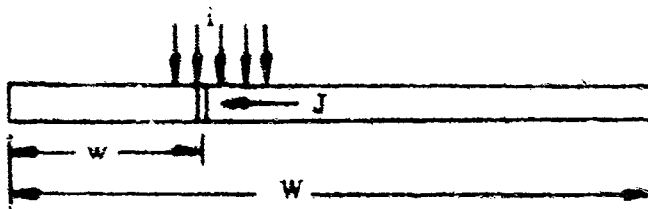
On the basis of the first assumption we can write

$$i = C\eta \tag{1}$$

where: i = current density - amps/cm^2

The current gives rise to an ohmic drop in the electrode, reducing the amount of polarization which influences the electrode reaction.

$$i = C(\eta - V_r) \tag{2}$$

If we write a current balance about a differential segment, we obtain:

$$i(l\, dw) = dJ \tag{3}$$

where: J = current parallel to surface
l = width of electrode

The current parallel to the surface can be derived from Ohm's law to be:

$$J = \frac{-lt}{\rho} \frac{dV_r}{dW} \tag{4}$$

Combining equation (3) and (4), the following differential equation is obtained:

$$\frac{d^2V_r}{dW^2} = \frac{-i\rho}{t} \tag{5}$$

Substituting equation (2) into equation (5) and rearranging:

$$\frac{d^2V_r}{dW^2} - \frac{C\rho}{t}V_r = \frac{-C\rho}{t}\eta \tag{6}$$

The complete solution can be determined from a knowledge of the boundary conditions:

$$V_r = 0 \quad \text{at} \quad w = 0$$

$$dV_r/dw = 0 \quad \text{at} \quad w = W$$

$$V_r = \eta\left[1 - \cosh\left(\frac{c\rho}{t}\right)^{\frac{1}{2}} w + \tanh\left[\left(\frac{c\rho}{t}\right)^{\frac{1}{2}} W\right] \sinh\left(\frac{c\rho}{t}\right)^{\frac{1}{2}} w\right] \tag{7}$$

84

An efficiency, E, is defined which is the electrode current at a given polarization with ohmic losses included divided by the current when the electrode ohmic drop is zero.

$$E = \frac{\displaystyle\int_0^W i(w)\,\ell\,dw}{\displaystyle\int_0^W c\eta\,\ell\,dw} = \frac{1}{c\eta\,\ell\,W}\int_0^W i(w)\,\ell\,dw \tag{8}$$

Substituting equation (7) into equation (2) yields the local current density as a function of position:

$$i = c\eta\left[\cosh\left(\frac{c\rho}{t}\right)^{\frac{1}{2}}w - \tanh\left(\frac{c\rho}{t}\right)^{\frac{1}{2}}W\sinh\left(\frac{c\rho}{t}\right)^{\frac{1}{2}}w\right] \tag{9}$$

The total current as a function of w is:

$$J = \int_0^W i\,\ell\,dw = \frac{c\eta\,\ell}{(c\rho/t)^{\frac{1}{2}}}\left[\sinh\left(\frac{c\rho}{w}\right)^{\frac{1}{2}}w - \tanh\left[\left(\frac{c\rho}{t}\right)^{\frac{1}{2}}W\cosh\left(\frac{c\rho}{t}\right)^{\frac{1}{2}}w\right]\Bigg|_0^W$$

$$= \frac{c\eta\,\ell}{\left(\frac{c\rho}{t}\right)^{\frac{1}{2}}}\left[\tanh\left(\frac{c\rho}{t}\right)^{\frac{1}{2}}W\right] \tag{10}$$

Substituting (10) into (8) gives,

$$E = \frac{\tanh\left[\left(\frac{c\rho}{t}\right)^{\frac{1}{2}}W\right]}{W\left(\frac{c\rho}{t}\right)^{\frac{1}{2}}}$$

85

APPENDIX II

LIST OF INPUT DATA SYMBOLS

CD MIN	Current density, minimum; amps/cm^2
CD MAX	Current density, maximum; amps/cm^2
CD INC	Current density increment; amps/cm^2
CAPMN	Capacity, minimum; watt-hours
CAPMX	Capacity, maximum; watt-hours
CAPIC	Capacity increment; watt-hours
DISMN	Discharge rate, minimum; hours
DISMX	Discharge rate, maximum; hours
DISIC	Discharge increment; hours
WMAX	Electrode width, maximum; cm
WMIN	Electrode width, minimum; cm
WINC	Electrode width increment; cm
VOLTN	Nominal voltage; volts
VCELL	Cell voltage; volts
FACT	Anode utilization factor
RES	Electrolyte resistivity, ohm-cm
E	Cathode polarization, volts
XKA	Lbs/amp-hr, consumable anode
TSMIN	Separator thickness, minimum; cm
SD	Thickness of gas space; cm
TTFE	Thickness of cathode; cm
TC	Cathode conductor thickness; cm
EXCES	Excess oxygen factor
RHOCA	Density of consumable anode; gm/cm^3
RHOCC	Density of cathode conductor; gm/cm^2
RHOTP	Density of Teflon-Pt; gm/cm^2
RHOA	Density of electrolyte; gm/cm^3
RHOE	Density of electrolyte; gm/cm^3
RHOGS	Density of gas separator; gm/cm^2
RHOAC	Density of electrolyte matrix
RHOT	Density of storage tank; gm/in^3
RHOHS	Density of heat sink; gm/cm^3
RHOEP	Density of epoxy; gm/cm^3
RHOGL	Density of glue; gm/cm
SIGY	Yield strength of storage tank; psi
XKO2	Lbs/amp-hr; cathode depolarizer
02P	Oxygen pressure; atmospheres
TAMP	Ambient temperature (maximum); °F
WT(10)	Weight of regulator; gms
REGV	Volume of regulator; in^3
BTULB	Thermal absorption capacity of heat sink; B TU/lb
EZERO	Thermoneutral voltage; volts

PIMEL	Melting point of heat sink; $^{\circ}F$
XKACT	Activation system proportionality constant; gms/cm^3
D	Distance between parallel modules; cm
CASEK	Battery case proportionality constant; gms/cm^3
XKC	Slope of cathode polarization curve; amps/volts
SPHT(1)	Specific heat of consumable anode; $cal/gm-^{\circ}C$
SPHT(2)	Specific heat of cathode conductor; $cal/gm-^{\circ}C$
SPHT(3)	Specific heat of TFE + Pt; $cal/gm-^{\circ}C$
SPHT(4)	Specific heat of anode conductor; $cal/gm-^{\circ}C$
SPHT(5)	Specific heat of electrolyte; $cal/gm-^{\circ}C$
SPHT(6)	Specific heat of electrolyte matrix; $cal/gm-^{\circ}C$
SIGC	Cathode conductor conductivity; $mho-cm^{-1}$
SIGA	Anode conductor conductivity; $mho-cm^{-1}$
XXKA	Slope of anode polarization curve; amps/volts
TAMIN	Minimum thickness of anode conductor; cm

IBM 1620 FORTRAN PROGRAM

```
C      PROGRAM 4018              JANUARY 28, 1966
C      OPTIMUM WEIGHT OF FUEL CELL
       DIMENSION SPHT(6), WT(15), PREV(15)
   999 READ 500, CDMIN, CDMAX, CDINC, CAPMN, CAPMX, CAPIC
       READ 500, DISMN, DISMX, DISIC, WMAX, WMIN, WINC
       READ 500, VOLTN, VCELL, FACT, RES, E, XKA
       READ 500, TSMIN, SD, TTFE, TTERM, TC, EXCES
       READ 500, RHOCA, RHOCC, RHOTP, RHOA, RHOE, RHOGS
       READ 500, RHOAC, RHOT, RHOHS, RHOEP, RHOGL, SIGY
       READ 500, XKO2, O2P, TAMB, WT(10), REGV, BTULB
       READ 500, EZERO, PTMEL, XKACT, D, CASEK, XKC
       READ 500, SPHT(1), SPHT(2), SPHT(3), SPHT(4), SPHT(5), SPHT(6)
       READ 500, SIGC, SIGA, XXKA, TAMIN
   500 FORMAT (SE12.1)
C      CONSTANTS
       CON1        = 453.5924
       CON1R       = 1.0/ CON1
       PI          = 3.1415927
       PI4         = 4.0 * PI
       CON2        = PI4 / 3.0
       BTULB       = 1.0 / BTULB
       TAMBK       = 5.0 * (TAMB - 32.0) / 9.0  +  273.16
       CD          = CDMIN
   995 CAP         = CAPMN
       E2          = 2.0 * E * CD / CDMIN
   996 DISCH       = DISMN
C      COMPUTE CURRENT AND AREA
   997 XI          = CAP / (VOLTN * DISCH)
       AIC         = XI / CD
       WTCA        = CAP * XKA * CON1 * FACT / VOLTN
       TCA         = WTCA / (RHOCA * AIC)
C      DETERMINE IF CONSUMABLE ANODE IS ZINC
       IF (RHOCA - 2.14) 200, 201, 200
   200 SL          = 3.0 * WTCA / (RHOE * AIC * 0.75)
       IF (SL - TSMIN) 904, 900, 900
   904 SL          = TSMIN
       GO TO 900
   201 TS          = WTCA / (RHOE * AIC * 0.915)  -  TCA * 0.933
       IF (TS - TSMIN) 905, 906, 906
   905 TS          = TSMIN
   906 SL          = TS  +  0.5 * TCA
   900 ERES        = SL * RES
       PHI         = CD * ERES
       VACT        = VCELL  -  PHI
       CELLS       = VOLTN / VACT
       NC          = CELLS
       CELL        = NC
       IF (CELL - CELLS) 202, 901, 202
   202 CELL        = CELL  +  1.0
   901 BV          = CELL * VACT
       XIA         = CAP / (BV * DISCH)
       ACELL       = XIA / (2.0 * CD)
       WTCA        = WTCA * XIA / XI
       PREVT       = 1.0E+08
       W           = WMAX
```

```
  998 XL            = ACELL / W
C     COMPUTE THE CATHODE EFFICIENCY
      DENO          = SQRT (XKC / (TC * SIGC)) * W
      EFFC          = DENO / SIN(DENO)
C     COMPUTE THE ANODE THICKNESS
      TA            = TC * (SIGC / SIGA) * (XXKA / XKC)
      IF (TA  -  TAMIN) 213, 213, 214
  213 TA            = TAMIN
C     COMPUTE THE ACTUAL LENGTH AND AREA OF CELL (ADJUST TA AND WTCA)
  214 XLACT         = XL * EFFC
      XAACT         = ACELL * EFFC
      TCA           = WTCA / (RHOCA * XAACT)
      WT(1)         = WTCA * CELL
C     DETERMINE THE NUMBER OF FOLDS
      FOLDS         = XLACT / (2.0 * W)
      NFOLD         = FOLDS
      FOLD          = NFOLD
      IF (FOLD - FOLDS) 203, 902, 203
  203 FOLD          = FOLD  +  1.0
  902 FOLDR         = 1.0 / FOLD
      FOLDA         = XAACT * FOLDR
      FOLDL         = XLACT * FOLDR
C     CALCULATE THE INACTIVE AREA DUE TO GAS SPACE
      AINAC         = SD * W * (FOLD - 1.0)
C     CALCULATE THE WEIGHTS OF CELL COMPONENTS
      ATOT          = XAACT  +  AINAC
      CN2           = 2.0 * CELL
      WT(2)         = ATOT * CN2 * RHOCC
      WT(3)         = ATOT * CN2 * RHOTP
      WT(4)         = TA * XAACT * CN2 * RHOA
C     DETERMINE IF THE CONSUMABLE ANODE IS ZINC
      IF (RHOCA - 2.14) 204, 205, 204
  204 ELECV         = CN2 * XAACT * TS * 0.75
      GO TO 903
  205 ELECV         = CN2 * XAACT * (0.75 * TS  +  0.7 * TCA)
  903 WT(5)         = ELECV * RHOE
      WT(7)         = RHOGS * FOLDA * CELL * (FOLD + 1.0)
      WT(6)         = CN2 * RHOAC * FOLDA * FOLD
C     CALCULATE THE WEIGHT OF THE OXYGEN AND RELATED COMPONENTS
      WT(8)         = EXCES * CAP * XKO2 * CON1 * CELL / BV
      VSTS          = WT(8) * CON1R * 19386.0
      VSTA          = VSTS * 262.2336 / (O2P * TAMBK)
      TANKR         = (VSTA / CONZ)**0.33333333
      TANKT         = 14.69 * O2P * TANKR / SIGY
      WT(9)         = PI4 * TANKR**2 * TANKT * RHOT
C     HEAT SINK
      AMPHR         = XIA * DISCH
      VOHM          = E2 * (1.0  -  COS(DENO))
      BGH           = AMPHR * CELL * 3.413 * (EZERO - VACT - VOHM)
      TINER         = 0.0
      DO  100  I  = 1, 6
  100 TINER         = TINER  +  WT(I) * SPHT(I)
      TINER         = TINER * (PTMEL - TAMB) * CON1R
      WT(11)        = (BGH - TINER) * CON1 * BTULB
      IF (WT(11)) 208, 209, 209
```

```
    208 WT(11)          = 0.0
C       COMPUTE THE INACTIVE CATHODE WEIGHT DUE TO FOLD
    209 THS             = WT(11) / (RHOHS * CELL * XAACT)
        CIA             = 4.0 * FOLD * CELL * W* (TS + TCA + TA + 0.5 * THS)
        CON10           = CN2 * CIA
        WT(2)           = WT(2)  +  CON10 * RHOCC
        WT(3)           = WT(3)  +  CON10 * RHOTP
C       FRAME WEIGHT
        TM              = 2.0 * (TC + TTFE + TS + TA + TCA) + THS + SD
        CON3            = CN2 * FOLD * FOLDL
        SLWT            = CON3 * (0.3175 * TM * RHOEP  +  2.0 * RHOGL)
        SACWT           = 0.3175 * CON3 * (2.0 * RHOCC  +  RHOA * TA)
        WT(12)          = SLWT  +  SACWT
C       CELL TERMINAL WEIGHT
        WT(13)          = FOLDL * FOLD * TM * (CELL + 1.0) * RHOA * TTERM
C       WEIGHT OF ACTIVATION SYSTEM
        WT(14)          = XKACT * ELECV**0.66666667
C       CASE WEIGHT
        VOLC            = TM * FOLD * W * (FOLDL + D)
        CASEV           = CELL * VOLC + ELECV + VSTA * 16.45 + REGV
        WT(15)          = CASEK * CASEV**0.66666667
C       TOTAL WEIGHT
        TOTWT           = 0.0
        DO  102  I  = 1, 15
    102 TOTWT           = TOTWT  +  WT(I)
        IF (TOTWT - PREVT) 206, 207, 207
    206 PREVT           = TOTWT
        PCASE           = CASEV / 16.45
        DO  103  I  = 1, 15
    103 PREV(I)         = WT(I)
        W               = W  - WINC
        GO TO 998
    207 PUNCH 553, CD
        PUNCH 554, CAP
        ODIS            = DISCH * 60.0
        PUNCH 555, ODIS
        PREVW           = W  +  WINC
        PUNCH 556, PREVW
        PUNCH 557, PCASE
        EDENS           = CAP / PCASE
        PUNCH 558, EDENS
        TOT             = PREVT / CON1
        PUNCH 559, TOT
        WHLB            = CAP / TOT
        PUNCH 560, WHLB
    553 FORMAT (19H CURRENT DENSITY = F12.4)
    554 FORMAT (19H WATT-HOURS      = F12.4)
    555 FORMAT (19H DISCHARGE RATE  = F12.4)
    556 FORMAT (19H WIDTH           = F12.4)
    557 FORMAT (19H TOTAL VOLUME    = F12.4)
    558 FORMAT (19H ENERGY DENSITY  = F12.4)
    559 FORMAT (19H TOTAL WEIGHT    = F12.4)
    560 FORMAT (19H WATT-HOURS/LB   = F12.4)
        CON4            = 100.0 / PREVT
        DO  101  I  = 1, 15
```

```
      PCT           = CON4 * PREV(I)
101   PUNCH 501, I, PREV(I), PCT
501   FORMAT (  I3, 3X F10.2, 3X F8.2)
      PUNCH 502, PREVT
502   FORMAT (9X F10.2, 9H    100.00)
      PUNCH 504, WHLB, ODIS
504   FORMAT (1X E14.7, 1X E14.7, 40X 2H 1)
      IF (DISCH  -  DISMX) 215, 216, 216
215   DISCH         = DISCH  + DISIC
      GO TO 997
216   IF (CAP  -  CAPMX) 210, 211, 211
210   CAP           = CAP  +  CAPIC
      GO TO 996
211   IF (CD  -  CDMAX) 212, 999, 999
212   CD            = CD  +  CDINC
      VCELL         = VCELL  -  CDINC / XXKA
      GO TO 995
      END
```

APPENDIX IV

DESIGN OF Zn/O_2 20 MINUTE RATE

1. **CELL SIZE**

   a. **Required Current**

   $$I = \frac{400 \text{ watt-hours}}{28V \times .333 \text{ hrs.}} = 43 \text{ amps}$$

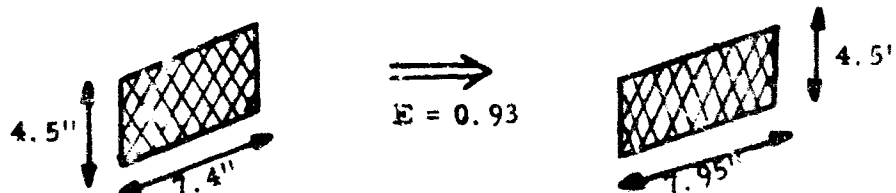   b. **Estimated capability of Zn/O_2 cell**

   @ 100 mA/cm^2

   $Vc = 1.24 \text{ volts}$

   $c = i/E = 2$

   No. of cells $= 28/1.24 = 23$

   c. **Required Area (Cell)**

   $$A = I/i = 43/0.100 = 430 \text{ cm}^2 = 66.6 \text{ in.}^2$$
   $$= 7.4" \times 4.5" \text{ for a bipolar cell}$$

   If we select a suitable nickel screen such as $5 \text{ Ni } 14 -2/o$, then the electrode efficiency for the cathode becomes

   $$E = \frac{\sin \sqrt{\frac{kp}{t}} L}{\sqrt{\frac{kp}{t}} L}$$

   where $c = $ slope of polar curve $= 2$

   $$p = \text{eff. resist.} = \frac{9.4 \times 10^{-6}}{.28} = 33.6 \times 10^{-6} \text{ -cm}$$

   $t = .005" \times 2.54 \quad .0127 \text{ cm}$

   $L = 10.4 \text{ cm}$

93

1. CELL SIZE

    c. (continued)

$$E = \frac{\sin (0.655)}{0.655} = 93\%$$

$$Lact = 7.4/.93 = 7.95''$$

Adj. Bipolar Area $= 35.8''^2 = 232$ cm^2
Cathode Area $= 71.6''^2 = 464$ cm^2

    d. Anode Thickness (Current Collector)

use silver screen, $\rho = 2.0 \times 7.7 \times 10^{-6} \,\Omega$ -cm, c= 2

Min. ta = tc $\dfrac{Pa}{Pc}$ = .0127 $2 \times 77/33.6$ = .0058 cm
= 2.3 mls

3 Ag 5 -2/0 screen can be used
+ ta = 3.0 mls

2. WEIGHT OF CELL COMPONENTS

    a. Weight of Cathode/Nickel

$$W_{Ni} = (gms/cm^2) \ (Ac) \ (N \ Cells)$$

$$(gms/cm^2 = \frac{10 \times 2 \times .014 \times .86 \times 8.9}{10.5 \times 6.45} = .0316$$

$$W_{Ni} = (.0316) \ (464) \ (23) = 336 \ gms$$

    b. Weight of Anode/Ag

$$W_{Ag} = (gms/cm^2) \ (Aa) \ (N \ Cells)$$

$$(gm^3/cm^2) = \frac{.13 \times .86 \times .6}{6.45} = .0104$$

$$W_{Ag} = (.0104) \ (232) \ (23) = 55.5 \ gms$$

94

c. Weight of Cathode/TFE + Pt

$$W_{TFE/Pt} = 0.0193 \text{ gms/cm}^2 \times 464 \text{ cm}^2 \times 23$$
$$= 206 \text{ gms}$$

d. Weight of Consumable Anode (Zinc)

Theoretical Wt. required = (amp-hrs) (G/amp-hr)
$$= 43/3 \times 1.22 = 17.5 \text{ gms/cell}$$

if we assume 50% availability, then

$Wa = 17.5 \times 2 \times 23 = 805 \text{ gms}$

$ta = (17.5 \text{ gms}/2.14 \text{ gms/cc}) \ (1/232 \text{ cm}^2) = .0352 \text{ cm} \times 2 = .07 \text{ cm}$
$$= 14 \text{ mils} \times 2 = 28 \text{ mils}$$

e. Electrolyte Requirements

(1) $\ Wt_{KOH} = 0.12 \left[\dfrac{7 \text{ gms } 30\% \text{ KOH}}{1.22 \text{ gms Zn}} \right] \times 35 \text{ gms Zn}$
$$= 24.1 \text{ gms/cell} \times 23 \text{ cells} = 555 \text{ gms}$$

Void thickness required = (24.1 gms/1.25 gms/cc) $(1/464 \text{ cm}^2)$
$$= .0416 \text{ cm} = 16.4 \text{ mls}$$

(2) Thickness KOH abs. by Zinc = $28/2 \times .7 = 9.8 \text{ mls}$

Separator thickness required = $(16.4 - 9.8)/.7 = 9.5 \text{ mils}$

$$W_{sep} = (.0226 \text{ gms/cm}^2) \ (464 \text{ cm}^2) \ (23)$$
$$= 241 \text{ gms}$$

f. Intercell Separators

Assume #20 nylon mesh is used

thickness $= .030''$
Wt. $= 0.19 \text{ gms/in.}^2$
Wt. $= 0.19 \times 35.8 \times 24 = 163 \text{ gms}$

95

3. HEAT SINK REQUIREMENTS

    a. Heat Generation, BTU's

$$G\text{-}BTU = (E^o - Vc)\,(amp\text{-}hrs)\,(3.413)\,(23)$$

$$Vc = 1.24 - (\phi_{KOH} + \phi_{cond.})$$

$$\phi_{KOH} = \frac{i \times \rho KOH}{.7} \times (ts + t\varkappa n/4) =$$

$$= (.100)\,(1.85/.7)\,(.042) = .011 \text{ Volts}$$

$$\phi_{cond} = 2 \times \eta \left[1 - \cos\,(\sqrt{\frac{cp}{t}}\ L) \right]$$

$$= 2 \times .050 \left[1 - \cos\ .655 \right]$$

$$= .020 \text{ Volts}$$

$$G\text{-}BTU = (1.80 - 1.21)\,(14.30)\,(3.413)\,(23)$$
$$660\ \ BTU's$$

    b. Thermal Inertia of Cell Components

$$A\text{-}BTU = \sum_{i=1}^{n} M_i\,C_i/454 \right]\ \ (MP\text{-}Ta)$$

$$= \left[\begin{array}{l} .25 \times 206 + .113 + .093 \times 905 \\ + .06 \times 55 + 0.9 \times 555 + .4 \times 241 \end{array} \right] (1/454)\,(46^o F)$$

$$= 78 \text{ BTU's}$$

    c. Weight of $Mg(NO_3)_2 \cdot 6 H_2O$ required

$$W_{HS} = (660 - 78)/106 \times 454$$

$$= 2500 \text{ gms}$$

$$t_{HS} = \frac{2500}{1.464} \times \frac{1}{23} \times \frac{1}{232}$$

$$= .32 \text{ cm} = 126 \text{ mils}$$

4. WEIGHT OF SEAL

    a. Weight of Seal with Heat Sink

$$*W_{seal} = (\text{frame perimeter, in.})(Pe, gm/in)(No. cells)$$

$$W_{seal} = (24.9)(0.878)(23) = 504 \text{ gms}$$

    b. Weight of Seal without Heat Sink

$$W_{seal} = (24.9)(.412)(23) = 236 \text{ gms}$$

5. WEIGHT OF OXYGEN + RELATED COMPONENTS

    a. Weight of Oxygen

$$W_{O_2} = (14.3 \text{ amp-hrs})(0.298 \text{ gm/amp-hrs})(23)(1.25)$$

$$= 122.5 \text{ gms}$$

    b. Volume of Storage Tank

$$Vol_{STP} = (122.5/32 \times 454)(359) = 3.02 \text{ ft}^3$$

$$Vol = \frac{3.02}{200 \text{ atm}} \times .96 \times 1728 = 25 \text{ in.}^3$$

$$r = (25/4.18)^{1/3} = 1.81 \text{ in.}$$

    c. Weight of Storage Tank (1/2 yield strength of Ti)

$$W = 4\pi r^2 t p$$

$$t_{min} = Pr/2\sigma_y = \frac{2930 \times 1.81}{2 \times 10^5} = 2.68 \times 10^{-2"}$$

use $t = .054"$ (safety factor = 2)

then $W = 4(3.14)(1.81)^2(.054)(16.45)(4.5) = 192 \text{ gms}$

$*W_{seal}$ includes weight of nylon frame, epoxy and sealed cathode screen.

97

d. Weight of Pressure Regulator = 70 gms

two stage regulator #25575, Scott Aviation Corp.

6. ELECTROLYTE ACTIVATION SYSTEM

The following relationship applied for all similarly shaped containers.

$$Wa = KV^{2/3}$$

where V = vol of electrolyte required

*$Ka = 0.6$

$$Wa = 0.6 (444)^{2/3} = 35 \text{ gms}$$

7. CASE WEIGHT

a. Volume, Total
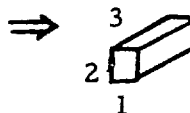
(1) with Heat Sink

$$V_t = 23 V_{cell} + V_{KOH} + V_{O_2} + V_{PR}$$

$$= 23 (7.75) + 27 + 25 + 2$$

$$= 233 \text{ in.}^3$$

(2) Volume w/o Heat Sink

$$V_t = 23 (3.2) + 27 + 25 + 2$$

$$= 127.5 \text{ in}^3$$

b. Weight of case by method of similar prisms, assume unit prism

then,

$$Wc = KcV^{2/3}$$

where

$Kc = 11.3$ (filament-wound, glass-filled epoxy, .040" thick)

*empirically determined for a "polyethylene syringe" prototype.

98

(1)   W/H.S.

$$W_c = 11.3 \, (233)^{2/3} = 430 \text{ gms}$$

(2)   w/o H.S.

$$W_c = 11.3 \, (127.5)^{2/3} = 288 \text{ gms}$$

8.   WATT-HOURS/#

a.   With Heat Sink

$$\text{Watt-hrs}/\# = 400 \text{ whrs}/ \quad W_i = 400/13.7\#$$

$$= 29.2$$

b.   W/O Heat Sink

$$\text{Watt-hrs}/\# = 400 \text{ whrs}/7.3\#$$

$$= 54.8$$

DOCUMENT CONTROL DATA - R&D

(Security classification of title, body of abstract and indexing annotation must be entered when the overall report is classified)

1. ORIGINATING ACTIVITY *(Corporate author)*	2a. REPORT SECURITY CLASSIFICATION
Leesona Moos Laboratories Division of Leesona Corporation Great Neck, New York	Unclassified
	2b. GROUP

3. REPORT TITLE

High Rate (5 Minute) Missile Battery Report

4. DESCRIPTIVE NOTES *(Type of report and inclusive dates)*

Final Report - 15 June 1965 through 30 April 1966

5. AUTHOR(S) *(Last name, first name, initial)*

Vertes, M. A. ; Oxley, J. E. ; Cohen, S.

6. REPORT DATE	7a. TOTAL NO. OF PAGES	7b. NO. OF REFS
June 1966	116	0

8a. CONTRACT OR GRANT NO. AF 33(615)-2680 b. PROJECT NO. 8173 c. Task No. 817304-010 d.	9a. ORIGINATOR'S REPORT NUMBER(S) As Applicable 9b. OTHER REPORT NO(S) *(Any other numbers that may be assigned this report)* AFAPL-TR-66-50

10. AVAILABILITY/LIMITATION NOTICES

This document is subject to special export controls and each transmittal to foreign governments and foreign nationals may be made only with prior approval of the Air Force Aero Propulsion Laboratory.

11. SUPPLEMENTARY NOTES	12. SPONSORING MILITARY ACTIVITY AF Aero Propulsion Laboratory, Attn: APIP, U. S. Air Force, Research & Technology, Wright-Patterson AFB, Ohio

13. ABSTRACT

The findings of an investigation of the aluminum/oxygen battery system in the 0.25 - 5 minute discharge time range are presented. Considerable improvement in the electrochemical reversibility of Al anodes was found in the Al-Sn alloys. This improvement, however, could not be achieved with a concurrent increase in hydrogen overvoltage. The high rate of corrosion accompanying the increased hydrogen evolution prevents the use of these alloys in batteries. A parallel study indicated that heat sinks would be required to absorb the waste heat generated during discharge - even if H_2 evolution is eliminated. Estimates of the battery weights at the various discharge rates were optimized using a computer program. It was shown that neither Al/O_2 or Zn/O_2 are capable of meeting the 100 watt-hour/lb. goal at the 5-minute rate. A general discussion is included identifying the weight contributing factors and their relative contributions towards total system weight. It is concluded that at the high rates couple reversibility, thermal efficiency and cell operating voltage have a much greater effect on overall battery weight than the theoretical energy density.

DD FORM 1 JAN 64 **1473**

14. KEY WORDS	LINK A		LINK B		LINK C	
	ROLE	WT	ROLE	WT	ROLE	WT
Aluminum, hydrogen overvoltage on						
Aluminum, surface oxide						
Aluminum/oxygen battery						
Anodes, aluminum						
Anodes, aluminum alloy						
Anodes, zinc						
Battery, high rate						
Battery, waste heat generation						
Cathodes, oxygen depolarized						
Electrodes, ohmic losses in						
Oxygen depolarized battery						
Zinc/oxygen battery						

INSTRUCTIONS

1. ORIGINATING ACTIVITY: Enter the name and address of the contractor, subcontractor, grantee, Department of Defense activity or other organization (corporate author) issuing the report.

2a. REPORT SECURITY CLASSIFICATION: Enter the overall security classification of the report. Indicate whether "Restricted Data" is included. Marking is to be in accordance with appropriate security regulations.

2b. GROUP: Automatic downgrading is specified in DoD Directive 5200.10 and Armed Forces Industrial Manual. Enter the group number. Also, when applicable, show that optional markings have been used for Group 3 and Group 4 as authorized.

3. REPORT TITLE: Enter the complete report title in all capital letters. Titles in all cases should be unclassified. If a meaningful title cannot be selected without classification, show title classification in all capitals in parenthesis immediately following the title.

4. DESCRIPTIVE NOTES: If appropriate, enter the type of report, e.g., interim, progress, summary, annual, or final. Give the inclusive dates when a specific reporting period is covered.

5. AUTHOR(S): Enter the name(s) of author(s) as shown on or in the report. Enter last name, first name, middle initial. If military, show rank and branch of service. The name of the principal author is an absolute minimum requirement.

6. REPORT DATE: Enter the date of the report as day, month, year; or month, year. If more than one date appears on the report, use date of publication.

7a. TOTAL NUMBER OF PAGES: The total page count should follow normal pagination procedures, i.e., enter the number of pages containing information.

7b. NUMBER OF REFERENCES: Enter the total number of references cited in the report.

8a. CONTRACT OR GRANT NUMBER: If appropriate, enter the applicable number of the contract or grant under which the report was written.

8b, 8c, & 8d. PROJECT NUMBER: Enter the appropriate military department identification, such as project number, subproject number, system numbers, task number, etc.

9a. ORIGINATOR'S REPORT NUMBER(S): Enter the official report number by which the document will be identified and controlled by the originating activity. This number must be unique to this report.

9b. OTHER REPORT NUMBER(S): If the report has been assigned any other report numbers (either by the originator or by the sponsor), also enter this number(s).

10. AVAILABILITY/LIMITATION NOTICES: Enter any limitations on further dissemination of the report, other than those imposed by security classification, using standard statements such as:

(1) "Qualified requesters may obtain copies of this report from DDC."

(2) "Foreign announcement and dissemination of this report by DDC is not authorized."

(3) "U. S. Government agencies may obtain copies of this report directly from DDC. Other qualified DDC users shall request through

_____ ."

(4) "U. S. military agencies may obtain copies of this report directly from DDC. Other qualified users shall request through

_____ ."

(5) "All distribution of this report is controlled. Qualified DDC users shall request through

_____ ."

If the report has been furnished to the Office of Technical Services, Department of Commerce, for sale to the public, indicate this fact and enter the price, if known.

11. SUPPLEMENTARY NOTES: Use for additional explanatory notes.

12. SPONSORING MILITARY ACTIVITY: Enter the name of the departmental project office or laboratory sponsoring (paying for) the research and development. Include address.

13. ABSTRACT: Enter an abstract giving a brief and factual summary of the document indicative of the report, even though it may also appear elsewhere in the body of the technical report. If additional space is required, a continuation sheet shall be attached.

It is highly desirable that the abstract of classified reports be unclassified. Each paragraph of the abstract shall end with an indication of the military security classification of the information in the paragraph, represented as (TS), (S), (C), or (U).

There is no limitation on the length of the abstract. However, the suggested length is from 150 to 225 words.

14. KEY WORDS: Key words are technically meaningful terms or short phrases that characterize a report and may be used as index entries for cataloging the report. Key words must be selected so that no security classification is required. Identifiers, such as equipment model designation, trade name, military project code name, geographic location, may be used as key words but will be followed by an indication of technical context. The assignment of links, rules, and weights is optional.